



UNIVERSITÀ
DEGLI STUDI
DI PADOVA

Head Office: UNIVERSITÀ DEGLI STUDI DI PADOVA

DIPARTIMENTO DI SALUTE DELLA DONNA E DEL BAMBINO

Ph.D. COURSE IN: MEDICINA DELLO SVILUPPO E SCIENZE DELLA PROGRAMMAZIONE SANITARIA

CURRICULUM: EMATO-ONCOLOGIA, GENETICA, MALATTIE RARE E MEDICINA PREDITTIVA

SERIES: XXXII

NOVEL HIGH RESOLUTION MASS SPECTROMETRY APPLICATIONS FOR THE STUDY OF LUNG DISEASES

Coordinator: Ch.mo Prof. Carlo Giaquinto

Supervisor: Ch.mo Prof. Carlo Giaquinto

Co-Supervisor: Ch.ma Prof.ssa Paola Cogo

Ph.D. student: Sonia Giambelluca

*Ai miei genitori,
Le mie radici, il mio faro*

INDEX

Abstract	1
Riassunto	3
Chapter 1: Respiratory Distress Syndrome and surfactant replacement therapy	
1.1 Respiratory Distress Syndrome	5
1.2 Lung surfactant	7
1.2.1 Alveolar system	7
1.2.2 Surfactant composition	8
1.3 Surfactant Replacement Therapy	10
Bibliography	12
Chapter 2: Contribution of surfactant replacement therapy by stable isotopes	
2.1 Stable isotopes	15
2.2 Mass spectrometry	17
2.2.1 Isotope ratio mass spectrometry (IRMS)	17
Bibliography	21
Publication 1: Estimating the contribution of surfactant replacement therapy to the alveolar pool: An <i>in vivo</i> study based on ¹³ C natural abundance in rabbits	23
Publication 2: Tracing exogenous surfactant <i>in vivo</i> in rabbits by the natural variation of ¹³ C	29
Chapter 3: Effect of chorioamnionitis on RDS	
3.1 Chorioamnionitis	37
3.2 Chorioamnionitis and neonatal outcome	39
3.2.1 Chorioamnionitis and respiratory outcome	41
Bibliography	43
Publication 3: Surfactant components and tracheal aspirate inflammatory markers in preterm infants with Respiratory Distress Syndrome	47

Chapter 4: Metabolomics in lung diseases	
4.1 Metabolomics	53
4.2 Metabolomics application for lung diseases	56
4.3 Liquid chromatography-mass spectrometry based metabolomics	57
Bibliography	61
Publication 4: Effects of maternal chorioamnionitis on epithelial lining fluid lipidomics and metabolomics in newborns with respiratory distress syndrome	65
Conclusions	93
Acknowledgment	95

ABSTRACT

Respiratory Distress Syndrome (RDS) is a respiratory disorder that can affect preterm newborns. It is due to lung immaturity and a deficiency of lung surfactant, a thin lipoprotein layer which allows lung expansion and prevents alveolar collapse during expiration. In these babies, nasal Continuous Positive Airway Pressure (nCPAP) provides non-invasive respiratory support by alveolar recruitment and improves functional residual capacity during spontaneous breathing. In case nCPAP fails, the next step is treatment with exogenous surfactant, which improves gas exchange and survival, reducing the need for mechanical ventilation and then the incidence of chronic lung disease. Although surfactant replacement therapy remains the gold standard for the treatment of RDS, failure rate ranges from 9% to 50%. The possibility of tracing the fate of the administered drug and estimate *in vivo* the amount of drug reaching the lung could help in improving the therapy and allow the premise to test different delivery systems.

RDS is a disorder related to prematurity. Among the factors responsible for premature birth, intrauterine infection (chorioamnionitis) is one of the main causes and it has been reported to have effects on the development of fetal organs. In particular, it has been reported that infants exposed to chorioamnionitis had a reduced risk to develop RDS but an increased risk for chronic lung diseases. Since the function of lung surfactant strictly depends on its composition, a better knowledge on surfactant metabolite and lipid changes would elucidate the effects of the exposition of the foetus to maternal intrauterine infection on RDS.

The PhD project focused on 2 objectives:

1. To validate natural abundance stable isotopes approach as a reliable method to quantify the contribution of exogenous surfactant to the alveolar surfactant pool in a rabbit model of RDS treated with a porcine exogenous surfactant
2. To assess the effect of maternal intrauterine infection on the surfactant composition of newborns affected by RDS by liquid chromatography-mass spectrometry (LC-MS/MS) based metabolomics

RIASSUNTO

La sindrome da distress respiratorio (RDS) è un disordine respiratorio che può colpire bambini nati prematuramente. È dovuta all'immaturità polmonare e ad una deficienza di surfattante polmonare, un sottile strato lipoproteico che permette l'espansione del polmone e previene il collasso alveolare durante l'espirazione. In questi bambini il supporto respiratorio tramite nasal Continuous Positive Airway Pressure (nCPAP) permette il reclutamento alveolare e migliora la capacità respiratoria. In caso la nCPAP fallisca, lo step successivo è il trattamento con un surfattante esogeno, che migliora lo scambio gassoso e la sopravvivenza, riducendo la necessità della ventilazione meccanica e quindi l'incidenza di malattie polmonari croniche. Nonostante la terapia con surfattante esogeno rimanga il gold standard per il trattamento della RDS, il tasso di fallimento può variare dal 9% al 50%. La possibilità di tracciare il destino del farmaco somministrato e stimare *in vivo* la quantità di farmaco che raggiunge i polmoni può aiutare a migliorare la terapia e permettere di testare diversi sistemi di somministrazione.

La RDS è un disordine correlato alla prematurità. Tra i fattori che predispongono alla prematurità, l'infezione intrauterina (corioamnionite) è una delle cause principali ed è stato riportato avere effetti sullo sviluppo degli organi fetali. In particolare, alcuni autori hanno riportato che l'esposizione alla corioamnionite possa, da una parte, ridurre il rischio di sviluppare la RDS, ma dall'altra aumentare il rischio di malattie polmonari croniche. Poiché la funzione del surfattante dipende fortemente dalla sua composizione, una maggiore conoscenza dei cambiamenti del profilo dei metaboliti e dei lipidi potrebbe chiarire gli effetti dell'esposizione del feto all'infezione intrauterina materna sulla RDS.

Il progetto di dottorato è stato strutturato secondo due obiettivi:

1. Validare l'utilizzo degli isotopi stabili ad abbondanza naturale come metodo affidabile per quantificare il contributo del surfattante esogeno nel pool alveolare di surfattante in un modello di RDS di coniglio trattato con surfattante esogeno di origine porcina.
2. Stabilire l'effetto della infezione intrauterina materna sulla composizione del surfattante in neonati affetti da RDS tramite metabolomica con cromatografia liquida accoppiata a spettrometria di massa (LC-MS/MS)

Chapter 1

RESPIRATORY DISTRESS SYNDROME AND SURFACTANT REPLACEMENT THERAPY

1.1 Respiratory Distress Syndrome

Preterm birth is defined as childbirth occurring at less than 37 completed gestational weeks (GWs). The worldwide incidence of preterm birth is 9.6% of all births, with higher rates in Africa (11.9%) and North America (10.6%) compared with the lowest rates in Europe (6.2%)[1]. It is a major determinant of neonatal mortality and morbidity, although improvements in neonatal care and clinical progress lead to 24 weeks newborn survival. Preterm newborns have higher rates of cerebral palsy, sensory deficits, learning disabilities and respiratory illnesses compared with children born at term. Among prematurity-related respiratory disorders, Respiratory Distress Syndrome (RDS) is the leading cause of respiratory insufficiency. Clinical characteristics of patients with RDS are[2]:

- Alveolar collapse (atelectasis)
- Decreased compliance (difficulties to inflate)
- Alveolar overexpansion (to overcome atelectasis of the other parts of the lung)
- Intrapulmonary shunting (impaired ventilation/perfusion)
- Hypoxemia
- Hypercapnia (thus, acidosis)

It was initially named hyaline membrane disease (HMD) because of the protein-rich, shiny appearance of alveoli and small airways found in preterm infants died for respiratory distress. Nowadays, it is well established that it is characterized by lung immaturity and a deficiency of surfactant, a thin layer of lipids and proteins which allows lung expansion and prevents alveolar collapse during expiration, thanks to tension-lowering properties. It has been reported that infants with RDS have surfactant lipid pools of less than 10 mg/kg compared with the surfactant lipid pool sizes in term infants of perhaps 100 mg/kg[3].

Lung development occurs in three main periods (Figure 1): the embryonic period, the fetal period and postnatal lung development. The embryonal period is characterized by lung organogenesis; fetal phase consists in the pseudoglandular, canalicular and sacular stages; postnatal lung development comprises the stages of classical and continued alveolarization, as

well as of microvascular maturation. During the saccular stage, peripheral airways enlarge and distal airways begin to dilate while their walls begin to thin. Type II pneumocytes, the cells responsible for surfactant production, are present and maturing. During alveolarization, alveoli form and mature and alveolar walls thin. All cell types proliferate during this phase, including type II pneumocytes. The overall result is a maturing lung with a larger surface area and a minimal diffusion distance for gas exchange[4]. With preterm birth this mechanism is interrupted. A foetus at 24 GW is completely surfactant deficient and unable to quickly synthesize or secrete surfactant if delivered. The tissues defining the potential air-blood barrier are thicker than at term newborn and pulmonary microvascular development has not fully vascularized the saccular mesenchyme, and is not ready to support air breathing. For this reason, the incidence of RDS increases with decreasing gestational age. Sixty per cent of infants born at <28 GW will develop RDS, with incidence of 30% in infants born between 28 and 34 GW, and less than 5% of infants born after 34 GW[4]. Other factors that increase the risk of RDS include male sex, maternal gestational diabetes, perinatal asphyxia, hypothermia, and multiple gestations.[5]

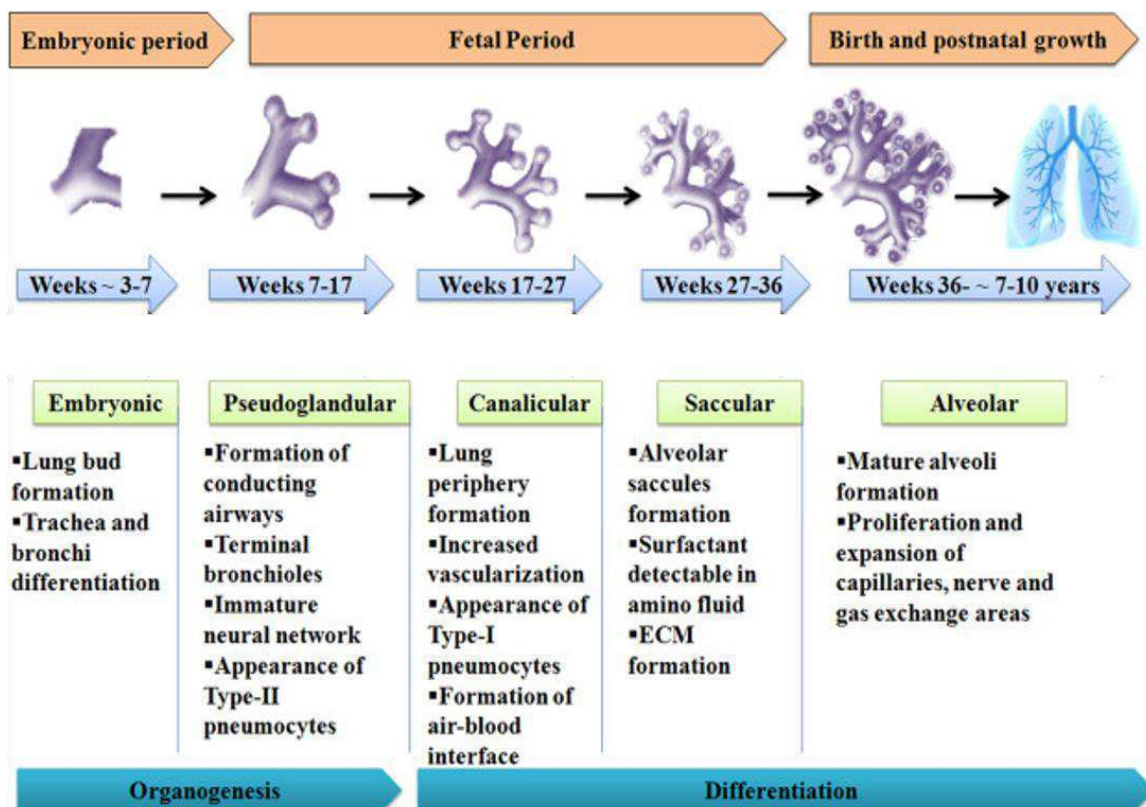


Figure 1. Lung development stages (adapted from Hussain et al.[6])

1.2 Lung surfactant

1.2.1 Alveolar system

In humans, the lung alveolar system represents the largest surface exposed to the environment covering up, in adults, 70-120 m², creating an extensive surface area through which oxygen and carbon dioxide are exchanged with blood. The alveolus (Figure 2), the basic respiratory exchange unit, consists of an epithelial layer and extracellular matrix surrounded by capillaries; it has a radius of about 0.1 mm, and a wall thickness of about 0.2 μ m. The alveolar surface is formed by two types of epithelial cells, pneumocytes I and pneumocytes II, or alveolar cells types I and II, respectively. Type I cells make up 95% of the alveolus, and serve as a thin barrier between blood and air[7]. Type II cells account the other 5% of epithelial cells, they can differentiate in type I cells, and take part in the immune defence, expressing receptors like Toll- like receptor. Also, they can regulate the transmigration of monocytes across the epithelial layer and participate in T-cell activation. However, the most important role of type II cells is to synthesize and secrete an aqueous fluid covering alveolar epithelial cells called pulmonary surfactant[8]. The alveoli have an innate tendency to collapse because of their spherical shape, small size and the contribution of water vapour to surface tension[9]. Surfactant forms a lipid monolayer at the air-water interphase that reduces the surface tension, hence stabilizing the alveoli and preventing their collapse at the end of expiration. Surfactant also exerts a critical role in host defence representing an efficient barrier against environmental insults, like pathogens.

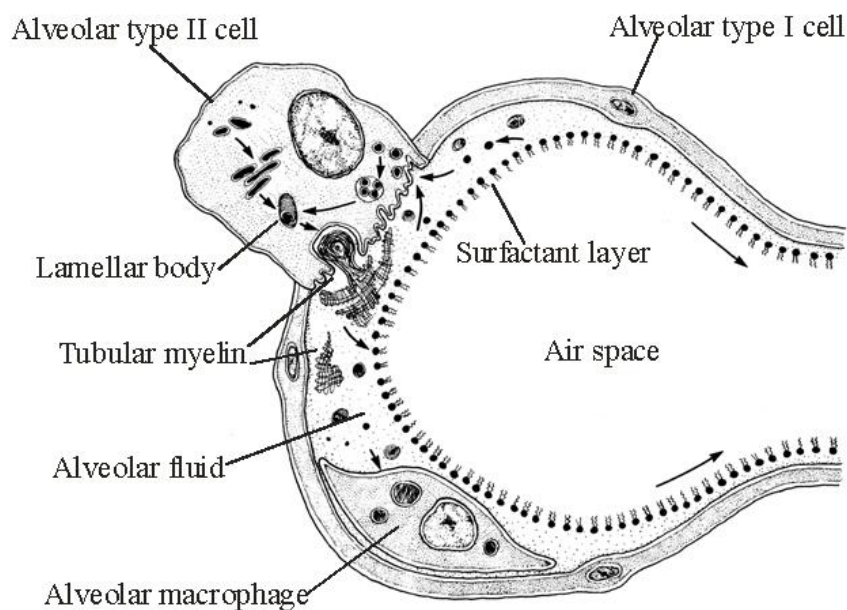


Figure 2. The structure of the alveolus. Tubular myelin is the form in which surfactant is secreted by Type II cells before spreading in a monolayer[10]

1.2.2 Surfactant composition

The function of surfactant in lowering surface tension is mainly due to its composition (Figure 3). Lipids constitute the major part (approximately 90%) of pulmonary surfactant; among these 80-90% are represented by phospholipids (PLs), whereas cholesterol comprises the largest amount of neutral lipids (10-20%). Among these PLs, phosphatidylcholine (PC) makes up the major part (80%), and around 60% of PC molecules contains two saturated fatty-acid moieties. This di-saturated PC (DSPC) contains mainly palmitic acid and is defined as 1,2-dipalmitoyl-sn-3-phosphocholine dipalmitoyl phosphatidylcholine (DPPC). The remaining PLs are a composite of phosphatidylglycerol (PG, 7–15%), and small quantities (<5% each) of phosphatidylinositol (PI), phosphatidylethanolamine (PE), and phosphatidylserine (PS). Finally, the most abundant neutral lipid is cholesterol, together with small amounts of free fatty acids and mono-, di-, and, triglycerides[11].

Aside the lipids, surfactant is constituted of proteins, which account for the remaining 10%. There are 4 surfactant's specific proteins (SP-A, B, C and D) that contribute to surfactant's formation and functions. SP-A is the most abundant protein followed by SP-B, SP-C and SP-D. SP-B and SP-C are hydrophobic proteins and play a direct role in structural organization of the surfactant at the interphase; mutations in the genes encoding SP-B and SP-C are associated with acute respiratory failure and interstitial lung diseases. The hydrophilic proteins, SP-A and SP-D, play a regulatory role in surfactant metabolism along with immunological functions.

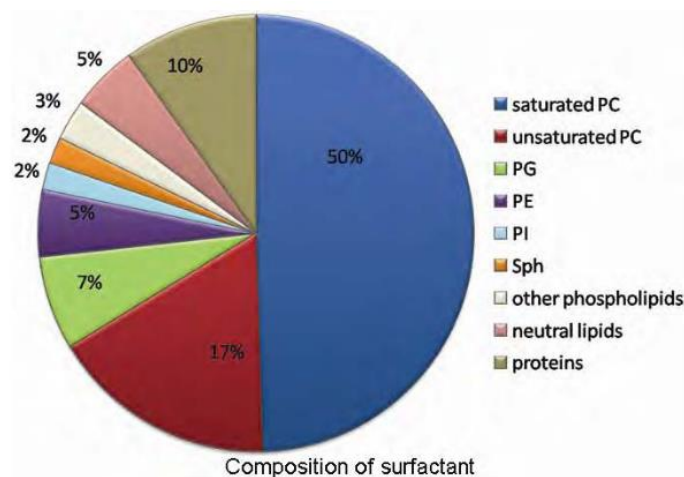


Figure 3. Composition of lung surfactant[12]

SP- B is an 18 kDa hydrophobic peptide composed of 79 amino acid expressed in Clara cells and alveolar type II cells. It has several functions in lung surfactant system, the most important one is its ability in enhancing the rate of adsorption and surface spreading of the phospholipids. SP-B interacts primarily with the head group region of the lipid bilayer. The positively charged amino acid residues of SP-B interact at the surface of surfactant lipids, together with SP-C, forming stable monolayers and bilayers that reduce surface tension and enhance the stability and spreading of the lipid film. It also plays a role in the packaging of surfactant phospholipids into lamellar bodies and contributes to recycling of surfactant from the alveolar space, enhancing the uptake of phospholipids by type II epithelial cells[13].

SP-C consists of a 35-amino-acid polypeptide has an important role in the surfactant system, and most of its properties are strictly linked to its extreme hydrophobicity. SP-C, inserted in the PL film, disrupts lipid packing promoting lipids movements between sheets of membranes[13]. Surfactant protein C also enhances the reuptake of surfactant phospholipids *in vitro* and may have a role in surfactant catabolism[14].

SP-A and SP-D are large glycosylated proteins belonging to collectin family, characterized by the presence of collagen like domain and carbohydrate binding properties. Thanks to a carbohydrate recognition domain, SP-A recognizes oligosaccharide moieties on various lung pathogens, thus opsonizes microorganisms, enhances their uptake by phagocytes, and stimulates the production of free oxygen radicals. SP-A also inhibits directly the proliferation of Gram-negative bacteria by increasing the permeability of the microbial cell membrane[15]. Beside its role in the innate defense of the lung, SP-A is important for the formation of tubular myelin, a structure formed by surfactant as soon as it is secreted from type II cells and thought to be the structure from which the surface film forms *in vivo*[16].

SP-D has a molecular weight of 43 kDa and shows structural similarities with SP-A but participates only to the host defense response agglutinating carbohydrates and participate to surfactant metabolism.

The interaction between lipids and proteins is important for the surface-active properties and homeostasis of the surfactant.

1.3 Surfactant Replacement Therapy

Since 1990 surfactant replacement has been recognized as an effective and safe therapy for immaturity-related surfactant deficiency. It has been reported that surfactant administration in preterm infants with established RDS reduces mortality, decreases the incidence of pneumothorax, pulmonary interstitial emphysema, and grade 3 or 4 intraventricular hemorrhage, and lowers the risk of chronic lung disease or death at 28 days of age[17–19]. Surfactant replacement has been used both as prophylactic and as a selective therapy. The prophylactic administration within 30 min after birth to infants who are at high risk for RDS ensures a normal surfactant pool and improve lung mechanics, thus reducing the need for mechanical ventilation[20], but on the other hand exposes infants to possibly unnecessary intubation and drug administration. Selective surfactant administration addresses the therapy only to those infants who really need it, but the administration is delayed allowing for lung inflammation and impaired gas exchange until the therapy is provided[17].

Exogenous surfactant preparations differ in both phospholipid and protein content and can be categorized as synthetic surfactants and animal derived surfactant extracts. Animal derived surfactant are derived from biologic sources including cows (bovactant, Boehringer Ingleheim, Bilberach, Germany; calfactant, ONY, Inc, Amherst, NY; beractant, Abbott Laboratories; Abbott Park, IL) and pigs (poractant alfa, Chiesi Farmaceutici SpA, Parma, Italy) and are obtained from bronchoalveolar lavage fluid or minced lung. Animal derived surfactants contain surfactant proteins SP-B and SP-C, that are thought to be crucial in promoting the adsorption and spread of monolayers of DPPC. However, foreign proteins in natural surfactant did not show significant allergic responses in treated infants[17]. They can also be supplemented with phospholipids or other surface active material while unmodified animal derived surfactant extract contains only the components remaining after the extraction process. Synthetic surfactants differ from natural surfactants mostly in their protein composition, can be protein free or contain peptides that are thought to mimic proteins found in pulmonary surfactant[21].

Currently the most common strategy for management of RDS is non-invasive ventilation with nasal continuous positive airway pressure (nCPAP) and when surfactant administration is required, the delivery involves endotracheal intubation and short-duration mechanical ventilation (InSurE, Intubation Surfactant Extubation). However, the lungs of premature infants are particularly susceptible to ventilator-induced lung injury because of their immaturity, the need for sedative medication, secondary effects such as bradycardia or hypotension, and difficulty in extubation. To prevent the intubation, new administration techniques have been described. Among these, less invasive surfactant administration (LISA) requires a thin catheter for intratracheal surfactant delivery in spontaneously breathing preterm infants on nCPAP[22]. Other

alternative procedures include pharyngeal deposition[23], application via laryngeal mask[24], and application of nebulized surfactant[25, 26].

InSurE still remains the most widely applied technique. Although beneficial in clinical practice, the InSurE method cannot be universally applied to all preterm neonates with RDS and is unsuccessful in a particular section of this population. The InSurE failure rate ranges from 9% to 50%[27, 28] with body weight <750 g, pO₂/FiO₂ <218, and a/ApO₂ <0.44 at the first blood gas analysis being independent risk factors for failure in infants with gestational age <30 weeks[29].

The estimation of the amount of the administered drug successfully delivered to the lungs represents a crucial point for the assessment of the efficiency of the procedure used. To this aim, during my PhD we developed a new non-invasive method to calculate *in vivo* the ratio between the exogenous and endogenous surfactant in an animal model of RDS by stable isotopes and isotopic ratio mass spectrometry. This led to the publication of two articles in peer-reviewed journals[30, 31]. Next chapter will deal with the stable isotope approach used and will report the two published articles.

Bibliography

1. Beck S, Wojdyla D, Say L, Betran AP, Merialdi M, Requejo JH, Rubens C, Menon R, Van Look PFA. The worldwide incidence of preterm birth: a systematic review of maternal mortality and morbidity. *Bull World Health Organ.* 2010; 88:31–8.
2. Crystal RG, West JB, Ronald Crystal BG. *The Lung: Scientific foundations.* Raven Press
3. Jobe AH. Why surfactant works for Respiratory Distress Syndrome. *Neoreviews.* 2006; 7:e95–e106.
4. Warren JB, Anderson JM. Core concepts: Respiratory Distress Syndrome. *Neoreviews.* 2009; 10:e351–e361.
5. Fraser J, Walls M, McGuire W. ABC of preterm birth: Respiratory complications of preterm birth. *Bmj.* 2005; 331:0507278.
6. Hussain M, Xu C, Lu M, Wu X, Tang L, Wu X. Wnt/ β -catenin signaling links embryonic lung development and asthmatic airway remodeling. *Biochim Biophys Acta - Mol Basis Dis.* 2017; 1863:3226–3242.
7. Berthiaume Y, Voisin G, Dagenais A. The alveolar type I cells: the new knight of the alveolus? *J Physiol.* 2006; 572:609–610.
8. Castranova V, Rabovsky J, Tucker JH, Miles PR. The alveolar type II epithelial cell: a multifunctional pneumocyte. *Toxicol Appl Pharmacol.* 1988; 93:472–83.
9. Bassett D, Fisher A, Rabinowitz J. Effect of hypoxia on incorporation of glucose carbons into lipids by isolated rat lung. *Am J Physiol Content.* 1974; 227:1103–1108.
10. Hawgood S, Clements JA. Pulmonary surfactant and its apoproteins. *J Clin.* 1990; 86:1–6.
11. Fessler MB, Summer RS. Surfactant lipids at the host-environment interface metabolic sensors, suppressors, and effectors of inflammatory lung disease. *Am J Respir Cell Mol Biol.* 2016; 54:624–635.
12. Akella A, Shripad &, Deshpande B. Pulmonary surfactants and their role in pathophysiology of lung disorders. *Indian J Exp Biol.* 2013; 51:5–22.
13. Whitsett JA, Weaver TE. Hydrophobic surfactant proteins in lung function and disease. 2002; 347:2141–2148.
14. Horowitz AD, Moussavian B, Whitsett JA. Roles of SP-A, SP-B, and SP-C in modulation of lipid uptake by pulmonary epithelial cells in vitro. *Am J Physiol.* 1996; 270:L69-79.

15. Wu H, Kuzmenko A, Wan S, Schaffer L, Weiss A, Fisher JH, Kim KS, McCormack FX. Surfactant proteins A and D inhibit the growth of Gram-negative bacteria by increasing membrane permeability. *J Clin Invest.* 2003; 111:1589–1602.
16. Pérez-Gil J. Structure of pulmonary surfactant membranes and films: The role of proteins and lipid–protein interactions. *Biochim Biophys Acta - Biomembr.* 2008; 1778:1676–1695.
17. Stevens TP, Sinkin RA. Surfactant replacement therapy. *Chest.* 2007; 131:1577–1582.
18. Seger N, Soll R. Animal derived surfactant extract for treatment of respiratory distress syndrome. *Cochrane Database Syst Rev.* 2009; 2:1–69.
19. Soll R, Blanco F. Natural surfactant extract versus synthetic surfactant for neonatal respiratory distress syndrome. *Cochrane Database Syst Rev.* 2001; 2:CD000144.
20. Rojas-Reyes MX, Morley CJ, Soll R. Prophylactic versus selective use of surfactant in preventing morbidity and mortality in preterm infants. *Cochrane Database Syst Rev.* 2012; 14:CD000510.
21. Pfister RH, Soll R, Wiswell TE. Protein-containing synthetic surfactant versus protein-free synthetic surfactant for the prevention and treatment of respiratory distress syndrome. *Cochrane Database Syst Rev.* 2009; 4:CD006180.
22. Kribs A, Roll C, Göpel W, Wieg C, Groneck P, Laux R, Teig N, Hoehn T, Böhm W, Welzing L, Vochem M, Hoppenz M, Bühner C, Mehler K, Stützer H, Franklin J, Stöhr A, Herting E, Roth B. Nonintubated surfactant application vs conventional therapy in extremely preterm infants: A randomized clinical trial. *JAMA Pediatr.* 2015; 169:723–730.
23. Kattwinkel J, Robinson M, Bloom BT, Delmore P, Ferguson JE. Technique for intrapartum administration of surfactant without requirement for an endotracheal tube. *J Perinatol.* 2004; 24:360–365.
24. Trevisanuto D, Grazzina N, Ferrarese P, Micaglio M, Verghese C, Zanardo V. Laryngeal mask airway used as a delivery conduit for the administration of surfactant to preterm infants with respiratory distress syndrome. *Biol Neonate.* 2005; 87:217–20.
25. Mazela J, Merritt TA, Finer NN. Aerosolized surfactants. *Curr Opin Pediatr.* 2007; 19:155–162.
26. Bianco F, Ricci F, Catozzi C, Murgia X, Schlun M, Bucholski A, Hetzer U, Bonelli S, Lombardini M, Pasini E, Nutini M, Pertile M, Minocchieri S, Simonato M, Rosa B, Pieraccini G, Moneti G, Lorenzini L, Catinella S, Villetti G, Civelli M, Pioselli B, Cogo P,

- Carnielli V, Dani C, Salomone F. From bench to bedside: in vitro and in vivo evaluation of a neonate-focused nebulized surfactant delivery strategy. *Respir Res.* 2019; 20:134.
27. Dani C, Corsini I, Bertini G, Pratesi S, Barp J, Rubaltelli FF. Effect of multiple INSURE procedures in extremely preterm infants. *J Matern Fetal Neonatal Med.* 2011; 24:1427–31.
 28. Reininger A, Khalak R, Kendig JW, Ryan RM, Stevens TP, Reubens L, D'Angio CT. Surfactant administration by transient intubation in infants 29 to 35 weeks' gestation with respiratory distress syndrome decreases the likelihood of later mechanical ventilation: a randomized controlled trial. *J Perinatol.* 2005; 25:703–708.
 29. Dani C, Corsini I, Poggi C. Risk factors for intubation-surfactant-extubation (INSURE) failure and multiple INSURE strategy in preterm infants. *Early Hum Dev.* 2012; 88:S3–S4.
 30. Giambelluca S, Ricci F, Simonato M, Correani A, Casiraghi C, Storti M, Cogo P, Salomone F, Carnielli VP. Estimating the contribution of surfactant replacement therapy to the alveolar pool: An in vivo study based on ¹³C natural abundance in rabbits. *J Mass Spectrom.* 2018; 53:560–564.
 31. Giambelluca S, Ricci F, Simonato M, Vedovelli L, Traldi U, Correani A, Casiraghi C, Storti M, Mersanne A, Cogo P, Salomone F, Carnielli VP. Tracing exogenous surfactant in vivo in rabbits by the natural variation of ¹³C. *Respir Res.* 2019; 20:1–7.

Chapter 2

CONTRIBUTION OF SURFACTANT REPLACEMENT THERAPY BY STABLE ISOTOPES

2.1 Stable isotopes

All atoms of one element have the same number of protons in their nucleus, but they may differ in the number of neutrons, giving each elemental isotope a different atomic mass. Isotopes with lower atomic mass are termed “light”, and isotopes with higher atomic mass are termed “heavy”. Due to the identical number of protons, they occupy the same (*isos*) position (*topos*) in the periodic table of elements. The stable isotopes have nuclei that do not decay to other isotopes on geologic timescales; radioactive (unstable) isotopes have nuclei that spontaneously decay over time to form other isotopes. The majority of chemical elements consists of a mixture of stable isotopes, which are not subjected to any radioactive disintegration. For example, carbon can have three main isotopes (figure 1): carbon-12 (^{12}C), with 6 protons and 6 neutrons, and carbon-13 (^{13}C) and -14 (^{14}C), with respectively 7 and 8 neutrons (Figure 1). ^{13}C is stable, while ^{14}C is not stable and decays at a known rate. ^{12}C represents about 98.9% of total carbon in nature, the remaining 1.1% is ^{13}C .

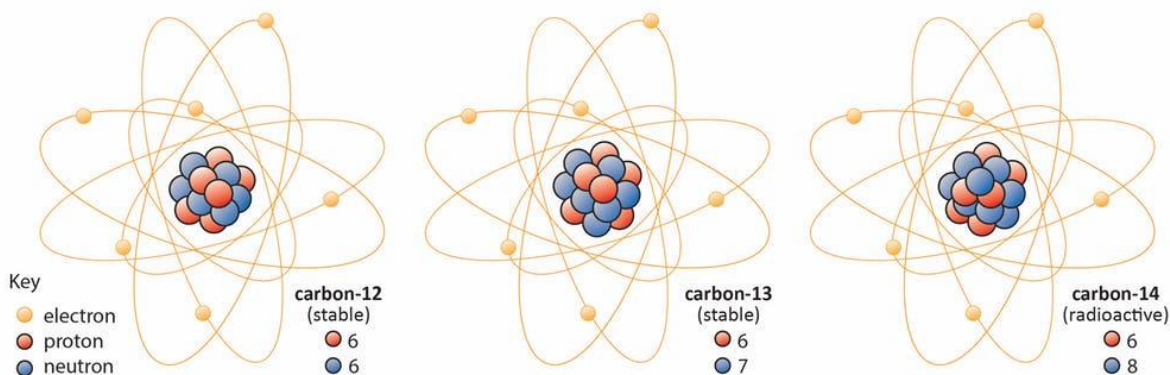


Figure 1. Isotopes of carbon

Stable isotopes are nearly chemically and functionally identical, but the difference in mass makes them analytically distinguishable from each other. In light of this, isotopes can be used in biological

science to discriminate or “trace” molecules. Molecules that differ by the number or arrangement of isotopically labelled position are referred to as “isotopomers”. Isotopic distribution of element derives from the origin and the evolution of component they derive from. Processes that impact on relative abundance of isotopes are known as “isotope fractionation” and can occur, for example during phase changes, or during specific biological processes. Thus, two components, with the same formula, can have different isotopic composition deriving from different origins and/or histories, due to natural fractionation processes. This principle, called stable isotope natural abundance approach, is used in several fields, as in example geology[1], archeology[2], forensic science[3] or human nutrition[4]. In human nutrition the natural abundance approach can be used for directly examining *in vivo* the fate of nutrients, and trace their uptake and elimination or to measure nutrient fluxes through specific pathways. In plants, carbon fractionation depends on the photosynthetic pathway used. Plants are in fact divided in C₃, C₄, and CAM (Crassulacean acid metabolism) each characterized by different speed of carbon fixation and a discrimination against ¹³C. C₃ plants use the Calvin-Benson photosynthetic pathway and they fix CO₂ by the action of ribulose phosphate carboxylase. Carboxylation step shows great fractionation leading to very low content of ¹³C in these plants. C₄ plants use the Hatch-Slack photosynthetic cycle, which does not show a strong fractionation effect. This results in different natural abundances of ¹³C in plants, with C₄ plants (e.g. corn or sugar cane) being more enriched in ¹³C than C₃ plants (e.g. tomato, potato, wheat, rice)[5]. CAM plants (e.g. pineapple and agave) have ¹³C values similar to C₄ plants. When animals consume plants, they incorporate carbon into their own tissues. Thus, in animals, ¹³C values typically reflect those of their diet[6], suggesting the use of stable isotopes as potential dietary biomarkers.

Besides the natural abundance approach, compounds that are artificially-labelled in one or several positions can be used.

In clinical diagnosis, stable isotopes are primarily employed for breath tests aiming at the evaluation of hepatic, gastric, small intestine and pancreatic functions, and for the diagnosis of *Helicobacter pylori* infection[7–9]. All these tests are based on ¹³C-urea breath test. *H. pylori* is able to survive in the stomach because it produces urease that cleavages urea locally lowering the pH value. After administration of a dose of ¹³C-urea, *H. pylori* produces ammonia and ¹³CO₂ that appears in the expired CO₂ of patients positive to the infection.

In pharmacology, studies using stable isotopes include pharmacokinetics and assessment of drug delivery systems[10]. These studies are based on the administration of a compound isotope-labelled, to the patient by single dose, multiple doses or constant infusion. These tracers can be instilled orally or intravenously, and modern analytical techniques allow the measurement of undifferentiated

molecules or after conversion into their metabolites. A large number of different isotopes are used for studies in humans, but most widely used are the stable isotopes of hydrogen, carbon, oxygen and nitrogen. Since the last two decades, our research group has been investigating on infant nutrition and pulmonary diseases by stable isotope tracers[11–15].

Administration of artificially labelled compound at low concentrations in humans has been proven to be risk-free, they can be used in paediatric research and during gestation since there is no exposition to radiation. Indeed, more stable isotopes can be administered simultaneously and in repeated doses allowing to study different biological aspects using the same sample. However, drugs and substances labelled with stable isotopes are produced by a limited number of companies and only those produced according to the Good Manufacturing Practice (GMP) regulations can be applied in human studies. Moreover, the production of other substances on request is very expensive[10].

Although previous pharmacological studies applying stable isotopes techniques were based solely on the use of artificially stable isotope labelled compounds, in the studies carried out during my PhD program, we explored the possibility of using the isotopes natural abundance approach applied to drug delivery.

2.2 Mass spectrometry

The most used analytical method for the measurement of isotopic differences is mass spectrometry, which separates and quantify ions on the basis of their mass-to-charge ratio (m/z). Any information gathered from a mass spectrometer comes from analysis of gas-phase ions[16]. To this aim, every mass spectrometer consists of three main components: an ionization source, a mass analyser and a detector. In the ionization source, analytes of interest are converted into gas-phase ions. The mass analyzer takes ionized masses and separates them based on m/z and outputs them to the detector where they are measured and later converted to a digital output.

2.2.1 Isotope ratio mass spectrometry (IRMS)

The measurement of isotopic differences at natural abundance can be carried out on spectrometers with lower sensitivity but higher precision and resolution than conventional mass spectrometers; the instrument utilized is an isotopic ratio mass spectrometer (IRMS). In a IRMS instrumentation there are two different systems for sample injection, the Dual Inlet (DI-IRMS) and Continuous Flow (CF-

IRMS). In the first case the sample is prepared for the analysis in off-line mode, transformed into gas before the injection. In CF technique, the sample is injected into a helium flow that, like a carrier, facilitate the introduction of the sample into the ion source. This system can be interfaced with preparative and/or separation techniques, such as elemental analyzer (EA), gas chromatography (GC) and more recently liquid chromatography (LC). The technique used to measure isotopic composition of organic samples is GC, that leads to separate samples previously derivatized in order to transform them in volatile phase (Figure 2).

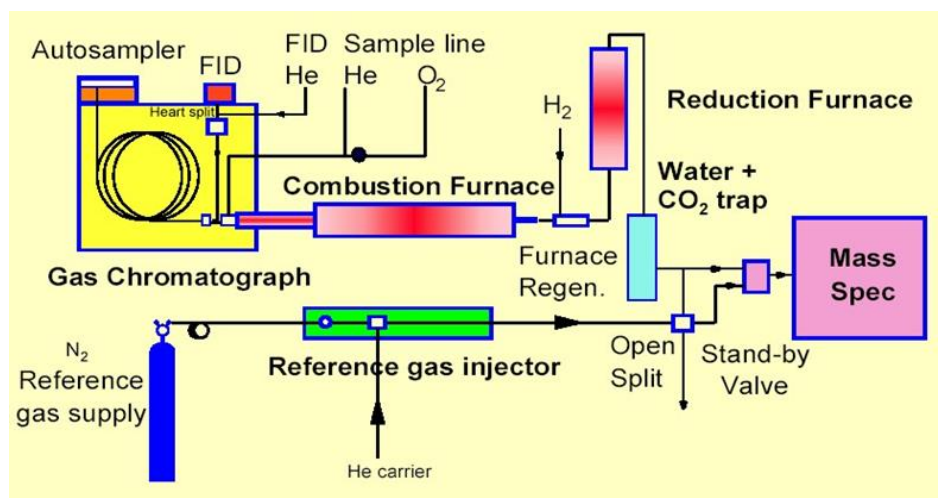


Figure 2. GC-C-IRMS scheme

One splitter at the end of the chromatographic column, leads to the sample to reach the combustion or pyrolysis tube, for nitrogen, carbon, hydrogen and oxygen analysis. For carbon analysis samples pass through oxidation tube made of ceramic and alumina containing a copper, platinum and nichel filaments[17]. The oxidation into the oven takes place for the reaction of copper with pure oxygen at 600-650°C to form CuO (copper oxide). Platinum then reacts as a catalyzer in the reaction between nichel and oxygen to form NiO (nickel oxide) at 960°C. The reduction oven removes the oxygen excess and reduces the eventually formed species of nitrogen oxide and nitrogen. After the sample combustion to CO₂ and H₂O, water is removed by a nafium trap. The final portion of interface is the open split that leads the helium flow to the magnetic analyzer (Figure 3).

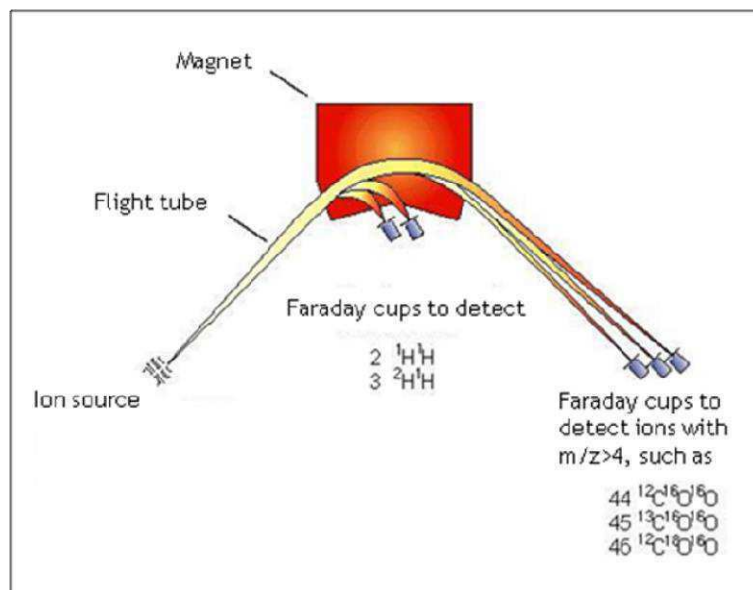


Figure 3. IRMS magnetic analyzer

Isotopic ratio can be calculated from simultaneous measurement of 44 m/z mass and 45 m/z mass, corresponding respectively to $^{12}\text{CO}_2$ and $^{13}\text{CO}_2$.

Isotopic ratios are usually expressed in term of δ (delta) that express the deviations, part per thousand, of a reference standard:

$$\delta X(\text{‰}) = \frac{R_{\text{sample}} - R_{\text{standard}}}{R_{\text{standard}}} * 1000$$

where R= heavy isotope mass/ light isotope mass ratio (i.e. $^{13}\text{C}/^{12}\text{C}$); $\delta X > 0$ when the heavy isotope is enriched versus standard in the sample; $\delta X < 0$ when the heavy isotope is impoverished or the light isotope is enriched versus standard in the sample. Reference standard are shown in Table 1.

Table 1. International standard references for the stable isotopes of hydrogen, carbon and oxygen.

Element	Stable isotopes	Natural mean abundance (%)	Standard ratio values	International standard reference
Hydrogen	1H 2H	99.985 0.015	$^2\text{H}/^1\text{H} = 0.000316$	VSMOW (Vienna Standard Mean Ocean Water)
Carbon	12C 13C	98.892 1.108	$^{13}\text{C}/^{12}\text{C} = 0.0112372$	PDB (Pee Dee Belemnite)
Oxygen	16O 18O	99.759 0.204	$^{18}\text{O}/^{16}\text{O} = 0.0039948$	VSMOW (Vienna Standard Mean Ocean Water)

For the PhD project, a GC Combustion (GC-Combustion III) coupled to a Delta V Advantage (Thermo Fisher Scientific, Waltham, MA, USA) isotopic ratio mass spectrometer was used.


Bibliography

1. Hoefs J. Stable isotope geochemistry, 6th ed. Springer
2. Sehrawat JS, Kaur J. Role of stable isotope analyses in reconstructing past life-histories and the provenancing human skeletal remains: a review. *Anthropol Rev.* 2017; 80:243–258.
3. Benson S, Lennard C, Maynard P, Roux C. Forensic applications of isotope ratio mass spectrometry - A review. *Forensic Sci Int.* 2006; 157:1–22.
4. O'Brien DM. Stable isotope ratios as biomarkers of diet for health research. *Annu Rev Nutr.* 2015; 35:565–594.
5. Bender MM. Mass spectrometric studies of carbon 13 variation in corn and other grasses. *Radiocarbon.* 1968; 10:468–472.
6. DeNiro MJ, Epstein S. Influence of diet on the distribution of carbon isotopes in animal. *Geochim Cosmochim Acta.* 1978; 42:495–506.
7. Hiele M, Ghos Y, Rutgeerts P, Vantrappen G. Starch digestion in normal subjects and patients with pancreatic disease, using a ^{13}C CO₂ breath test. *Gastroenterology.* 1989; 96:503–509.
8. Atherton JC, Spiller RC. The urea breath test for *Helicobacter pylori*. *Gut.* 1994; 35:723–725.
9. Koletzko S, Koletzko B, Haisch M, Hering P, Seeboth I, Hengels K, Braden B, Hering P. Isotope-selective non-dispersive infrared spectrometry for detection of *Helicobacter pylori* infection with ^{13}C -urea breath test. *Lancet.* 1995; 345:961–962.
10. Schellekens RCA, Stellaard F, Woerdenbag HJ, Frijlink HW, Kosterink JGW. Applications of stable isotopes in clinical pharmacology. *Br J Clin Pharmacol.* 2011; 72:879–897.
11. Cogo PE, Zimmermann LJI, Verlato G, Midrio P, Gucciardi A, Ori C, Carnielli VP. A dual stable isotope tracer method for the measurement of surfactant disaturated-phosphatidylcholine net synthesis in infants with congenital diaphragmatic hernia. *Pediatr Res.* 2004; 56:184–190.
12. Cogo PE, Toffolo GM, Ori C, Vianello A, Chierici M, Gucciardi A, Cobelli C, Baritussio A, Carnielli VP. Surfactant disaturated-phosphatidylcholine kinetics in acute respiratory distress syndrome by stable isotopes and a two compartment model. *Respir Res.* 2007; 8:13.

13. Cogo PE, Facco M, Simonato M, De Luca D, De Terlizi F, Rizzotti U, Verlato G, Bellagamba MP, Carnielli VP. Pharmacokinetics and clinical predictors of surfactant redosing in respiratory distress syndrome. *Intensive Care Med.* 2011; 37:510–517.
14. Cogo PE, Ori C, Simonato M, Verlato G, Isak I, Hamvas A, Carnielli VP. Metabolic precursors of surfactant disaturated-phosphatidylcholine in preterms with respiratory distress. *J Lipid Res.* 2009; 50:2324–31.
15. Cogo PE, Gucciardi A, Traldi U, Hilker AW, Verlato G, Carnielli V. Measurement of pulmonary surfactant disaturated-phosphatidylcholine synthesis in human infants using deuterium incorporation from body water. *J Mass Spectrom.* 2005; 40:876–881.
16. Glish GL, Vachet RW. The basics of mass spectrometry in the twenty-first century. *Nat Rev Drug Discov.* 2003; 2:140–150.
17. Merritt DA, Freeman KH, Ricci MP, Studley SA, Hayes JM. Performance and optimization of a combustion interface for isotope ratio monitoring gas chromatography/mass spectrometry. *Anal Chem.* 1995; 67:2461–2473.

RESEARCH ARTICLE

Estimating the contribution of surfactant replacement therapy to the alveolar pool: An *in vivo* study based on ^{13}C natural abundance in rabbits

Sonia Giambelluca¹  | Francesca Ricci² | Manuela Simonato³ | Alessio Correani⁴ | Costanza Casiraghi² | Matteo Storti² | Paola Cogo³ | Fabrizio Salomone² | Virgilio Paolo Carnielli⁴

¹Department of Women's and Children's Health, Padova University Hospital, Padova, Italy

²R&D Department, Chiesi Farmaceutici, Parma, Italy

³Division of Pediatrics, Department of Medicine, University of Udine, Udine, Italy

⁴Division of Neonatology, Department of Clinical Sciences, Polytechnic University of Marche and Azienda Ospedaliero-Universitaria Ospedali Riuniti, Ancona, Italy

Correspondence

Manuela Simonato, University of Udine, Department of Medicine, 33100 Udine, Italy.
Email: m.simonato@irpcds.org

Abstract

Variation of the isotopic abundance of selected nutrients and molecules has been used for pharmacological and kinetics studies under the premise that the administered molecule has a different isotopic enrichment from the isotopic background of the recipient subject. The aim of this study is to test the feasibility of assessing the contribution of exogenous surfactant phospholipids to the endogenous alveolar pool *in vivo* after exogenous surfactant replacement therapy in rabbits.

The study consisted in measuring the consistency of $^{13}\text{C}/^{12}\text{C}$ ratio of disaturated-phosphatidylcholine palmitate (DSPC-PA) in 7 lots of poractant alfa, produced over a year, and among bronchoalveolar lavages of 20 rabbits fed with a standard chow. A pilot study was performed in a rabbit model of lavage-induced surfactant deficiency: 7 control rabbits and 4 treated with exogenous surfactant. The contribution of exogenous surfactant to the alveolar pool was assessed after intra-tracheal administration of 200 mg/kg of poractant alfa. The ^{13}C content of DSPC-PA was measured by isotope ratio mass spectrometry.

The mean DSPC-PA $^{13}\text{C}/^{12}\text{C}$ ratio of the 7 lots of poractant alfa was -18.8‰ with a SD of 0.1‰ (range: -18.9‰ ; -18.6‰). The mean $^{13}\text{C}/^{12}\text{C}$ ratio of surfactant DSPC recovered from the lung lavage of 20 rabbits was $-28.8 \pm 1.2\text{‰}$ (range: -31.7‰ ; -25.7‰). The contribution of exogenous surfactant to the total alveolar surfactant could be calculated in the treated rabbits, and it ranged from 83.9% to 89.6%.

This pilot study describes a novel method to measure the contribution of the exogenous surfactant to the alveolar pool. This method is based on the natural variation of ^{13}C , and therefore it does not require the use of chemically synthesized tracers. This method could be useful in human research and especially in surfactant replacement studies in preterm infants.

KEYWORDS

^{13}C natural abundance, GC-C-IRMS, RDS, stable isotope, surfactant

1 | INTRODUCTION

The natural stable isotopes fingerprint approach has been used in the past in many different fields, ie, ecology, archaeology, and food and beverage industries.¹⁻³ This approach has been also applied to human nutritional studies involving dietary intake, because many commonly consumed traditional and market foods are isotopically distinct.⁴

In plants, carbon isotopic fractionation depends on the used photosynthetic pathway (C_3 or C_4), each characterized by different speed of CO_2 carbon fixation and a discrimination against ^{13}C . This results in different natural abundances of ^{13}C in plants, with C_4 plants (eg, corn or sugar cane) being more enriched in ^{13}C than C_3 plants (eg, tomato, potato, wheat, rice). In animals, ^{13}C values typically reflect those of their diet,⁵ suggesting the use of stable isotopes as potential dietary biomarkers.⁶ In the United States, livestock are predominately raised on corn, which gives to their meat a higher abundance of ^{13}C .⁴ The corresponding meat or meat products made in Europe have significantly lower ^{13}C abundance, because European diet is based on a higher consumption of C_3 plants.⁷

Studies describing the metabolic fate of nutrients based on the variation of ^{13}C content have been performed in the past by our group and by several other investigators.⁸⁻¹¹ In the present study, we explored the feasibility of using the isotopes natural abundance approach applied to drug delivery, in particular the delivery of poractant alfa (Curosurf®, Chiesi pharmaceuticals, Parma, Italy). This approach is based on a difference in stable isotopes content between an exogenous compound and the endogenous isotopic content of the recipient subject. The constancy of these 2 components through the study is mandatory.

We tested the suitability of our method by means of an *in vivo* model of respiratory distress syndrome (RDS),¹² a breathing disorder affecting a large portion (approximately 50%) of the smaller preterm newborns.¹³ RDS is characterised by lung immaturity and lack of lung surfactant, a thin layer of lipids and proteins with tension-lowering properties. The lipid portion of pulmonary surfactant is mainly composed of phospholipids (PL, 80%–85% by weight), with a predominant presence of disaturated-phosphatidylcholine (DSPC, approximately 50% of total PL).¹⁴ In RDS newborns, treatment with exogenous surfactant improves gas exchange and survival, and the InSurE (Intubation-Surfactant-Extubation) procedure has been widely used since has been shown to reduce both the need for mechanical ventilation and death.

Among commercial surfactants, poractant alfa is an extract of natural porcine lung surfactant obtained from pigs that are raised on a corn predominant diet. We postulated a marked difference between the carbon stable isotopes ratio of poractant alfa and the endogenous surfactant of animals raised on a C_3 predominant diet. If this were to be correct, our novel stable isotope natural abundance approach could allow to study *in vivo* the metabolism of exogenous DSPC without interfering with metabolic processes, and without the need of administering the expensive chemically synthesized stable isotope tracers. The possibility of monitoring the fate of the administered surfactant and calculating the amount of drug reaching the lungs could improve treatment dosing strategies and then the therapy success rate.

In this study, we tested the hypothesis of a constant isotopic abundance among different lots of the drug and among the animals included in the study and the hypothesis of a difference between the isotopic abundance of recipient animals and the administered drug.

2 | MATERIALS AND METHODS

2.1 | Extraction and isolation of DSPC from poractant alfa

A 200- μ L aliquot of 7 different lots of poractant alfa produced over a period of a year were provided by Chiesi pharmaceuticals (Parma, Italy). Poractant alfa aliquots were heated at 37°C in a water bath, then diluted 1:81 with NaCl 0.9%, processed and analysed in triplicate. Lipids were extracted by the method of Bligh and Dyer¹⁵ after addition of the internal standard, dipentadecanoyl phosphatidylcholine (PC-C15). Extracted lipids were oxidized with osmium tetroxide, resuspended in chloroform and spotted on silica gel G thin-layer plates (Merck, Darmstadt, Germany). The plates were developed with chloroform:methanol:isopropanol:0.25% KCl:trimethylamine (40:12:33:8:24). DSPC was visualized against a standard and scraped off from the silica gel plate. DSPC fatty acids were derivatized as methyl ester by adding 2-mL 3 M HCl methanol and heating at 100°C for 1 hour. Methyl esters were then extracted with hexane.

2.2 | Collection and analysis of rabbit bronchoalveolar lavages

The experimental procedure was approved by the intramural Animal Welfare Body and the Italian Ministry of Health (Prot.n° 1300-2015-PR) and complied with the European and Italian regulations for animal care. A total of 31 rabbits were studied: 20 rabbits for the feasibility study and 11 rabbits for the pilot study. Rabbits were 7 to 8 weeks old, with a body weight of 1.7 ± 0.3 kg. Water and diet were provided ad libitum. All rabbits underwent surfactant depletion procedure as previously described.¹² For each rabbit, the entire volume of all bronchoalveolar lavages (BALs) necessary for surfactant depletion were merged into a pool (BAL pool). After homogenization, a 10-mL aliquot of the BAL pool was immediately centrifuged at 100 \times g for 10 minutes in order to sediment cells and debris. Obtained supernatant was transferred in a new tube, aliquoted and stored at -80°C until analysis.

For the analysis, BALs were slowly thawed on ice, then homogenised by vortex for 10 seconds. Lipids were extracted, and DSPC fatty acids were derivatized as described for poractant alfa.

2.3 | Isotopic analysis of rabbit BAL

To evaluate the inter-individual variability of $^{13}C/^{12}C$ alveolar DSPC-PA, a feasibility study was performed in 20 rabbits with surfactant deficiency induced by BALs. For each rabbit, the BAL pool was collected and processed. BAL samples were preserved and processed as previously mentioned.

2.4 | Exogenous surfactant therapy

To test the modification of DSPC-PA ^{13}C abundance in rabbit lungs after surfactant administration, a pilot study was performed in 11 rabbits with surfactant deficiency induced by BALs. For each rabbit, the BAL pool was collected. After surfactant depletion: 4 rabbits received 200 mg/kg of poractant alfa using the InSurE technique; 7 rabbits served as a negative control group and did not receive exogenous surfactant. After 90 minutes, all rabbits underwent repeated depletion BALs again using 20 mL/kg of pre-warmed saline (37°C) until visual inspection showed transparent solution. An additional pool of all BALs made at the end of the experiment (BAL end experiment) was collected from both treated and control rabbits.

BAL samples were preserved and processed as previously mentioned.

2.5 | Stable isotopes analysis

In order to assess DSPC concentration, a prior quantitative analysis of DSPC was performed by a GC-FID (Agilent 5890).

DSPC-PA $^{13}\text{C}/^{12}\text{C}$ ratio was analysed by gas chromatograph coupled with isotope ratio mass spectrometer (GC-IRMS, Thermo Fisher Scientific Delta V Advantage).

For GC-IRMS analysis, the DSPC fatty acids separation was achieved on an Ultra-2 (25 m, 0.32 mm, 0.52- μm film thickness) column (Agilent J&W). Helium was used as carrier gas, and on-column injection was applied. The initial temperature gradient was 60°C, 1-minute hold; then increased to 195°C with a rate of 30°C/minute, 2-minute hold; finally, 30°C/min to 240°C, with a hold of 7 minutes.

Fatty acids were then combusted online at 960°C and introduced as CO_2 into the ion source. Finally, the $^{13}\text{C}/^{12}\text{C}$ ratio of the ionized CO_2 was measured.

Carbon isotopic analysis was performed in triplicate and normalized against Vienna Pee Dee Belemnite (V-PDB) standard. Results are expressed as $\delta\text{‰}$ (delta permil) of $^{13}\text{C}/^{12}\text{C}$, which indicate the difference, in part per thousand, from the standard:

$$\delta X(\text{‰}) = [(R_{\text{sample}} - R_{\text{standard}}) / R_{\text{standard}}] \times 1000$$

where "R" is the ratio of the heavy to light isotope in the sample or standard.

2.6 | Analytical error of GC-IRMS method

The linearity range of our GC-IRMS for methylated PA is 2 to 200 ng. The analytical error, expressed as standard deviation, for $^{13}\text{C}/^{12}\text{C}$ tested for alveolar DSPC-PA from rabbit BALs at DSPC concentrations within the instrumental linearity range was $\pm 0.2\text{‰}$ (with $\delta^{13}\text{C}$: -30.2‰).

The inter-assay repeatability was measured by injecting a certified standard solution of 3 alkanes (Alkane-Mix C14-C16 in Isooctane 15 ng/ μL , IVA Analysentechnik e. K., Meerbusch, Deutschland) at the beginning of each sequence. The inter-assay precision measured on 10 days for C15 alkane was $\pm 0.2\text{‰}$ (with $\delta^{13}\text{C}$: -28.0‰).

2.7 | Statistical analysis

A paired *t* test was performed to assess the difference between BAL pool and BAL end experiment in control group. Statistical analysis was performed with Prism 5 software (GraphPad Prism 5, San Diego, CA, USA). A *P*-value < 0.05 was considered significant.

Data are presented as mean \pm SD and min-max range.

3 | RESULTS

3.1 | Isotopic analysis of poractant alfa

DSPC-PA $^{13}\text{C}/^{12}\text{C}$ ratio was measured in 7 batches of poractant alfa to test the constancy of carbon stable isotope abundance. The mean value was $-18.8 \pm 0.1\text{‰}$ (-18.9‰ ; -18.6‰).

3.2 | Isotopic analysis of rabbit BALs

BALs from 20 adult rabbits were studied to assess the inter-individual variability of $^{13}\text{C}/^{12}\text{C}$ alveolar DSPC-PA. The mean value obtained was $-28.8 \pm 1.2\text{‰}$ (-31.7‰ ; -25.7‰).

3.3 | Exogenous surfactant therapy

BAL pool and BAL end experiment from 7 negative control rabbits and 4 rabbits treated with poractant alfa were analysed for DSPC-PA $^{13}\text{C}/^{12}\text{C}$ ratio to verify the contribution of exogenous surfactant to the alveolar pool. No significant difference was found between DSPC-PA $^{13}\text{C}/^{12}\text{C}$ ratio in BAL pool (mean \pm SD: $-29.0 \pm -0.6\text{‰}$) and BAL end experiment (mean \pm SD: $-28.9 \pm -0.6\text{‰}$) for control rabbits (*P* = 0.884).

Results for treated rabbits are resumed in Figure 1. The InSurE administration of 200 mg/kg of exogenous surfactant causes a mean variation of $-8.0 \pm 0.3\text{‰}$ (-7.6‰ , -8.2‰) of DSPC-PA ^{13}C abundance in rabbit alveolar pool. Based on mean poractant alfa DSPC-PA $^{13}\text{C}/^{12}\text{C}$ ratio of -18.8‰ , the percentages of exogenous

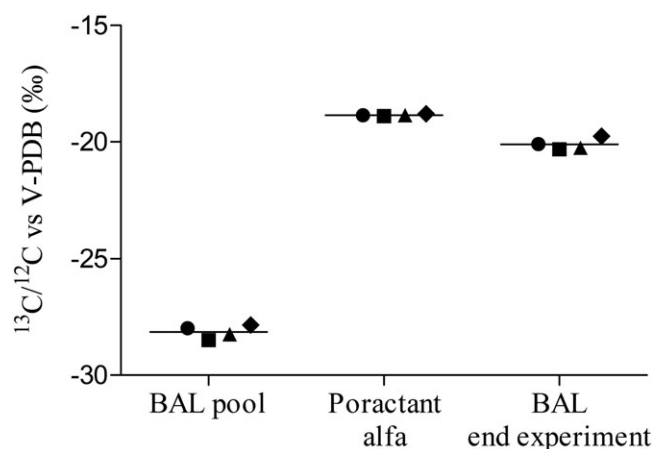


FIGURE 1 DSPC-PA $\delta^{13}\text{C}/^{12}\text{C}$ (‰) in poractant alfa and in rabbit BAL fluids before and after 200 mg/kg poractant alfa administration. Data presented as mean of triplicate injections; different symbols correspond to different rabbits. BAL pool: pool of all BALs collected before poractant alfa administration; BAL end experiment: pool of all BALs collected after poractant alfa administration

surfactant calculated for the 4 rabbits were: 83.9%, 89.6%, 84.4%, and 86.3%.

4 | DISCUSSION

The aim of this work was to describe the feasibility of measuring the contribution of the exogenous surfactant to the intrapulmonary endogenous pool. We demonstrate that, under the premise that exogenous surfactant is isotopically different from the endogenous counterpart, this is doable.

In this study, we designed a new method based on stable isotope natural abundance using gas chromatography coupled to isotope ratio mass spectrometry. To this purpose, we verified the suitability of our method in lung-lavaged adult rabbits by assessing the constancy of poractant alfa $^{13}\text{C}/^{12}\text{C}$ among different batches, the inter-individual variability of alveolar DSPC-PA ^{13}C natural abundance in rabbits, the difference in carbon stable isotopes abundance between endogenous and exogenous surfactant, and the effect of poractant alfa administration on rabbit alveolar DSPC-PA ^{13}C content.

According to studies reporting the influence of diet stable isotopes composition on that of animal tissues,⁵ the isotopic analysis of DSPC-PA of poractant alfa extracted from lungs of pigs fed on a C_4 diet showed a high $^{13}\text{C}/^{12}\text{C}$ ratio. Moreover, this ratio is constant among different batches, reflecting the standardization of animal breeding and raising system used. On the other hand, the carbon isotopic analysis of DSPC-PA in rabbits showed the typical $\delta^{13}\text{C}$ bulk of C_3 plants (-34% to -22% ¹⁶) and confirmed a significant lower ^{13}C abundance than poractant alfa, with a mean difference of 10.0%.

Our precision (expressed as standard deviation) for GC-IRMS analysis of BAL processed in single and injected in triplicate is $\pm 0.2\%$, and no significant effect of DSPC concentration on $^{13}\text{C}/^{12}\text{C}$ ratio (vs V-PDB) of alveolar DSPC-PA was found. Under these conditions, the difference in DSPC-PA ^{13}C natural abundance between poractant alfa and rabbits alveolar pool is wide enough to distinguish the endogenous compound from the exogenous one. Considering a mean difference of 10% and an error of 0.2%, the endogenous/exogenous (and vice versa) ratio we are able to discriminate is 1/49 (2%). In the clinical practise, this ratio could allow to detect even a small quantity of administrated surfactant, in order to potentially assess the efficacy of conventional and other newer surfactant delivery systems (LISA, aerosol).¹⁷

Our pilot study on 4 rabbits receiving poractant alfa showed a significant variation of alveolar DSPC-PA ^{13}C abundance after administration, which could be exploited to measure the percentage of exogenous and endogenous surfactant. In fact, it is well known that surfactant administration stimulates endogenous surfactant synthesis.¹⁸ Exogenous surfactant rapidly spreads throughout airways and airspaces. Immediately after administration, the amount of exogenous surfactant in lavage fluid decreases, and during the first 3 hours, most of it become associated to lung parenchyma.¹⁹ However, the epithelial uptake of surfactant is balanced by surfactant secretion into the epithelial lining fluid.²⁰ Then, the $^{13}\text{C}/^{12}\text{C}$ ratio found in treated rabbits, 90 minutes after treatment administration, represents the contribution of both lung, new synthesized and secreted DSPC and poractant alfa

^{13}C content (the latter providing for approximately the 86% of measured DSPC). In control rabbits, no significant difference in DSPC-PA ^{13}C was found 90 minutes after depletion, corroborating the hypothesis that the re-secreted DSPC from lung has the same ^{13}C content of DSPC recovered in the alveolar spaces at the beginning of the experiment.

Surfactant has been historically studied with radioactive isotopes in cell cultures and in animals.²¹⁻²³ More recently, administration of ^{13}C -labelled endogenous substances, such as carbohydrates and lipids, has been widely applied in biochemical studies and also for surfactant kinetics.²⁴

Application of stable isotope technology in humans has proved to be risk-free. However, drugs and substances labelled with stable isotopes are produced by a limited number of companies and only those produced according to the Good Manufacturing Practice regulations for active pharmaceutical ingredients can be applied in human studies. Actually, only few substances are available in the Good Manufacturing Practice grade (ie, ^{13}C -urea and ^{13}C -octanoic acid), and the production of other substances on request is very expensive.²⁵ Our novel stable isotopes approach at ^{13}C natural abundance overcomes the problem of administering any artificially labelled tracer because it is based on a different isotopic background. Thus, poractant alfa behaves as a naturally and uniformly labelled tracer. We foresee that surfactant kinetic studies will be at reach in any infant who receives the commercially available poractant alfa and in whom sampling from the airways will be possible through the endotracheal tube. Repeated sampling at different time points should give data on surfactant kinetics.

Nevertheless, we tested here an animal model raised on a controlled diet. The difference between endogenous and exogenous ^{13}C natural abundance could decrease when considering to apply this approach in infants fed with variable diets or with a more C_4 plants enriched diet. Further studies are necessary to assess the isotopic background and the feasibility of natural abundance approach in humans. Moreover, additional studies should address the isotopic content of other selected fatty acids as well. If this method will be proven to be reliable and thus suitable for clinical applications in human as well as in animal research, this could represent an advance for surfactant replacement therapy in the treatment of RDS, even in very low birth weight infants.

5 | CONCLUSION

Here, we report a novel method that allows for the contribution of the exogenous surfactant to the alveolar surfactant in treated rabbits by exploiting the difference in stable isotopes content at natural abundance. This method could serve in understanding treatment failures after surfactant administration and then increase therapy success rate.

CONFLICT OF INTEREST DECLARATION

F. Ricci, C. Casiraghi, M. Storti, and F. Salomone are Chiesi Farmaceutici employees. Chiesi Farmaceutici supplied its own products (Poractant Alfa) without limitations to the study. Apart of this, the authors declare no other conflict of interests.

ORCID

Sonia Giambelluca  <http://orcid.org/0000-0001-7425-7958>

REFERENCES

- Thompson DR, Bury SJ, Hobson KA, Wassenaar LI, Shannon JP. Stable isotopes in ecological studies. *Oecologia*. 2005;144(4):517-519.
- Schoeller DA. Isotope fractionation: why aren't we what we eat? *J Archaeol Sci*. 1999;26(6):667-673.
- van Leeuwen KA, Prenzler PD, Ryan D, Camin F. Gas chromatography-combustion-isotope ratio mass spectrometry for traceability and authenticity in foods and beverages. *Compr Rev Food Sci Food Saf*. 2014;13(5):814-837.
- Nash SH, Bersamin A, Kristal AR, et al. Stable nitrogen and carbon isotope ratios indicate traditional and market food intake in an indigenous circumpolar population. *J Nutr*. 2012;142(1):84-90.
- DeNiro MJ, Epstein S. Influence of diet on the distribution of carbon isotopes in animal. *Geochim Cosmochim Acta*. 1978;42(5):495-506.
- O'Brien DM. Stable isotope ratios as biomarkers of diet for health research. *Annu Rev Nutr*. 2015;35(1):565-594.
- Morrison DJ, Dodson B, Slater C, Preston T. ^{13}C natural abundance in the British diet: implications for ^{13}C breath tests. *Rapid Commun Mass Spectrom*. 2000;14(15):1321-1324.
- Demmelmair H, Kuhn A, Dokoupil K, Hegele V, Sauerwald T, Koletzko B. Human lactation: oxidation and maternal transfer of dietary ^{13}C -labelled α -linolenic acid into human milk. *Isotopes Environ Health Stud*. 2016;52(3):270-280.
- Larqué E, Pagán A, Prieto MT, et al. Placental fatty acid transfer: a key factor in fetal growth. *Ann Nutr Metab*. 2014;64(3-4):247-253.
- Carnielli VP, Sulkers EJ, Moretti C, et al. Conversion of octanoic acid into long-chain saturated fatty acids in premature infants fed a formula containing medium-chain triglycerides. *Metabolism*. 1994;43(10):1287-1292.
- Carnielli VP, Simonato M, Verlato G, et al. Synthesis of long-chain polyunsaturated fatty acids in preterm newborns fed formula with long-chain polyunsaturated fatty acids. *Am J Clin Nutr*. 2007;86(5):1323-1330.
- Ricci F, Catozzi C, Murgia X, et al. Physiological, biochemical, and biophysical characterization of the lung-lavaged spontaneously-breathing rabbit as a model for respiratory distress syndrome. *PLoS one*. 2017;12(1):e0169190.
- Walther FJ, Hernández-Juviel JM, Waring AJ. Aerosol delivery of synthetic lung surfactant. *PeerJ*. 2014;2:e403.
- Vedovelli L, Baritussio A, Carnielli VP, Simonato M, Giusti P, Cogo PE. Simultaneous measurement of phosphatidylglycerol and disaturated-phosphatidylcholine palmitate kinetics from alveolar surfactant. Study in infants with stable isotope tracer, coupled with isotope ratio mass spectrometry. *J Mass Spectrom*. 2011;46(10):986-992.
- Bligh EG, Dyer WJ. Rapid method of total lipid extraction and purification. *Can J Biochem Physiol*. 1959;37(1):911-917.
- Spangenberg JE. Bulk C, H, O, and fatty acid C stable isotope analyses for purity assessment of vegetable oils from the southern and northern hemispheres. *Rapid Commun Mass Spectrom*. 2016;30(23):2447-2461.
- More K, Sakhuja P, Shah PS. Minimally invasive surfactant administration in preterm infants. *JAMA Pediatr*. 2014;168(10):901-908.
- Bunt JE, Carnielli VP, Janssen DJ, et al. Treatment with exogenous surfactant stimulates endogenous surfactant synthesis in premature infants with respiratory distress syndrome. *Crit Care Med*. 2000;28(10):3383-3388.
- Alberti A, Pettenazzo A, Enzi GB, et al. Uptake and degradation of Curosurf after tracheal administration to newborn and adult rabbits. *Eur Respir J*. 1998;12(2):294-300.
- Jobe A. Metabolism of endogenous surfactant and exogenous surfactants for replacement therapy. *Semin Perinatol*. 1988;12:231.
- Jobe A. The labeling and biological half-life of phosphatidylcholine in subcellular fractions of rabbit lung. *Biochim Biophys Acta (BBA)/Lipids Lipid Metab*. 1977;489(3):440-453.
- Jobe A, Gluck L. The labeling of lung phosphatidylcholine in premature rabbits. *Pediatr Res*. 1979;13(5):635-640.
- Jacobs HC, Ikegami M, Jobe AH, Berry DD. Reutilization of surfactant phosphatidylcholine in adult rabbits. *Biochim Biophys Acta*. 1985;837(1):77-84.
- Torresin M, Zimmermann LJI, Cogo PE, et al. Exogenous surfactant kinetics in infant respiratory distress syndrome: a novel method with stable isotopes. *Am J Respir Crit Care Med*. 2000;161(5):1584-1589.
- Schellekens RCA, Stellaard F, Woerdenbag HJ, Frijlink HW, Kosterink JGW. Applications of stable isotopes in clinical pharmacology. *Br J Clin Pharmacol*. 2011;72(6):879-897.


How to cite this article: Giambelluca S, Ricci F, Simonato M, et al. Estimating the contribution of surfactant replacement therapy to the alveolar pool: An *in vivo* study based on ^{13}C natural abundance in rabbits. *J Mass Spectrom*. 2018;53:560-564. <https://doi.org/10.1002/jms.4088>

RESEARCH

Open Access



Tracing exogenous surfactant in vivo in rabbits by the natural variation of ^{13}C

Sonia Giambelluca^{1,2}, Francesca Ricci³, Manuela Simonato^{2,4*} , Luca Vedovelli², Umberto Traldi⁵, Alessio Correani⁶, Costanza Casiraghi³, Matteo Storti³, Arianna Mersanne³, Paola Cogo⁷, Fabrizio Salomone³ and Virgilio P. Carnielli⁶

Abstract

Background: Respiratory Distress Syndrome (RDS) is a prematurity-related breathing disorder caused by a quantitative deficiency of pulmonary surfactant. Surfactant replacement therapy is effective for RDS newborns, although treatment failure has been reported. The aim of this study is to trace exogenous surfactant by ^{13}C variation and estimate the amount reaching the lungs at different doses of the drug.

Methods: Forty-four surfactant-depleted rabbits were obtained by serial bronchoalveolar lavages (BALs), that were merged into a pool (BAL pool) for each animal. Rabbits were in nasal continuous positive airway pressure and treated with 0, 25, 50, 100 or 200 mg/kg of poractant alfa by InSurE. After 90 min, rabbits were depleted again and a new pool (BAL end experiment) was collected. Disaturated-phosphatidylcholine (DSPC) was measured by gas chromatography. DSPC-Palmitic acid (PA) $^{13}\text{C}/^{12}\text{C}$ was analyzed by isotope ratio mass spectrometry. One-way non-parametric ANOVA and post-hoc Dunn's multiple comparison were used to assess differences among experimental groups.

Results: Based on DSPC-PA $^{13}\text{C}/^{12}\text{C}$ in BAL pool and BAL end experiment, the estimated amount of exogenous surfactant ranged from 61 to 87% in dose-dependent way ($p < 0.0001$) in animals treated with 25 up to 200 mg/kg. Surfactant administration stimulated endogenous surfactant secretion. The percentage of drug recovered from lungs did not depend on the administered dose and accounted for 31% [24–40] of dose.

Conclusions: We reported a risk-free method to trace exogenous surfactant in vivo. It could be a valuable tool for assessing, alongside the physiological response, the delivery efficiency of surfactant administration techniques.

Keywords: Respiratory distress syndrome, Lung surfactant, Surfactant replacement therapy, ^{13}C natural abundance, Stable isotope

Background

RDS is a respiratory disorder that mostly affects preterm infants and it is characterised by lung immaturity and critically low amounts of pulmonary surfactant [1, 2]. To overcome pulmonary surfactant deficiency, exogenous surfactant replacement therapy represents a crucial achievement in the care of the preterm newborn [3], reducing death and pneumothorax [4]. There are several modalities to administer exogenous surfactant, including InSurE (*Intubation-Surfactant-Extubation*) [5], aerosolization [6], laryngeal mask [7], and intratracheal catheters

[8]. Among these, InSurE procedure has been widely used since it has been shown to improve gas exchange and survival, and to reduce the duration of mechanical ventilation. However, treatment failure after InSurE has been reported to be from 9 to 50% [9], with the need of repeating the treatment in some patients [10].

During clinical development of a therapy, definition of the dosage and dosage schedule is a key question, and it is the objective of the so-called dose-finding studies. [11] Although the performance of a therapy can be evaluated by different clinical parameters, monitoring the fate of a drug in vivo remains a main concern, since it usually entails the need for dispensing labelled compounds [12]. The possibility of estimating the amount of drug reaching the target organ could improve treatment dosing

* Correspondence: m.simonato@irpcds.org

²PCare Laboratory, Fondazione Istituto di Ricerca Pediatrica Città della Speranza, Corso Stati Uniti, 4F, Padova 35121, Italy

⁴Institute of Anesthesiology and Intensive Care, Department of Medicine – DIMED, University of Padova, Padova, Italy

Full list of author information is available at the end of the article



strategies, help in comparing different delivery systems, thus increasing the therapy success rate.

We recently developed a new method to estimate the contribution of exogenous surfactant to the alveolar pool in a rabbit model of RDS based on carbon stable isotope natural abundance of the disaturated-phosphatidylcholine palmitic acid (DSPC-PA) [13], the main phospholipid component of pulmonary surfactant. Briefly, we verified the suitability of our method in lung-lavaged adult rabbits by assessing the constancy of poractant alfa DSPC-PA carbon stable isotopes ratio among different batches, the difference in carbon stable isotopes abundance between endogenous and exogenous surfactant, and the effect of poractant alfa administration on rabbit alveolar DSPC-PA ^{13}C content. Our novel method allowed to discriminate an endogenous/exogenous (and vice versa) ratio of 1/49 (2%), without the need for dispensing any artificially labelled compound [14, 15]. This aspect makes the stable isotope natural abundance approach safe and exploitable to study in vivo different doses and surfactant administration methods.

In the present work, we further investigated the efficacy and the reliability of our method in lung-lavaged adult rabbits managed with a nasal continuous positive airway pressure [16] (nCPAP) and treated with increasing doses of poractant alfa in a dose-ranging study.

Materials and methods

Animals and sample collection

The experimental procedure was approved by the intramural Animal Welfare Body and the Italian Ministry of Health (Prot. n° 1300–2015-PR) and complied with the European and Italian regulations for animal care. A total of 44 adult rabbits were included in the study. Rabbits (male) were 7 to 8 weeks old, with a body weight of 1.9 ± 0.3 kg (min 1.2, max 2.8 Kg). Water and diet were provided ad libitum. The diet was the same for all animals (3409 Rabbit, maintenance and breeding - Kliba Nafag, Kaiseraugst, Switzerland) and was kept constant for at least six days before the studies.

All rabbits underwent a standardized surfactant depletion procedure, using 20 mL/kg of pre-warmed saline (37 °C) until visual inspection showed transparent lavage fluid, as previously described [16].

For each rabbit, the entire volume of all bronchoalveolar lavages (BALs) necessary for surfactant depletion was pooled (BAL pool). After surfactant depletion, rabbits were randomly assigned to 5 treatment groups and received different doses of poractant alfa using the InSurE technique according to a procedure previously described [16]: 0 mg/kg ($N = 11$); 25 mg/kg ($N = 6$); 50 mg/kg ($N = 11$); 100 mg/kg ($N = 8$); 200 mg/kg ($N = 8$).

The dose-range 50–200 mg/kg was previously used to assess the performances of poractant alfa [17] and synthetic surfactant CHF5633 [18].

Ninety minutes after exogenous surfactant administration, all rabbits underwent a second surfactant depletion with the same technique as described above. For each animal, all BALs performed at the end of the experiment were pooled (BAL end experiment).

After homogenization, a 10-mL aliquot of the BAL pool and of BAL end experiment was immediately centrifuged at $100\times g$ for 10 min in order to sediment cells and debris. The supernatant was transferred in a new tube, aliquoted and stored at -80 °C until analysis.

Aliquots of all the lots of poractant alfa used for the study were provided by Chiesi Farmaceutici (Parma, Italy) and kept at 4 °C until analysis.

Extraction and isolation of DSPC

BALs were slowly thawed on ice, then homogenised by vortex for 10 s. Lipids were extracted by the method of Bligh and Dyer [19] after addition of the internal standard, dipentadecanoyl phosphatidylcholine (PC-C15) 1 mg/mL. Extracted lipids were oxidized with osmium tetroxide, resuspended in chloroform and spotted on silica gel G thin-layer plates (Merck, Darmstadt, Germany). The plates were developed with chloroform:methanol:isopropanol:0.25% KCl:trimethylamine (40:12:33:8:24).

DSPC was visualized against a standard and scraped off from the silica gel plate. DSPC saturated fatty acids were derivatized as methyl ester by adding 2-mL 3 M HCl methanol and heating at 100 °C for 1 h. Methyl esters were then extracted with hexane.

Poractant alfa aliquots were heated at 37 °C in a water bath, then diluted 1:81 with NaCl 0.9%, processed and analysed in triplicate by following the same procedure used for BAL lipids extraction.

Stable isotopes analysis

In order to assess DSPC concentration, a prior quantitative analysis of DSPC was performed by Gas Chromatography - Flame Ionization Detector (GC-FID, HP 5890, Agilent Technologies, Santa Clara, CA, USA). DSPC-PA $^{13}\text{C}/^{12}\text{C}$ ratio was analysed by Gas chromatography - Combustion - Isotope Ratio Mass Spectrometry (GC-C-IRMS, Delta V Advantage, Thermo Fisher Scientific, Waltham, MA, USA).

For GC-C-IRMS analysis, the DSPC fatty acids separation was achieved on an Ultra-2 (25 m, 0.32 mm, 0.52- μm film thickness) column (Agilent). Helium was used as carrier gas, and on-column injection was applied. The initial temperature gradient was 60 °C, 1-min hold; then increased to 195 °C with a rate of 30 °C/minute, 2-min hold; finally, 30 °C/min to 240 °C, with a hold of 7 min.

Fatty acids were then combusted online at 960 °C and introduced as CO_2 into the ion source. Finally, the

$^{13}\text{C}/^{12}\text{C}$ ratio of the ionized CO_2 was measured by detecting mass 44/45.

Carbon isotopic analysis was performed in triplicate and normalized against Vienna Pee Dee Belemnite (V-PDB) standard. Results are expressed as $\delta\%$ (delta per-mil) of $^{13}\text{C}/^{12}\text{C}$, which indicate the difference, in part per thousand, from the standard:

$$\delta X (\%) = \frac{R_{\text{sample}} - R_{\text{standard}}}{R_{\text{standard}}} * 1000$$

where “R” is the ratio of the heavy to light isotope in the sample or standard.

Calculations

Data analysis was carried out with Microsoft Excel 2016 (Microsoft Corp). The contribution of exogenous surfactant to the alveolar pool was calculated as follows:

$$\text{BAL DSPC (mg/Kg)} = \frac{\text{DSPC (mg/ml)} * \text{BAL Volume (ml)}}{\text{Rabbit body weight (Kg)}}$$

$$\text{Dilution factor} = \frac{\text{PA } ^{13}\text{C}/^{12}\text{C of BAL end experiment} - \text{PA } ^{13}\text{C}/^{12}\text{C of BAL pool}}{\text{PA } ^{13}\text{C}/^{12}\text{C of administered DSPC} - \text{PA } ^{13}\text{C}/^{12}\text{C of BAL pool}}$$

$$\text{Exogenous DSPC (mg/Kg)} = \text{DSPC in BAL end experiment (mg/Kg)} * \text{dilution factor}$$

$$\text{Endogenous DSPC (mg/Kg)} = \text{Total DSPC in BAL end experiment} - \text{exogenous DSPC}$$

$$\% \text{ of administered in lungs} = \frac{\text{administered DSPC} * 100}{\text{Exogenous DSPC}}$$

Data for each lot of administered poractant alfa were used for the calculations relative to the receiving rabbits.

For rabbits receiving 0 mg/kg of poractant alfa the DSPC recovered in BAL end experiment was assumed to be 100% endogenous.

Statistical analysis

Wilcoxon signed rank test was performed to compare carbon stable isotopes ratio in BAL pool and BAL end experiment of control rabbits. One-way non-parametric ANOVA (Kruskal-Wallis) and post-hoc Dunn’s multiple

comparison were used to assess differences among experimental groups.

Kendall’s Tau-b (τ_b) coefficient of correlation was used to measure the degree of association between the dose administered and changes in DSPC amount and carbon stable isotopes content in treated rabbits.

Statistical analysis was performed using GraphPad Prism 5 (GraphPad Software Inc., San Diego, CA, USA) and SPSS 25 (IBM Corp, Armonk, NY, USA) software. A p -value < 0.05 was considered significant. Data are presented as median and interquartile range [IQR] or as mean \pm SD, according to data distribution.

Results

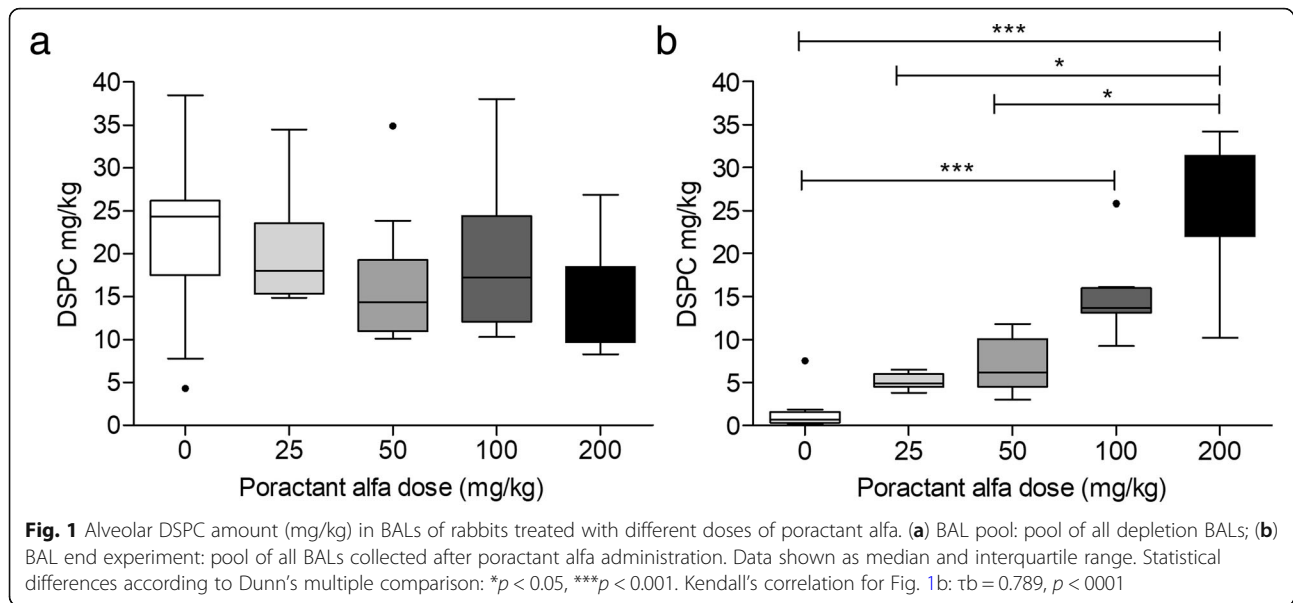
BAL pool and BAL end experiment from 44 rabbits treated with different doses of poractant alfa were analysed for DSPC content and DSPC-PA $^{13}\text{C}/^{12}\text{C}$ ratio to assess the contribution of exogenous surfactant to the alveolar pool. The alveolar DSPC content in BAL pool and BAL end experiment of rabbit experimental groups are shown in Fig. 1. No differences were found for BAL pool ($p = 0.177$), while the DSPC amount in BAL end experiment was significantly different ($p < 0.0001$) and positively correlated ($\tau_b 0.789$, $p < 0.0001$) with the dose administered.

The ^{13}C abundance of alveolar DSPC-PA was constant during the experiment for rabbits treated with 0 mg/kg of poractant alfa: BAL pool -29.1% [-29.5 , -28.8]; BAL end experiment -29.0% [-29.3 , -28.1] ($p = 0.41$). A positive correlation ($\tau_b 0.654$, $p < 0.0001$) was found between the differences in $^{13}\text{C}/^{12}\text{C}$ of DSPC-PA in BAL end experiment and BAL pool and the administered dose.

Comparison of the difference between DSPC-PA $^{13}\text{C}/^{12}\text{C}$ in BAL end experiment and BAL pool in rabbits treated with different doses of poractant alfa is shown in Fig. 2. All groups (50 mg/kg 6.9% [5.1 , 7.6]; 100 mg/kg 6.7% [6.0 , 8.4]; 200 mg/kg 8.2% [7.8 , 8.9]), except animals treated with a dose of 25 mg/kg (6.5% [5.4 , 6.7]), significantly differed from rabbits treated with 0 mg/kg (0.0% [-0.3 , 0.8]) ($p < 0.0001$).

Based on the differences on $^{13}\text{C}/^{12}\text{C}$ of alveolar DSPC-PA in BAL pool and BAL end experiment, the contribution of exogenous DSPC to the rabbit alveolar pool and the percentage of administered poractant alfa recovered from the lungs were calculated in all treated rabbits. The percentage of administered poractant alfa recovered from the lungs did not correlate with the administered dose ($p = 0.80$) and accounted for 38% [20, 43], 24% [14, 48], 29% [21, 22] and 35% [23, 40] of the dose with 25, 50, 100, and 200 mg/kg, respectively.

The mean ratio between endogenous and exogenous DSPC in the rabbit alveolar pool of the different experimental groups is shown in Fig. 3. The estimated amount



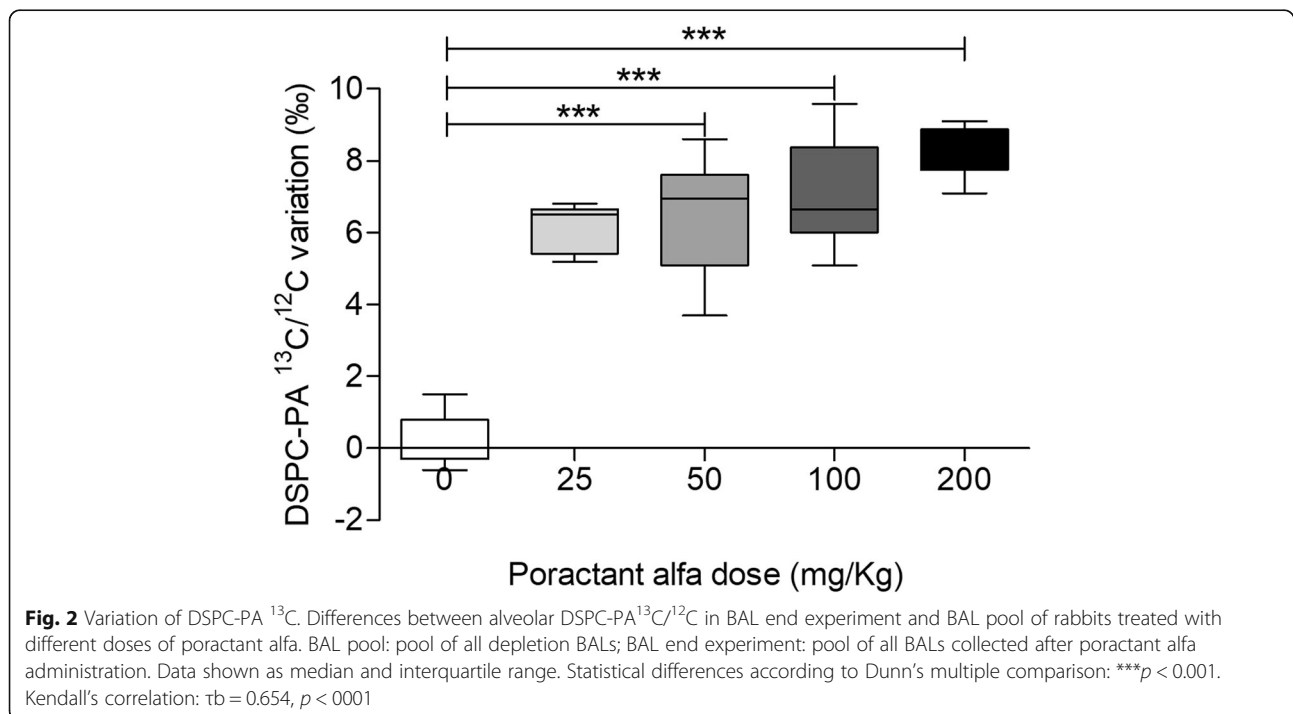
of exogenous surfactant in the alveolar pool increased in a dose-dependent way ($\tau_b 0.710$, $p < 0.0001$). A significantly higher amount was found for 200 mg/kg group (24.4 mg/kg [19.1, 26.7]) compared to rabbits treated with 25 mg/kg (3.0 mg/kg [2.5, 3.7], $p < 0.001$) and 50 mg/kg (4.1 mg/kg [2.7, 8.5], $p < 0.001$), and for 100 mg/kg group (9.4 mg/kg [8.9, 12.1]) compared to rabbits treated with 25 mg/kg ($p < 0.05$).

The estimated amount of endogenous surfactant secreted into the airways during 90 min after exogenous

surfactant administration was higher in rabbits treated with 100 mg/kg (4.0 mg/kg [2.2, 4.3]) and 200 mg/kg (3.8 mg/kg [2.7, 4.6]) than in rabbits receiving 0 mg/kg of poractant alfa (0.7 mg/kg [0.3, 1.6]) ($p < 0.01$).

Discussion

In the present study, we showed the feasibility of using the ^{13}C natural abundance approach to trace exogenous surfactant (poractant alfa) at progressively increasing doses in a rabbit model of RDS. To this purpose, we



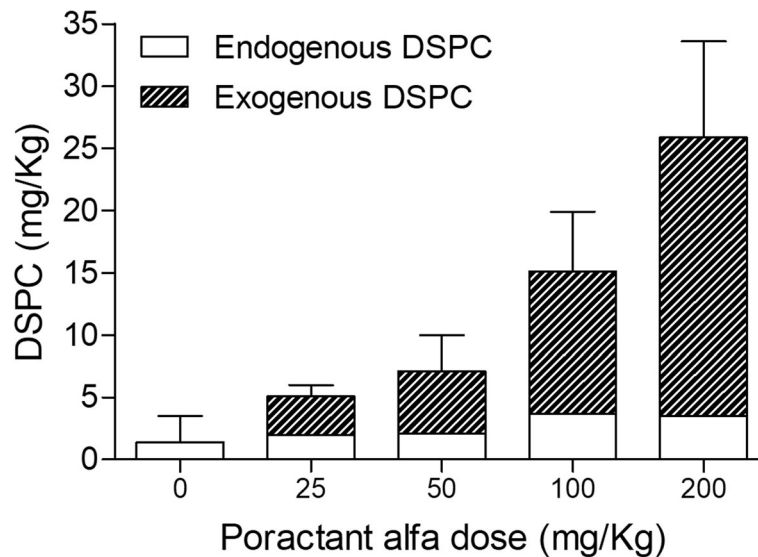


Fig. 3 Estimated contribution of exogenous surfactant. Ratio between exogenous and endogenous DSPC (mg/kg) in the alveolar pool of rabbits treated with different doses of poractant alfa by InSurE. Data shown as mean. Standard deviation bars refer to the total amount of DSPC. Kendall's correlation for the exogenous surfactant dose: $\tau_b = 0.710$, $p < 0.0001$

verified: the constancy of alveolar DSPC-PA $^{13}\text{C}/^{12}\text{C}$ during the experiment in a group of untreated rabbits (0 mg/kg dose); the correlation between the dose administered and changes in alveolar DSPC-PA $^{13}\text{C}/^{12}\text{C}$ before and after treatment with poractant alfa. Since these premises were satisfied in our model, we calculated the contribution of poractant alfa to the surfactant alveolar pool. Dose-dependent studies have been previously published for different animal-derived surfactants, including bovectant (Alveofact, Boehringer-Ingelheim, Ingelheim am Rhein, Germany) [20] and poractant alfa [17, 18]. However, those studies focused on the clinical effects of the administered dose and on the performance of the exogenous surfactant. Data about the amount of drug reaching the lungs are scarce. Here we investigated the possibility to estimate the percentage of surfactant delivered to the lung by InSurE procedure at increasing doses of the drug. The percentage of administered exogenous surfactant recovered from the BAL was only 31%. This is because an important fraction of the administered surfactant becomes inaccessible to lavage already at 1 min after administration [21]. Moreover, the percentage of recovery was independent from the dose instilled. This is a crucial result for allowing users to confidently apply this technique in different surfactant replacement studies where often different surfactant dosages need to be compared. There was a positive correlation between the administered dose and the differences in DSPC-PA $^{13}\text{C}/^{12}\text{C}$ before and after treatment. Based on the multiple comparison test used, significant difference in the variation of ^{13}C was not reached only for the comparison between rabbits receiving 0 and 25 mg/kg of

surfactant, because the reported p -value is adjusted for the number of rabbits (11 vs 6, respectively). These data, taken together, corroborate the power of our method, highlighting both a standardization of drug administration and BAL collection procedures on one side and the sensitiveness of the natural abundance approach to the dose administered on the other. Of interest, we used doses of poractant alfa which are much lower than the recommended dose of 200 mg/kg. We showed the suitability of our method to quantify “rather low” therapeutic doses allowing the premises to apply this approach also for animal studies on new less-invasive surfactant application (LISA) systems or for aerosolized or nebulized surfactant administrations, exploiting the present results as a calibration curve for the total delivered surfactant dose.

The combination of both quantitative data on DSPC amount and on carbon modification after treatment resulted in a clear picture of DSPC alveolar pool, which was a combination of both poractant alfa and new synthesized and/or secreted DSPC. The possibility to accurately estimate the ratio between the exogenous and the alveolar DSPC also allowed for the knowledge that a greater endogenous portion can be detected in rabbits who underwent therapy (at clinical dosages) compared to animals who did not receive the drug. The effect of the administration of exogenous surfactant on the synthesis and secretion of endogenous lung surfactant have been extensively studied, although the results are still controversial [22–24]. In vivo studies suggested an enhanced synthesis of endogenous surfactant PC both in rabbits [25, 26] and preterm infants [27], while no

noticeable effects on the endogenous synthesis have been described in mice treated with a therapeutic dose of both synthetic or natural exogenous surfactant [28]. In the present study, a clear dose-dependent tendency was observed for the comparison of the endogenous DSPC amount in the alveolar pool among the experimental groups, confirming a stimulation of endogenous DSPC secretion or synthesis after treatment, mainly when a therapeutic dose is administered. Of note, the present study was conducted in adult rabbits thus with mature lungs and, likely, with normal amounts of intracellular surfactant. Preterm infants with RDS have low amounts of both alveolar and lung tissue associated surfactant and in addition DSPC synthesis is much reduced. We speculate that endogenous surfactant synthesis/secretion is less likely to occur in preterm infants in the time frame of our animal studies. Pilot feasibility studies in preterm infants are ethically acceptable and they need to be done. Worth of note, in previous reports the contribution of newly synthesized surfactant has been estimated by the use of radio-labelled [24, 29] or stable isotope-labelled precursors of surfactant phospholipids [27, 28]. This is the first study in which the exogenous and endogenous surfactant can be distinguished in the alveolar pool without the need for administering any artificially labelled compound. This aspect supports a higher suitability of our method for research in human medicine, even for in vivo studies involving a vulnerable target population like preterm infants.

This approach is non-invasive and risk-free, but studies in infants carry some limitations. The first is that it requires patients to be intubated to allow for airways sampling. Sample collection is not possible in case of non-invasive surfactant administration techniques, however the need for reintubation after such techniques was reported to be as high as 75% [30]. Data on the contribution of exogenous surfactant to the total amount of surfactant from tracheal aspirates in case of reintubation after the first surfactant administration is of interest to clinicians and it may help in understanding the cause of the respiratory failure. Our method could help in distinguishing respiratory (surfactant related) from non-respiratory causes of CPAP failure, and could provide information on the endogenous or exogenous origin of the surfactant deficiency [31]. Our technique has theoretical limitations as well. One of these could be represented by the inter-individual variability of ^{13}C content. This approach is based on a different isotopic background between the drug and the biological pool. It is well known that in animal tissues ^{13}C values typically reflect those of diet [32]. Here we reported a study conducted on rabbits with a controlled diet. A restriction could be represented by the inconsistency of carbon stable isotope background moving from the animal model to infants fed

with variable diets. We have no data on the feasibility of our method in countries where the ^{13}C dietary abundance of the population is high as this will likely be the case of countries with high corn-based food consumption [33, 34]. Data collection about intra- and inter-individual variability of DSPC-PA $^{13}\text{C}/^{12}\text{C}$ in infants who needed intubation are under way.

Despite these limitations, if this method will be proven to be suitable for clinical applications in human research, this could represent a significant advancement in surfactant replacement therapy for the treatment of RDS, especially in extremely low birth weight infants.

Under the premises of an appreciable difference in stable isotope content between the exogenous compound and the biological counterpart, and of a constancy of drug stable isotope content in different lots, this method could also be extended to other drug therapies.

Conclusion

We demonstrated the reliability of carbon stable isotopes approach at natural abundance to trace in vivo the fate of surfactant replacement therapy. Since the administered drug behaves as a natural tracer, no other labelled compound is required. This approach could be a valuable tool for assessing, alongside the physiological response, the delivery efficiency of different less-invasive administration techniques in in vivo studies. However, the feasibility of this approach in infants deserves further investigations.

Abbreviations

BAL: Bronchoalveolar Lavage; DSPC: Disaturated-phosphatidylcholine; GC-C-IRMS: Gas Chromatography – Combustion – Isotope Ratio Mass Spectrometry; GC-FID: Gas Chromatography - Flame Ionization Detector; InSurE: Instillation Surfactant Extubation; IQR: Interquartile Range; LISA: Less Invasive Surfactant Administration; nCPAP: nasal Continuous Positive Airway Pressure; PA: Palmitic Acid; PC: Phosphatidylcholine; RDS: Respiratory Distress Syndrome; V-PDB: Vienna Pee Dee Belemnite

Acknowledgements

Not applicable.

Authors' contributions

GS performed the laboratory analysis, contributed to data interpretation and wrote the initial draft of the manuscript; FS, FR contributed to the experimental plan design and to manuscript drafting and revision; SM supervised laboratory analysis and gave a substantial contribution in the interpretation of data; VL performed data analysis and contributed to the data interpretation; CA contributed to the laboratory analysis; FR, CC, AM, MS carried out the in vivo experiments; FS, FR, CC contributed to the interpretation of the results; UT contributed to the method development; CVP and CP conceptualized and designed the study, made a substantial contribution to the interpretation of the data and revised the manuscript. All the authors read and approved the final manuscript as submitted, and agree to be accountable for all aspects of the work.

Funding

The study was performed with no specific financial support.

Availability of data and materials

The datasets used and/or analysed during the current study are available from the corresponding author on reasonable request.

Ethics approval and consent to participate

The experimental procedure was approved by the intramural Animal Welfare Body and the Italian Ministry of Health (Prot. n° 1300–2015-PR) and complied with the European and Italian regulations for animal care.

Consent for publication

Not applicable.

Competing interests

F. Ricci, C. Casiraghi, M. Storti, A. Mersanne and F. Salomone are Chiesi Farmaceutici employees. Chiesi Farmaceutici supplied its own products (poractant alfa) without limitations to the study. Apart of this, the authors declare that they have no competing interests.

Author details

¹Department of Women's and Children's Health, University of Padova, Padova, Italy. ²PCare Laboratory, Fondazione Istituto di Ricerca Pediatrica Città della Speranza, Corso Stati Uniti, 4F, Padova 35121, Italy. ³R&D Department, Chiesi Farmaceutici, Parma, Italy. ⁴Institute of Anesthesiology and Intensive Care, Department of Medicine – DIMED, University of Padova, Padova, Italy. ⁵Thermo Fisher Scientific Spa, Rodano, Milan, Italy. ⁶Division of Neonatology, Department of Clinical Sciences, Polytechnic University of Marche and Azienda Ospedaliero-Universitaria Ospedali Riuniti, Ancona, Italy. ⁷Department of Medicine, University of Udine, Udine, Italy.

Received: 3 May 2019 Accepted: 3 July 2019

Published online: 18 July 2019

References

1. Jobe AH. Why surfactant works for respiratory distress syndrome. *Neoreviews*. 2006;7:e95–e106.
2. Verlato G, Simonato M, Giambelluca S, Fantinato M, Correani A, Cavicchiolo ME, Priante E, Carnielli V, Cogo P. Surfactant components and tracheal aspirate inflammatory markers in preterm infants with respiratory distress syndrome. *J Pediatr*. 2018;203:442–6.
3. Halliday HL. Surfactants: past, present and future. *J Perinatol*. 2008;28:S47–56.
4. Seger N, Soll R. Animal derived surfactant extract for treatment of respiratory distress syndrome. *Cochrane Database Syst Rev*. 2009;2:1–69.
5. Verderer H, Robertson B, Greisen G, Ebbesen F, Albertsen P, Lundstrom K, Jacobsen T. Surfactant therapy and nasal continuous positive airway pressure for newborns with respiratory distress syndrome. *N Engl J Med*. 1994;331:1051–5.
6. Finer NN, Merritt TA, Bernstein G, Job L, Mazela J, Segal R. An open label, pilot study of Aerosurf® combined with nCPAP to prevent RDS in preterm neonates. *J Aerosol Med Pulm Drug Deliv*. 2010;23:303–9.
7. Trevisanuto D, Grazzina N, Ferrarese P, Micaglio M, Verghese C, Zanardo V. Laryngeal mask airway used as a delivery conduit for the administration of surfactant to preterm infants with respiratory distress syndrome. *Biol Neonate*. 2005;87:217–20.
8. Kribs A, Pillekamp F, Hünseler C, Vierzig A, Roth B. Early administration of surfactant in spontaneous breathing with nCPAP: feasibility and outcome in extremely premature infants (postmenstrual age ≤ 27 weeks). *Pediatr Anesth*. 2007;17:364–9.
9. Dani C, Corsini I, Poggi C. Risk factors for intubation-surfactant-extubation (INSURE) failure and multiple INSURE strategy in preterm infants. *Early Hum Dev*. 2012;88:53–4.
10. Dani C, Corsini I, Bertini G, Pratesi S, Barp J, Rubaltelli FF. Effect of multiple INSURE procedures in extremely preterm infants. *J Matern Fetal Neonatal Med*. 2011;24:1427–31.
11. Schmidt R. Dose-finding studies in clinical drug development. *Eur J Clin Pharmacol*. 1988;34:15–9.
12. Cogo PE, Facco M, Simonato M, Verlato G, Rondina C, Baritussio A, Toffolo GM, Carnielli VP. Dosing of porcine surfactant: effect on kinetics and gas exchange in respiratory distress syndrome. *Pediatrics*. 2009;124:e950–7.
13. Giambelluca S, Ricci F, Simonato M, Correani A, Casiraghi C, Storti M, Cogo P, Salomone F, Carnielli VP. Estimating the contribution of surfactant replacement therapy to the alveolar pool: an in vivo study based on ¹³C natural abundance in rabbits. *J Mass Spectrom*. 2018;53:560–4.
14. Cogo PE, Ori C, Simonato M, Verlato G, Isak I, Hamvas A, Carnielli VP. Metabolic precursors of surfactant disaturated-phosphatidylcholine in preterms with respiratory distress. *J Lipid Res*. 2009;50:2324–31.
15. Vedovelli L, Baritussio A, Carnielli VP, Simonato M, Giusti P, Cogo PE. Simultaneous measurement of phosphatidylglycerol and disaturated-phosphatidylcholine palmitate kinetics from alveolar surfactant. Study in infants with stable isotope tracer, coupled with isotope ratio mass spectrometry. *J Mass Spectrom*. 2011;46:986–92.
16. Ricci F, Catozzi C, Murgia X, Rosa B, Amidani D, Lorenzini L, Bianco F, Rivetti C, Catinella S, Villetti G, Civelli M, Pioselli B, Dani C, Salomone F. Physiological, biochemical, and biophysical characterization of the lung-lavaged spontaneously-breathing rabbit as a model for respiratory distress syndrome. *PLoS One*. 2017;12:1–19.
17. Bongrani S, Fornasier M, Papotti M, Razzetti R, Curstedt T, Robertson B. Dose-response study of surfactant replacement in immature newborn rabbits. *Prenat Neonatal Med*. 1999;4:71–8.
18. Ricci F, Murgia X, Razzetti R, Pelizzi N, Salomone F. In vitro and in vivo comparison between poractant alfa and the new generation synthetic surfactant CHF5633. *Pediatr Res*. 2017;81:369–75.
19. Bligh EG, Dyer WJ. Rapid method of total lipid extraction and purification. *Can J Biochem Physiol A*. 1959;37:911–7.
20. Gortner LN. High-dose versus low-dose bovine surfactant treatment in very premature infants. *Acta Paediatr*. 1994;83:135–41.
21. Baritussio A, Pettenazzo A, Benevento M, Alberti A, Gamba P. Surfactant protein C is recycled from the alveoli to the lamellar bodies. *Am J Phys*. 1992;263:L607–11.
22. Gilfillan AM, Chu AJ, Rooney SA. Stimulation of phosphatidylcholine synthesis by exogenous phosphatidylglycerol in primary cultures of type II pneumocytes. *Biochim Biophys Acta*. 1984;794:269–73.
23. Griese M, Dietrich P, Reinhardt D. Pharmacokinetics of bovine surfactant in neonatal respiratory distress syndrome. *Am J Respir Crit Care Med*. 1995;152:1050–4.
24. Miles PR, Wright JR, Bowman L, Castranova V. Incorporation of [³H] palmitate into disaturated phosphatidylcholines in alveolar type II cells isolated by centrifugal elutriation. *Biochim Biophys Acta*. 1983;753:107–18.
25. Bambang Oetomo S, Lewis J, Ikegami M, Jobe AH. Surfactant treatments alter endogenous surfactant metabolism in rabbit lungs. *J Appl Physiol*. 1990;68:1590–6.
26. Amato M, Petit K, Fiore HH, Doyle CA, Frantz ID, Nielsen HC. Effect of exogenous surfactant on the development of surfactant synthesis in premature rabbit lung. *Pediatr Res*. 2003;53:671–8.
27. Bunt JE, Carnielli VP, Janssen DJ, Wattimena JL, Hop WC, Sauer PJ, Zimmermann LJ. Treatment with exogenous surfactant stimulates endogenous surfactant synthesis in premature infants with respiratory distress syndrome. *Crit Care Med*. 2000;28:3383–8.
28. Madsen J, Panchal MH, Mackay R-MA, Echaide M, Koster G, Aquino G, Pelizzi N, Perez-Gil J, Salomone F, Clark HW, Postle AD. Metabolism of a synthetic compared with a natural therapeutic pulmonary surfactant in adult mice. *J Lipid Res*. 2018;59:1880–92.
29. Bourbon JR, Chailley-Heu B, Gautier B. The exogenous surfactant Curosurf enhances phosphatidylcholine content in isolated type II cells. *Eur Respir J*. 1997;10:914–9.
30. Kribs A, Roll C, Göpel W, Wieg C, Groneck P, Laux R, Teig N, Hoehn T, Böhm W, Welzing L, Vochem M, Hoppenz M, Bühner C, Mehler K, Stützer H, Franklin J, Stöhr A, Herting E, Roth B. Nonintubated surfactant application vs conventional therapy in extremely preterm infants: a randomized clinical trial. *JAMA Pediatr*. 2015;169:723–30.
31. Cogo PE, Facco M, Simonato M, De Luca D, De Terlizzi F, Rizzotti U, Verlato G, Bellagamba MP, Carnielli VP. Pharmacokinetics and clinical predictors of surfactant redosing in respiratory distress syndrome. *Intensive Care Med*. 2011;37:510–7.
32. DeNiro MJ, Epstein S. Influence of diet on the distribution of carbon isotopes in animal. *Geochim Cosmochim Acta*. 1978;42:495–506.
33. O'Brien DM. Stable isotope ratios as biomarkers of diet for Health Research. *Annu Rev Nutr*. 2015;35:565–94.
34. Nakamura K, Schoeller DA, Winkler FJ, Schmidt H-L. Geographical variations in the carbon isotope composition of the diet and hair in contemporary man. *Biol Mass Spectrom*. 1982;9:390–4.

Publisher's Note

Springer Nature remains neutral with regard to jurisdictional claims in published maps and institutional affiliations.

Chapter 3

EFFECT OF CHORIOAMNIONITIS ON RDS

3.1 Chorioamnionitis

The placenta is composed of three major structures: the placental disc, the chorioamniotic membranes, and the umbilical cord. Inflammatory lesions of the placenta are characterized by the infiltration of neutrophils in each of these structures. Specifically, when the inflammatory process affects the chorion and amnion, this is termed acute chorioamnionitis (CA).

The definition of CA varies between clinicians and across epidemiologic studies (Table 1), and this led to conflicting associations between CA and fetal outcomes. The most rigorous definition is inflammation of the chorionic and amniotic layers of the fetal membranes confirmed by pathologic review of the placenta[1]. The pathologic diagnosis requires the presence of a neutrophilic infiltrate in the placental tissues.

Table 1. Definitions of chorioamnionitis[2]

Definitions of chorioamnionitis	
Histologic CA	Pathologic diagnosis, inflammatory cells are present in the fetal membranes[3, 4]
Clinical CA	Typically maternal fever + at least 2 of: uterine tenderness, fetal or maternal tachycardia, maternal leukocytosis, foul smelling amniotic fluid[5]
Maternal inflammatory response	Inflammatory changes limited to the subchorion, chorion and amnion[6]
Fetal inflammatory response	Umbilical vasculitis, funisitis, elevated inflammatory markers in the cord blood[6]

CA is recognized as a primary cause of preterm delivery, being present in approximately 40–70% of women who deliver prematurely[7]. It results from ascending bacteria from the vagina and cervix, while an uncommon pathway of intrauterine infection is by bloodborne spread.

Most identified pathogens in the uterus that are associated with preterm labor are of vaginal origin. Examples of such pathogens are *Ureaplasma urealyticum*, *Chlamydia trachomatis*, *Neisseria gonorrhoea*, *Mycoplasma hominis*, Group B Streptococcus, and *Trichomonas vaginalis*. The fetal response will depend on the organisms and the duration of the exposure[8]. Vaginal organisms appear to ascend first into the choriodecidual space; in some women they then cross the intact chorioamniotic membranes into the amniotic fluid, and some of the fetuses ultimately become infected (Figure 1)[7]. Pathogenic colonization of the intrauterine space leads to placental inflammatory response, which is associated with preterm labor. The mechanisms through which intrauterine infection leads to preterm labor are the result of activation of the innate immune system. Bacteria release endotoxins and exotoxins, which are recognised by Toll-like receptors on the surface of leukocytes, and dendritic, epithelial, and trophoblast cells. The infectious insult triggers a cascade of events that leads to the release of numerous inflammatory mediators (cytokines, chemokines, prostaglandins, proteases, etc.). Inflammatory cytokines stimulate the production of prostaglandins and initiate neutrophil chemotaxis, infiltration, and activation, resulting in the synthesis and release of metalloproteases[9] resulting in uterine contractions and rupture of the membrane[10].

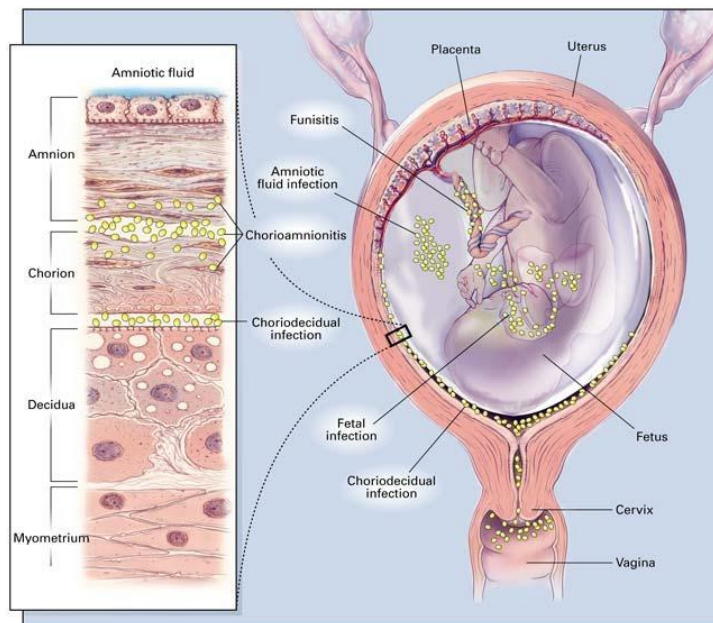


Figure 1. Potential sites of bacterial infection within the uterus[7]

Histological examination of the placenta is the gold standard for evaluating inflammatory processes. Other criteria are: clinical signs of inflammation in the mother, microbiological detection of pathogens, and biochemical criteria[11]. Clinical diagnosis of CA is most frequently based on the following criteria[12]: maternal fever $>38^{\circ}\text{C}$, uterine tenderness defined as pain referred by the mother on abdominal examination in the absence of uterine contractions, leukocytosis ($>15,000$ cells/mm³), maternal tachycardia (>100 bpm), fetal tachycardia (>160 bpm), or foul smelling vaginal discharge. The microbiological diagnosis is based on the isolation of the causative microorganism by PCR or from culture of amniotic fluid obtained by amniocentesis, but this procedure is performed during labor, and the results can be delayed for some days. This makes the microbiological diagnosis less useful for decision-making during labor. Biochemical criteria are: elevated cytokine levels in amniotic fluid, elevated maternal serum C-reactive protein concentration, presence of fetal fibronectin in cervical and vaginal secretions, etc.[13]. Histology remains the most sensitive method for diagnosis, however this finding is available only after delivery.

3.2 Chorioamnionitis and neonatal outcome

The consequent fetal response to chorioamnionitis has been referred to as the fetal inflammatory response syndrome (FIRS)[14]. As recently reviewed by Galan Henriquez[15] many studies have associated chorioamnionitis with adverse neonatal outcome in newborn infants, with fetal consequences described in several organ systems. Moreover, evidence is increasing that the effects of chorioamnionitis on health and disease may extend beyond the neonatal period. In order to investigate the correlation with neonatal morbidities, most of these studies are performed *in vivo* on animal models of intrauterine inflammation obtained by exposition (intracervical, intravenous, intraperitoneal or into the amniotic cavity) of fetus to lipopolysaccharide (LPS), thus triggering the inflammatory cascade[16–18]. Many organs of the fetus may then be affected.

Brain

Perinatal brain damage is a fundamental cause of developmental delay and lifelong neurological disabilities, such as mental retardation, cerebral palsy as well as learning and behavioral difficulties. CA and vasculitis in the umbilical cord (funisitis) have a high incidence in preterm deliveries and are important risk factor of preterm cerebral white matter disease. Furthermore, hypoxia–ischemia in association with CA markedly increases the vulnerability of the immature brain to the cerebral deficits. White matter disease, usually described as periventricular leukomalacia, has been shown to be the predominant feature of brain damage in premature newborns of <32 weeks of gestation[19]. In

clinical studies, antenatal exposure to inflammation has been implicated as a potential cause of cerebral palsy[20]. Moreover, neurodevelopmental delay has been linked with previous exposure to CA by some studies, although others have failed to reproduce these findings[21]. In a fetal sheep model, CA induced by the intra-amniotic administration of LPS caused microglial activation[22], which plays a central role in the onset of white matter disease leading to the apoptotic death of the developing oligodendrocytes.

Heart

CA may predispose to adverse neurological outcome through cardiovascular instability. Although findings are not conclusive about the association between antenatal inflammation and postnatal circulatory disturbance many studies in both humans and animal models, reported that intrauterine inflammation may result in abnormal fetal cardiac function and impaired development of the myocardium[23]. In particular, intrauterine inflammation has been associated with: increased left ventricular compliance/dilatation[24]; reduced mean and diastolic blood pressure, which may contribute to the increased incidence of periventricular leukomalacia and cerebral palsy[25]; impaired contractility and relaxation of the myocardial tissue[26]; increased cardiac afterload[27].

Retina

Retinopathy of prematurity (ROP) is an eye disease that can occur in premature babies and causes abnormal blood vessels growing in the retina, and can lead to blindness. Antenatal exposure to HCA was correlated to an increased risk of ROP. Two possible mechanisms have been reported to explain this correlation: a direct sensitization of the developing retina to oxygen-induced changes in vascular endothelial growth factor availability and subsequent vascular development; and/or by causing systemic hypotension resulting in retinal hypoperfusion/ischemia[28].

Sepsis

Sepsis greatly contributes to the mortality and morbidity of preterm infants. Early onset sepsis (with onset <72 hours of age) is typically associated with vertical transmission of infection from the mother to her infant and can be caused by the infectious pathogens that drive perinatal inflammation. A cohort study of 3094 infants showed that clinical CA was associated with a 5.5-fold increase in the incidence of early onset sepsis[29]. Other studies also indicate that HCA seemed to increase the risk of early onset sepsis in preterm infants[30].

3.2.1 Chorioamnionitis and respiratory outcome

There is no consensus about the relationships between chorioamnionitis and pulmonary outcomes. The exposure is complex as both the bacteria and products of the inflammation bathe the chorioamnion and the fetal skin. The fetal gut is exposed from swallowed amniotic fluid[9]. Amniotic fluid also mixes with fetal lung fluid by fetal breathing causing a lung exposure.

However, the association of chorioamnionitis with RDS, is not straightforward. In 1996, Watterberg and colleagues [31] were the first to report a decrease in the incidence of RDS, while the incidence of chronic lung injury, marked by the presence of bronchopulmonary dysplasia (BPD), was increased in preterm newborns with HCA. For this reason, this paradoxical effect of prenatal inflammation on pulmonary outcome has been referred to as the “Watterberg effect” and it is basically an “early protection, late-damage” mechanism of action whereby antenatal inflammation promotes lung maturation in the premature infant, thus reducing the risk of RDS, and simultaneously causing an acute injury.

Fetal exposure to inflammation may initiate events that progress toward lung injury in the preterm infant. However, inflammatory mediators also can regulate lung development. Studies in animal models aimed to assess the involvement of infection related cytokines causing inflammatory responses in lung maturation were performed by injection of pro-inflammatory mediators such as *Escherichia coli* LPS, interleukins or single live organisms as Ureaplasma. The effect of cytokines on lung development and injury has both pre and postnatal influences. Intra-amniotic interleukin (IL)-1 stimulates the production of SP-A and SP-B in the immature rabbit lung, but decreases their production in the more mature rabbit lung[17]. In the same way, intra-amniotic *E. coli* endotoxin in fetal sheep improves postnatal lung function and increases the production of surfactant proteins[32]. The increase in surfactant protein production was associated with an increase in type 2 alveolar epithelial cells by *in vivo* and *in vitro* studies on fetal mice subject to intra-amniotic LPS exposure [33]. On the other side the potential benefits of an enhanced lung maturation can be counterbalanced by an injury caused by the inflammation to the developing lung.

In human studies, it was reported that infants exposed to HCA and diagnosed with FIRS had an increased risk of developing RDS and were less responsive to surfactant treatment relative to infants exposed to HCA but without FIRS, which in turn had less severe RDS than infants who were not exposed to HCA[34]. Moreover, the incidence of RDS was decreased in infants exposed HCA plus funisitis compared to no HCA[35]. On the other hand, other studies reported no association between CA and RDS[29]. The reasons for the discrepancy on the relationship between CA and RDS outcome

were summarized by Jobe[8] and include imprecise diagnosis of CA and/or of RDS and interferences due to surfactant treatment and mechanical ventilation.

Since the function of lung surfactant strictly depends on its composition, during my PhD we carried out two studies aimed to assess differences in lung epithelial lining fluid (ELF) composition in preterm infants with RDS exposed or not to HCA.

In the first study, we assessed the effect of gestational age and of the inflammatory state induced by HCA on the principal components of surfactant (DSPC, SP-A, and SP-B) and on the alveolar capillary permeability in preterm infants with RDS. The results of this study were published in the paper reported below in this chapter[36].

In the second study, we investigated the metabolome and lipid profiles of the ELF of newborns with RDS by liquid chromatography-mass spectrometry (LC-MS/MS) based metabolomics. Next chapter will deal with the application of metabolomics as a good approach to identify metabolic changes related to a particular pathophysiological state, and the paper relative to the second study will be reported.

In both studies, samples have been obtained from tracheal aspirates (TAs). We have decided to use TA instead of broncholaveolar lavage (BAL) fluid because of ethical concerns since tracheal aspiration is a procedure routinely performed in intubated infants as part of the clinical care, whereas BAL technique is rarely done and only for specific clinical indication (i.e. bacterial pneumonia, atelectasis). Lung fluid obtained by TA originated more proximally in the airways than did that obtained by BAL. However, after a comparison of 53 paired TA and BAL specimens Dargaville et al.[37] found that the surfactant indices obtained by TA were at least equivalent to those obtained in BAL for predicting the degree of lung dysfunction. This suggest that, even in lavage samples from the proximal airway, the concentration of alveolar component in the return fluid is indicative of their concentration in alveolar ELF. In a recent work, Dushianthan et al.[38] reported that phospholipid molecular species composition did not significantly differ between TA and BAL samples and that TA fluid may be of value as a surrogate to assess ELF composition in patients unable to tolerate invasive procedures without clinical compromise.

Bibliography

1. Hecht JL, Allred EN, Kliman HJ, Zambrano E, Doss BJ, Husain A, Pflueger SM V, Chang C-H, Livasy CA, Roberts D, Bhan I, Ross DW, Senagore PK, Leviton A, Elgan Study Investigators. Histological characteristics of singleton placentas delivered before the 28th week of gestation. *Pathology*. 2008; 40:372–6.
2. Ericson JE, Laughon MM. Chorioamnionitis: implications for the neonate. *Clin Perinatol*. 2015; 42:155–65.
3. Lee SYR, Leung CW. Histological chorioamnionitis – implication for bacterial colonization, laboratory markers of infection, and early onset sepsis in very-low-birth-weight neonates. *J Matern Neonatal Med*. 2012; 25:364–368.
4. Torricelli M, Voltolini C, Toti P, Vellucci FL, Conti N, Cannoni A, Moncini I, Occhini R, Severi FM, Petraglia F. Histologic chorioamnionitis: different histologic features at different gestational ages. *J Matern Neonatal Med*. 2014; 27:910–913.
5. Curtin WM, Katzman PJ, Florescue H, Metlay LA. Accuracy of signs of clinical chorioamnionitis in the term parturient. *J Perinatol*. 2013; 33:422–428.
6. Liu Z, Tang Z, Li J, Yang Y. Effects of placental inflammation on neonatal outcome in preterm infants. *Pediatr Neonatol*. 2014; 55:35–40.
7. Goldenberg RL, Hauth JC, Andrews WW. Intrauterine infection and preterm delivery. *N Engl J Med*. 2000; 342:1500–1507.
8. Jobe A. Effects of chorioamnionitis on the fetal lung. *Clin Perinatol*. 2012; 39:441–457.
9. Romero R, Espinoza J, Chaiworapongsa T, Kalache K. Infection and prematurity and the role of preventive strategies. *Semin Neonatol*. 2002; 7:259–274.
10. Romero R, Gomez R, Ghezzi F, Yoon BH, Mazor M, Edwin SS, Berry SM. A fetal systemic inflammatory response is followed by the spontaneous onset of preterm parturition. *Am J Obstet Gynecol*. 1998; 179:186–193.
11. Pagni L, Pietrasanta C, Acaia B, Merlo D, Ronchi A, Ossola MW, Bosari S, Mosca F. Chorioamnionitis and neonatal outcome in preterm infants: A clinical overview. *J Matern Neonatal Med*. 2016; 29:1525–1529.
12. Gibbs RS, Duff P. Progress in pathogenesis and management of clinical intraamniotic

- infection. *Am J Obstet Gynecol.* 1991; 164:1317–1326.
13. Romero R, Miranda J, Kusanovic JP, Chaiworapongsa T, Chaemsaihong P, Martinez A, Gotsch F, Dong Z, Ahmed AI, Shaman M, Lannaman K, Yoon BH, Hassan SS, Kim CJ, Korzeniewski SJ, Yeo L, Kim YM. Clinical chorioamnionitis at term I: microbiology of the amniotic cavity using cultivation and molecular techniques. *J Perinat Med.* 2015; 43:19–36.
 14. Gotsch F, Romero R, Kusanovic JP, Mazaki-Tovi S, Pineles BL, Erez O, Espinoza J, Hassan SS. The fetal inflammatory response syndrome. *Clin Obstet Gynecol.* 2007; 50:652–83.
 15. Galan Henriquez GM, Garcia-Munoz Rodrigo F. Chorioamnionitis and neonatal morbidity: current perspectives. *Res Reports Neonatol.* 2017; Volume 7:41–52.
 16. Dombroski RA, Woodard DS, Harper MJK, Gibbs RS. A rabbit model for bacteria-induced preterm pregnancy loss. *Am J Obstet Gynecol.* 1990; 163:1938–1943.
 17. Bry K, Lappalainen U. Intra-amniotic endotoxin accelerates lung maturation in fetal rabbits. *Acta Paediatr.* 2001; 90:74–80.
 18. Abdulkadir AA, Kimimasa T, Bell MJ, MacPherson TA, Keller BB, Yanowitz TD. Placental inflammation and fetal hemodynamics in a rat model of chorioamnionitis. *Pediatr Res.* 2010; 68:513–518.
 19. Berger R, Garnier Y. Pathophysiology of perinatal brain damage. *Brain Res Rev.* 1999; 30:107–134.
 20. Wu YW, Colford, Jr JM. Chorioamnionitis as a risk factor for cerebral palsy. *J Am Med Assoc.* 2000; 284:1417.
 21. Been J V, Kramer BW, Zimmermann LJI. In utero and early-life conditions and adult health and disease. *N Engl J Med.* 2008; 359:1523–4; author reply 1524.
 22. Gavilanes AWD, Strackx E, Kramer BW, Gantert M, Van den Hove D, Steinbusch H, Garnier Y, Cornips E, Steinbusch H, Zimmermann L, Vles J. Chorioamnionitis induced by intraamniotic lipopolysaccharide resulted in an interval-dependent increase in central nervous system injury in the fetal sheep. *Am J Obstet Gynecol.* 2009; 200:437.e1-437.e8.
 23. Galinsky R, Polglase GR, Hooper SB, Black MJ, Moss TJM. The consequences of chorioamnionitis: Preterm birth and effects on development. *J Pregnancy.* 2013; 2013:.
 24. Romero R, Espinoza J, Gonçalves LF, Gomez R, Medina L, Silva M, Chaiworapongsa T,

- Yoon BH, Ghezzi F, Lee W, Treadwell M, Berry SM, Maymon E, Mazor M, DeVore G. Fetal cardiac dysfunction in preterm premature rupture of membranes. *J Matern Neonatal Med.* 2004; 16:146–157.
25. Mitchell T, Macdonald JW, Srinouanpranchanh S, Bammler TK, Merillat S, Boldenow E, Coleman M, Agnew K, Baldessari A, Stencel-baerenwald JE, Adams Waldorf K, Rajagopal L, Tisoncik-go J, Green RR, GALE Jr MJ, Adams Waldorf KM. Evidence of cardiac involvement in the fetal inflammatory response syndrome: disruption of gene networks programming cardiac development in nonhuman primates. *Am J Obs Gynecol.* 2018; 218:438–439.
 26. Rounioja S, Räsänen J, Glumoff V, Ojaniemi M, Mäkikallio K, Hallman M. Intra-amniotic lipopolysaccharide leads to fetal cardiac dysfunction. A mouse model for fetal inflammatory response. *Cardiovasc Res.* 2003; 60:156–64.
 27. Rounioja S, Räsänen J, Ojaniemi M, Glumoff V, Autio-Harmainen H, Hallman M. Mechanism of acute fetal cardiovascular depression after maternal inflammatory challenge in mouse. *Am J Pathol.* 2005; 166:1585–92.
 28. Lee J, Dammann O. Perinatal infection, inflammation, and retinopathy of prematurity. 2011; 17:26–29.
 29. Soraisham AS, Singhal N, McMillan DD, Sauve RS, Lee SK. A multicenter study on the clinical outcome of chorioamnionitis in preterm infants. *Am J Obstet Gynecol.* 2009; 200:372.e1-372.e6.
 30. Korbage de Araujo MC, Schultz R, do Rosário Dias de Oliveira Latorre M, Ramos JLA, Vaz FAC. A risk factor for early-onset infection in premature newborns: invasion of chorioamniotic tissues by leukocytes. *Early Hum Dev.* 1999; 56:1–15.
 31. Watterberg KL, Demers LM, Scott SM, Murphy S. Chorioamnionitis and early lung inflammation in infants in whom bronchopulmonary dysplasia develops. *Pediatrics.* 1996; 97:210–215.
 32. Jobe AH, Newnham JP, Willet KE, Sly P, Ervin MG, Bachurski C, Possmayer F, Hallman M, Ikegami M. Effects of antenatal endotoxin and glucocorticoids on the lungs of preterm lambs. *Am J Obstet Gynecol.* 2000; 182:401–408.
 33. Prince LS, Okoh VO, Moninger TO, Matalon S. Lipopolysaccharide increases alveolar type II

- cell number in fetal mouse lungs through Toll-like receptor 4 and NF- κ B. *Am J Physiol Cell Mol Physiol*. 2004; 287:L999–L1006.
34. Been J V., Rours IG, Kornelisse RF, Jonkers F, de Krijger RR, Zimmermann LJ. Chorioamnionitis alters the response to surfactant in preterm infants. *J Pediatr*. 2010; 156:10-15.e1.
 35. Lahra MM, Beeby PJ, Jeffery HE, Lahra MM. Maternal versus fetal inflammation and respiratory distress syndrome: a 10-year hospital cohort study. *Arch Dis Child Fetal Neonatal*. 2009; 94:F13-16.
 36. Verlatto G, Simonato M, Giambelluca S, Fantinato M, Correani A, Cavicchiolo ME, Priante E, Carnielli V, Cogo P. Surfactant components and tracheal aspirate inflammatory markers in preterm infants with Respiratory Distress Syndrome. *J Pediatr*. 2018; 203:442–446.
 37. Dargaville PA, South M, McDougall PN. Comparison of two methods of diagnostic lung lavage in ventilated infants with lung disease. *Am J Respir Crit Care Med*. 1999; 160:771–777.
 38. Dushianthan A, Goss V, Cusack R, Grocott MP, Postle AD. Phospholipid composition and kinetics in different endobronchial fractions from healthy volunteers. *BMC Pulm Med*. 2014; 14:10.



Surfactant Components and Tracheal Aspirate Inflammatory Markers in Preterm Infants with Respiratory Distress Syndrome

Giovanna Verlatto, MD, PhD¹, Manuela Simonato, PhD^{2,3}, Sonia Giambelluca, MSc⁴, Margherita Fantinato, MD¹, Alessio Correani, MSc⁵, Maria Elena Cavicchiolo, MD¹, Elena Priante, MD¹, Virgilio Carnielli, MD, PhD⁵, and Paola Cogo, MD, PhD³

In 93 preterm infants ≤ 32 weeks of gestational age and 12 control infants, epithelial lining fluid disaturated-phosphatidylcholine, surfactant protein A and B, albumin, and myeloperoxidase activity were assessed after intubation and before exogenous surfactant administration. We found that disaturated-phosphatidylcholine, surfactant protein B, and myeloperoxidase were significantly higher in preterms with chorioamnionitis. (*J Pediatr* 2018;203:442-6).

Deficiency or dysfunction of pulmonary surfactant plays a critical role in the pathogenesis of respiratory diseases in newborns.¹ Surfactant provides surface-tension-lowering activity to the lungs and consists of about 90% lipids and 10% of specific surfactant proteins (surfactant protein A [SP-A], surfactant protein B [SP-B], surfactant protein C, and surfactant protein D).² Dipalmitoyl-phosphatidylcholine is about 60% of the disaturated-phosphatidylcholine (DSPC) species and it is the most important tensioactive component of surfactant. Among surfactant proteins, SP-A is the most abundant and plays an important role in the lung innate immune system³ and SP-B is considered to be the most important protein for sustaining respiratory physiology.⁴

Surfactant synthesis and secretion are regulated by chemical and physical factors. Among perinatal factors, inflammation, such as chorioamnionitis, could enhance lipid and protein synthesis, but also alter lung growth and predispose the preterm lung to the development of bronchopulmonary dysplasia (BPD).⁵ It was reported that preterm newborns with respiratory distress syndrome (RDS)⁶ and experiencing extubation failure⁷ have a reduced surfactant pool size compared with term newborns with normal lungs.⁸

Few studies have reported on surfactant status at birth in preterm infants^{9,10} and no published data have evaluated surfactant composition in patients with chorioamnionitis before exogenous surfactant administration and mechanical ventilation. We assessed the effect of gestational age and of the inflammatory state induced by chorioamnionitis on the principal components of surfactant (DSPC, SP-A, and SP-B) and on the alveolar capillary permeability in preterm infants with RDS.

Methods

Between January 2016 and December 2017 we prospectively recruited 98 preterm newborns with a gestational age of >23 and ≤ 32 weeks admitted to the Neonatal Intensive Care Unit of the University Hospital of Padova who needed intubation for RDS. Exclusion criteria were severe congenital malformations, chromosomal abnormalities, exogenous surfactant administration (200 mg/kg at first dose and 100 mg/kg the following doses) before collection of tracheal aspirate samples, and lack of placenta histologic examination report. RDS was defined as a PaO_2 of <50 mm Hg (<6.6 kPa) on room air, central cyanosis, or necessity of supplemental oxygen to maintain a PaO_2 of >50 mm Hg (>6.6 kPa) together with the classical findings on chest radiograph.¹¹ Chorioamnionitis was diagnosed by histologic examination of the placenta and fetal membranes according to the classification of Redline.¹² BPD was assessed at 28 days and 36 weeks of gestational age and defined as indicated by Jobe and Bancalari.¹³ Respiratory failure was assessed by PaO_2 /fraction of inspired oxygen (FiO_2), mean airway pressure (MAP), oxygenation index, and alveolar-arterial oxygen gradient (AaDO_2), calculated as $([\text{MAP} \times \text{FiO}_2 / \text{PaO}_2] \times 100)$ and $([\text{FiO}_2 \times (760 - 47)] - [\text{PaCO}_2 / 0.8]) - \text{PaO}_2$, respectively.

Patients were divided into 2 groups according to their gestational age: group A was composed of preterm infants with gestational ages of >23 and ≤ 28 weeks and group B included preterm infants with gestational age of >28 and ≤ 32 weeks.

To evaluate the effect of the gestational age on surfactant composition and on alveolar capillary permeability,

AaDO ₂	Alveolar-arterial oxygen gradient
BPD	Bronchopulmonary dysplasia
DSPC	Disaturated-phosphatidylcholine
MPO	Myeloperoxidase
RDS	Respiratory distress syndrome
SP-A	Surfactant protein A
SP-B	Surfactant protein B

From the ¹Neonatal Intensive Care Unit, Department of Women's and Children's Health, University Hospital of Padova, Padova, Italy; ²Pediatric Research Foundation Institute "Città della Speranza", Padova; ³Division of Pediatrics, Department of Medicine, University of Udine, Udine, Italy; ⁴Department of Women's and Children's Health, University of Padova, Padova, Italy; and ⁵Department of Clinical Sciences, Polytechnic University of Marche, Ancona, Italy

The authors declare no conflicts of interest.

Portions of this study were presented at the Pediatric Academic Societies Annual Meeting, May 5-8, 2018, Toronto, Canada.

0022-3476/\$ - see front matter. © 2018 Elsevier Inc. All rights reserved.
<https://doi.org/10.1016/j.jpeds.2018.08.019>

we selected all newborns in groups A and B without chorioamnionitis. To examine the possible influence of inflammation on surfactant composition we identified all preterm infants with histologic chorioamnionitis (group positive histologic chorioamnionitis [HCA+]) and compared them with infants without chorioamnionitis, matched by gestational age (group negative histologic chorioamnionitis [HCA-]). Twelve term infants with no lung disease served as a reference group. Vital signs and ventilator parameters were recorded at the time of tracheal aspirate collection. The study protocol was approved by the local ethics committee and written informed consent was obtained from parents.

TAs were collected immediately after intubation and before surfactant administration in preterm infants with RDS and immediately after intubation in the infants. All samples were processed and stored, together with leftover blood from arterial blood gas analysis, as previously reported.¹⁴

DSPC was extracted from TAs according to the method of Bligh and Dyer¹⁵ after the addition of 50 µg of internal standard (pentadecanoyl-phosphatidylcholine; Sigma-Aldrich, Milan, Italy). DSPC amount was quantified by gas chromatography as previously reported.¹⁶ SP-A and SP-B concentration were measured by enzyme-linked immunosorbent assay.¹⁷⁻¹⁹ Albumin concentration and myeloperoxidase (MPO) activity were measured by spectrophotometric assay.^{20,21} Plasma and tracheal aspirate samples were analyzed for urea using a colorimetric method (QuantiChrom Urea Assay kit, BioAssay Systems, Hayward, California) to normalize the tracheal aspirate components for the epithelial lining fluid volume.²²

Statistical Analyses

We expressed data as median and IQR (25th-75th) or as mean ± SD, according to the variable distribution. Comparisons were made by the *t* test or by Mann-Whitney *U* test for continuous variables, and by χ^2 for categorical variables. Spearman analysis was performed to test the correlation between clinical parameters and biochemical dosage. Multiple regression analysis was used to identify predictors of prolonged mechanical ventilation. *P* < .05 was considered as statistically significant. Statistical analysis was performed using PASW Statistics 20.0 for Windows (SPSS Inc, Chicago, Illinois).

Results

We prospectively enrolled 98 preterm infants with RDS and 12 term infants with no lung disease. Five patients with RDS with tracheal aspirate samples with visible blood (*n* = 2) or with a urea concentration of <0.08 mg/dL (kit linear detection range, 0.08-100 mg/dL; *n* = 3) were not included in this study. The remaining 93 preterm infants had a median postnatal age at the time of sample collection of 2.1 hours (range, 0.6-7.2 hours). The clinical characteristics of the 3 study groups are reported in **Table I**. Group A (*n* = 46) had a significantly higher incidence of HCA, lower serum albumin, and higher percentage of BPD at 28 days and at 36 weeks of gestational age compared with group B (*n* = 47). The HCA+ and HCA- group of newborns with RDS had similar gestational ages and birth weights (25.3 ± 1.8 weeks vs 26.1 ± 1.5 weeks [*P* = .30] and 816 ± 255 g vs 783 ± 186 g; *P* = 0.998, respectively). There were

Table I. Demographic and clinical characteristics of the study population of preterm (gestational age of ≤ 32 weeks) and term infants (gestational age of ≥ 37 weeks)

	Group A (<i>n</i> = 46; 23 > gestational age ≤ 28 wk)	Group B (<i>n</i> = 47; 28 < gestational age ≤ 32 wk)	<i>P</i> *	Term Reference Group (<i>n</i> = 12)
Birth weight (g)	745 (181)	1224 (318)	<.001	3144 (609)
Gestational age (wk)	25.7 (1.4)	29.9 (1.2)	<.001	38.6 (1.5)
Sex (female/male)	20/26	18/29	.68	3/9
Age ss (h)	1.0 (0.4-3.1)	3.9 (1.2-12.8)	.001	116.7 (23.5-1400.4)
Maternal steroid (%)	86	93	.52	
IUGR (%)	22	26	.79	
CRP max (mg/L)	7.7 (2.9-17.1)	4.2 (2.9-16.4)	.36	4.6 (2.9-10.6)
WBC max (N ^o /mm ³)	13 410 (7367-20 658)	6535 (5272-10 592)	.001	
Albumin (g/L)	26.0 (3.9)	28.1 (3.7)	.02	33.7 (5.2)
Oi	7.9 (4.3-9.8)	6.3 (3.4-8.2)	.07	
MAP	8.5 (8.0-9.4)	8.2 (6.0-8.9)	.04	
FiO ₂	0.40 (0.30-0.60)	0.37 (0.30-0.41)	.17	
AaDO ₂	192 (101-266)	158 (107-207)	.16	
PaO ₂ /FiO ₂	108 (90-183)	133 (93-184)	.21	
MV time (1 st intubation) (h)	158 (69-333)	28 (10-97)	<.001	14 (4-37)
MV time (1 st intubation) (d)	6.6 (2.9-13.9)	1.2 (0.4-4.0)	<.001	0.6 (0.2-1.5)
Total MV (d)	8.9 (5.4-31.8)	1.8 (0.8-4.1)	<.001	0.6 (0.2-1.5)
Total amount of surfactant (mg/kg)	245 (200-300)	200 (200-255)	.05	
HCA (%)	44	9	<.001	
BPD at 28 gg (%)	87	32	<.001	
BPD at 36 gestational age (%)	45	25	.04	
Survival (%)	89	100	.02	100

CRP, C-reactive protein; FiO₂, fraction of inspired oxygen; IUGR, intrauterine growth restriction; MAP, mean airway pressure; MV, mechanical ventilation; Oi, oxygenation index; WBC, white blood cells.

Values are expressed as median and IQR (25th-75th) or as mean (SD) as appropriate.

The total amount of surfactant comprises first dose (200 mg/kg) and following doses (100 mg/kg) each.

*Differences between group A and group B were assessed by the independent *t* test or Mann-Whitney *U* test, χ^2 test, or Fisher exact tests as appropriate.

Table II. Effect of gestational age and of chorioamnionitis on tracheal aspirate biomarker concentrations in preterm and in term infants (gestational age of ≥ 37 weeks)

	23 < Gestational age \leq 28 wk (n = 24)	28 < Gestational age \leq 32 wk (n = 43)	<i>P</i> *	HCA+ (n = 23)	HCA- (n = 24)	<i>P</i> *	Control (n = 12)
Epithelial lining fluid DSPC (mg/mL)	0.6 (0.2-0.9) [‡]	0.6 (0.2-1.0) [‡]	.79	3.0 (0.8-7.3)	0.6 (0.2-0.9) [‡]	.009	3.0 (1.4-6.4)
Epithelial lining fluid albumin (mg/mL)	12.0 (8.0-19.0)	7.0 (5.0-12.2)	.10	15.0 (5.0-27.0) [†]	12.0 (8.0-19.0)	.26	6.0 (2.0-10.7)
Epithelial lining fluid SP-A (μ g/mL)	5.7 (1.2-20.3) [†]	10.8 (3.2-26.9) [‡]	.83	24.1 (10.4-58.6)	10.1 (1.9-46.0)	.18	31.9 (15.4-41.0)
Epithelial lining fluid SP-B (μ g/mL)	5.3 (2.2-12.4)	5.9 (3.6-15.0)	.48	12.7 (7.0-38.6) [†]	5.3 (2.2-12.3)	.007	5.6 (2.5-8.9)
Epithelial lining fluid MPO (mU/mL)	101 (0-531)	27 (0-484)	.99	1513 (401-2664) [‡]	101 (0-531)	.002	2 (0-102)
Tracheal aspirate/plasma albumin	0.51 (0.30-0.81) [‡]	0.24 (0.18-0.46)	.03	0.65 (0.20-1.11) [‡]	0.51 (0.30-0.81)	.47	0.16 (0.05-0.37)

Controls = term infants (gestational age of ≥ 37 weeks).

Preterms in group 23 < gestational age \leq 28 wk and 28 < gestational age \leq 32 wk have no chorioamnionitis.

HCA+ and HCA- groups are matched by gestational age.

Values are expressed as median and IQR (25th-75th).

*Differences between Groups (23 < gestational age \leq 28 wk vs 28 < gestational age \leq 32 wk and HCA+ vs HCA-) were assessed by the Mann-Whitney *U* test.

[†]*P* < .05 vs control group by the Mann-Whitney *U* test.

[‡]*P* < .01 vs control group by the Mann-Whitney *U* test.

no differences in the development of BPD (either at 28 days or 36 weeks gestational age) between infants in HCA+ group and those in HCA- group (data not shown).

To evaluate the effect of the gestational age on surfactant composition and on alveolar capillary permeability, we selected all newborns in groups A and B without chorioamnionitis. We found no significant differences in the epithelial lining fluid DSPC, SP-A, or SP-B concentrations between the 2 preterm groups (Table II). In contrast, infants with a gestational age of >23 and ≤ 28 weeks had a significantly higher TA/plasma albumin ratio ($P = .03$) compared with those with a gestational age of >28 and ≤ 32 weeks. Although epithelial lining fluid DSPC and SP-A concentrations were significantly lower in the preterm groups compared with term controls, epithelial lining fluid SP-B amount was similar among the 3 groups (Table II). We found that newborns who were HCA+ had higher concentrations of epithelial lining fluid DSPC, SP-B and MPO activity than infants who were HCA- and higher SP-B and MPO activity and albumin ratio with respect to the term reference group (Table II).

In the whole cohort of patients ($n = 93$) epithelial lining fluid DSPC inversely correlated with oxygenation index and AaDO₂ ($r = -0.295$, $P = .02$; $r = -0.341$, $P = .006$) and positively with PaO₂/FiO₂ ($r = 0.296$, $P = .02$). Serum albumin concentration inversely correlated with respiratory outcomes for BPD at 28 days and 36 weeks, respectively ($r = -0.394$, $P = .001$; $r = -0.289$, $P = .02$) and with the total duration of invasive mechanical ventilation ($r = -0.506$; $P < .001$).

Multiple regression analysis in the newborns with RDS without chorioamnionitis ($n = 70$) showed that serum albumin concentration and gestational age were significant predictors of length of mechanical ventilation ($R^2 = 0.512$; $P < .001$). By increasing gestational age of 1 week, we found a decrease in mechanical ventilation of 1.4 days and an increase of serum albumin of 1 g/L was associated with a decrease of 1.0 days of mechanical ventilation.

Discussion

We compared surfactant composition of preterm infants within the first hours of life before exogenous surfactant administration with the surfactant composition of term infants with no lung disease.

We observed that, in the tracheal aspirate of preterm infants with chorioamnionitis, DSPC was >4 -fold and SP-B was 2-fold higher than in age-matched infants without chorioamnionitis. MPO activity, a marker of inflammation,²³ was 15-fold higher in infants with vs without chorioamnionitis. In animals, inflammation caused by intra-amniotic injection of cytokines induced the messenger RNA transcription of surfactant lipids and proteins SP-A and SP-B.²⁴ In newborns with pneumonia, SP-B was significantly higher vs controls at the peak of lung disease and SP-B decreased as pulmonary function improved.²⁵ This finding was also reported in animal studies^{21,26} and in newborns after lung injury^{27,28} and with suspected chorioamnionitis.¹⁰ Specifically, Ikegami et al found that, in healthy mice, the induction of lung injury by the intratracheal injection of LPS increased bronchoalveolar lavage fluid DSPC and SP-B in a STAT-3-dependent way.²⁶ Another study described higher levels of SP-B associated with reduced lung damage after endotoxin exposure in transgenic mice, suggesting a protective role of SP-B during inflammation.²⁸ Nonetheless, inflammation in sheep fetuses induced a permanent change in pulmonary structure, similar to BPD, and an altered distribution of elastin, a mesenchymal protein necessary for normal alveolar septation.^{29,30} The increased levels of DSPC found in the group with chorioamnionitis could be an advantage; we found that higher DSPC pools accompanied lower degrees of respiratory failure (as measured by oxygenation index and AaDO₂) in the study infants. In contrast, the increase in surfactant components in newborns with chorioamnionitis could be counterbalanced by higher levels of inflammatory markers as MPO activity. Of note, we did not find differences

in clinical outcomes or the rate of BPD in patients with or without chorioamnionitis, although more patients with longer follow-up are required to support this preliminary observation.

In infants without chorioamnionitis, the extremely premature group (with gestational age of >23 and ≤28 weeks) did not have lower epithelial lining fluid DSPC, SP-A or SP-B compared with the older group (with gestational age of >28 and ≤32 weeks), but had a higher tracheal aspirate/plasma albumin ($P = .003$), indicating increased alveolar capillary permeability. We also found that lower plasma albumin concentration at birth significantly correlated with more days of mechanical ventilation and oxygen dependency. Recently, hypoalbuminemia, a predictor of mortality in adult patients,³¹ was found to be associated with severe adverse outcomes in preterm infants.^{32,33} In our study, we found that lower tracheal aspirate to plasma albumin ratios, an index of altered alveolar-capillary permeability, correlated with a higher $\text{PaO}_2/\text{FiO}_2$ ($r = 0.319$; $P = .02$). Albumin leak in the alveolar space induces surfactant inactivation that leads to respiratory failure.^{34,35} Increased alveolar capillary permeability was found in preterm infants, especially in those with a lower gestational age,³⁶ although a higher tracheal aspirate/plasma albumin ratio could be due to other perinatal factors. Interestingly, we found that, in patients without chorioamnionitis, an increase in serum albumin of 1 g/L was associated with a decrease in mechanical ventilation of 1 day. This finding suggests that optimizing albumin synthesis in the first days of life through nutritional interventions may be important. Moreover tailored anti-inflammatory therapy could be useful to reduce the release of inflammatory mediators (leukotrienes, prostacyclin, and endothelin-1) and to maintain the microvascular integrity.

We are aware that samples obtained by tracheal aspiration could be a limitation of our study. However, surfactant extracted by tracheal aspiration closely resembles that obtained by bronchoalveolar lavage³⁷ and tracheal aspirate samples may be an alternative for surfactant isolation in preterm infants otherwise unable to tolerate invasive procedures.

In conclusion, we found that preterm newborns with chorioamnionitis had higher concentrations of epithelial lining fluid DSPC, SP-B, and MPO activity than those without chorioamnionitis. Extremely preterm newborns showed similar amounts of epithelial lining fluid DSPC, SP-A, and SP-B compared with more mature infants. A lower gestational age was associated with increased markers of alveolar capillary leak. Further studies will provide more information on the evolution of surfactant components and outcome in preterm newborns with chorioamnionitis and on value of perinatal anti-inflammatory interventions. ■

We are grateful to the nurses of the Neonatal Intensive Care who helped us to conduct the study. Without their enthusiasm and support this study would not have been possible.

Submitted for publication May 17, 2018; last revision received Jul 11, 2018; accepted Aug 9, 2018

References

- Zimmermann LJ, Janssen DJ, Tibboel D, Hamvas A, Carnielli VP. Surfactant metabolism in the neonate. *Biol Neonate* 2005;87:296-307.
- Haagsman HP, Diemel RV. Surfactant-associated proteins: functions and structural variation. *Comp Biochem Physiol A Mol Integr Physiol* 2001;129:91-108.
- LeVine AM, Whitsett JA. Pulmonary collections and innate host defense of the lung. *Microbes Infect* 2001;3:161-6.
- Perez-Gil J. Structure of pulmonary surfactant membranes and films: the role of proteins and lipid-protein interactions. *Biochim Biophys Acta* 2008;1778:1676-95.
- Watterberg KL, Demers LM, Scott SM, Murphy S. Chorioamnionitis and early lung inflammation in infants in whom bronchopulmonary dysplasia develops. *Pediatrics* 1996;97:210-5.
- Torresin M, Zimmermann LJ, Cogo PE, Cavicchioli P, Badon T, Giordano G, et al. Exogenous surfactant kinetics in infant respiratory distress syndrome: a novel method with stable isotopes. *Am J Respir Crit Care Med* 2000;161:1584-9.
- Verlato G, Cogo PE, Balzani M, Gucciardi A, Burattini I, De Benedictis F, et al. Surfactant status in preterm neonates recovering from respiratory distress syndrome. *Pediatrics* 2008;122:102-8.
- Cogo PE, Zimmermann LJ, Meneghini L, Mainini N, Bordignon L, Suma V, et al. Pulmonary surfactant disaturated-phosphatidylcholine (DSPC) turnover and pool size in newborn infants with congenital diaphragmatic hernia (CDH). *Pediatr Res* 2003;54:653-8.
- Ballard PL, Merrill JD, Godinez RI, Godinez MH, Truog WE, Ballard RA. Surfactant protein profile of pulmonary surfactant in premature infants. *Am J Respir Crit Care Med* 2003;168:1123-8.
- Beresford MW, Shaw NJ. Bronchoalveolar lavage surfactant protein A, B, and D concentrations in preterm infants ventilated for respiratory distress syndrome receiving natural and synthetic surfactants. *Pediatr Res* 2003;53:663-70.
- Sweet DG, Carnielli V, Greisen G, Hallman M, Ozek E, Plavka R, et al. European consensus guidelines on the management of neonatal respiratory distress syndrome in preterm infants—2013 update. *Neonatology* 2013;103:353-68.
- Redline RW. Inflammatory responses in the placenta and umbilical cord. *Semin Fetal Neonatal Med* 2006;11:296-301.
- Jobe AH, Bancalari E. Bronchopulmonary dysplasia. *Am J Respir Crit Care Med* 2001;163:1723-9.
- Simonato M, Baritussio A, Carnielli VP, Vedovelli L, Falasco G, Salvagno M, et al. Influence of type of congenital heart defects on epithelial lining fluid composition in infants undergoing cardiac surgery with cardiopulmonary-bypass. *Pediatr Res* 2017;83:791-7.
- Bligh EG, Dyer WJ. A rapid method of total lipid extraction and purification. *Can J Biochem Physiol* 1959;37:911-7.
- Facco M, Nespeca M, Simonato M, Isak I, Verlato G, Ciambra G, et al. In vivo effect of pneumonia on surfactant disaturated-phosphatidylcholine kinetics in newborn infants. *PLoS ONE* 2014;9:e93612.
- Baritussio A, Alberti A, Quaglino D, Pettenazzo A, Dalzoppo D, Sartori L, et al. SP-A, SP-B, and SP-C in surfactant subtypes around birth: reexamination of alveolar life cycle of surfactant. *Am J Physiol* 1994;266:L436-47.
- Simonato M, Baritussio A, Vedovelli L, Lamonica G, Carnielli VP, Cogo PE. Surfactant protein B amount and kinetics in newborn infants: an optimized procedure. *J Mass Spectrom* 2012;47:1415-9.
- Kramer HJ, Schmidt R, Gunther A, Becker G, Suzuki Y, Seeger W. ELISA technique for quantification of surfactant protein B (SP-B) in bronchoalveolar lavage fluid. *Am J Respir Crit Care Med* 1995;152:1540-4.
- Shirole R, Kshatriya AA, Kshatriya AA, Sutariya B, Sutariya B, Saraf MN, et al. Mechanistic evaluation of butea monosperma using in vitro and in vivo murine models of bronchial asthma. *Int J Res Ayurveda Pharmacy* 2013;4:322-31.
- Lamonica G, Amigoni M, Vedovelli L, Zambelli V, Scanziani M, Bellani G, et al. Pulmonary surfactant synthesis after unilateral lung injury in mice. *J Appl Physiol* 2014;116:210-5.

22. Dargaville PA, South M, Vervaart P, McDougall PN. Validity of markers of dilution in small volume lung lavage. *Am J Respir Crit Care Med* 1999;160:778-84.
23. Engels GE, van Oeveren W. Biomarkers of lung injury in cardiothoracic surgery. *Dis Markers* 2015;2015:472360.
24. Bry K, Lappalainen U, Hallman M. Intraamniotic interleukin-1 accelerates surfactant protein synthesis in fetal rabbits and improves lung stability after premature birth. *J Clin Invest* 1997;99:2992-9.
25. D'Aronco S, Simonato M, Vedovelli L, Baritussio A, Verlato G, Nobile S, et al. Surfactant protein B and A concentrations are increased in neonatal pneumonia. *Pediatr Res* 2015;78:401-6.
26. Ikegami M, Falcone A, Whitsett JA. STAT-3 regulates surfactant phospholipid homeostasis in normal lung and during endotoxin-mediated lung injury. *J Appl Physiol* 2008;104:1753-60.
27. Griese M, Dietrich P, Reinhardt D. Pharmacokinetics of bovine surfactant in neonatal respiratory distress syndrome. *Am J Respir Crit Care Med* 1995;152:1050-4.
28. Epaud R, Ikegami M, Whitsett JA, Jobe AH, Weaver TE, Akinbi HT. Surfactant protein B inhibits endotoxin-induced lung inflammation. *Am J Respir Cell Mol Biol* 2003;28:373-8.
29. Collins JJ, Kallapur SG, Knox CL, Nitsos I, Polglase GR, Pillow JJ, et al. Inflammation in fetal sheep from intra-amniotic injection of *Ureaplasma parvum*. *Am J Physiol Lung Cell Mol Physiol* 2010;299:L852-60.
30. Kramer BW, Ladenburger A, Kunzmann S, Speer CP, Been JV, van Iwaarden JF, et al. Intravenous lipopolysaccharide-induced pulmonary maturation and structural changes in fetal sheep. *Am J Obstet Gynecol* 2009;200:e1-10.
31. Vincent JL, Dubois MJ, Navickis RJ, Wilkes MM. Hypoalbuminemia in acute illness: is there a rationale for intervention? A meta-analysis of cohort studies and controlled trials. *Ann Surg* 2003;237:319-34.
32. Yang C, Liu Z, Tian M, Xu P, Li B, Yang Q, et al. Relationship between serum albumin levels and infections in newborn late preterm infants. *Med Sci Monit* 2016;22:92-8.
33. Torer B, Hanta D, Yapakci E, Gokmen Z, Parlakgumus A, Gulcan H, et al. Association of serum albumin level and mortality in premature infants. *J Clin Lab Anal* 2016;30:867-72.
34. Groneck P, Gotze-Speer B, Oppermann M, Eiffert H, Speer CP. Association of pulmonary inflammation and increased microvascular permeability during the development of bronchopulmonary dysplasia: a sequential analysis of inflammatory mediators in respiratory fluids of high-risk preterm neonates. *Pediatrics* 1994;93:712-8.
35. Wirbelauer J, Speer CP. The role of surfactant treatment in preterm infants and term newborns with acute respiratory distress syndrome. *J Perinatol* 2009;29(Suppl 2):S18-22.
36. Czernik C, Schmalisch G, Buhner C, Proquitte H. Fetal and neonatal samples of a precursor surfactant protein B inversely related to gestational age. *BMC Pediatr* 2013;13:164.
37. Dushianthan A, Goss V, Cusack R, Grocott MP, Postle AD. Phospholipid composition and kinetics in different endobronchial fractions from healthy volunteers. *BMC Pulm Med* 2014;14:10.

Chapter 4

METABOLOMICS IN LUNG DISEASES

4.1 Metabolomics

Metabolites are small molecules (<1 kDa) that participate in chemical reactions within living organisms, and they include endogenous (amino acids, lipids, organic acids, nucleotides, etc) and exogenous (drugs, toxins) chemicals. Metabolomics is an “omic” strategy that entails the comprehensive analysis of endogenous metabolites in biological systems (metabolome) in order to describe changes related to particular stress factors such as e.g. disease or drugs. The complexity and size of the metabolome is dependent on the organism and sample type. Together with genomics, transcriptomics, proteomics, and epigenomics studies (Figure 1), metabolomics can provide more comprehensive insights into biological processes. Compared to transcriptomics and proteomics, metabolomics is ‘downstream’ which means that changes in the metabolome are amplified. It is the endpoint of the “omics cascade” and is the closest to phenotype. Moreover, metabolic profiling is cheaper allowing for the examination of large numbers of samples from organisms at specific conditions. Finally, the technology used is generic, as a given metabolite is the same in every organism that contains it.[1]

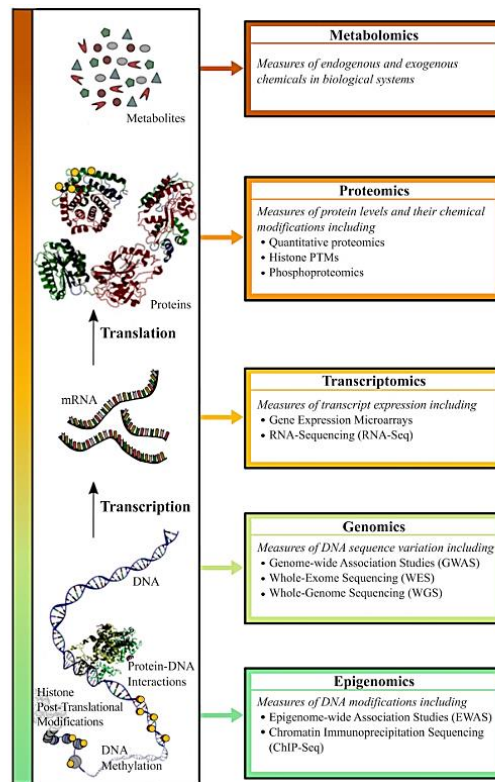


Figure 1. Omic science: biological levels with corresponding omics techniques used for their characterization[2]

Thanks to increasing awareness of the central role of metabolic pathways in biological processes, metabolomics approach have been applied in many fields of health research, including prenatal and infant health[3–5]. The rising number of publications demonstrates that metabolomics is a valuable emerging tool to study phenotype changes caused by environmental influences, disease, or changes in genotype. To this aim, a wide range of biological samples have been used for metabolomics studies, including blood serum and plasma, urine, tissues, cells, amniotic fluid, and cerebrospinal fluid[6].

There are three commonly used analytical metabolomics approaches[7]:

Untargeted assays are used for discovery/hypothesis generating studies, aiming to measure as many metabolites as possible (low thousands of metabolites) and provide semi-quantitative data. The chemical identity of metabolites is not necessarily known before data are acquired. Samples are prepared to minimize loss of any metabolites and identification is performed post hoc. Untargeted metabolomics is applied to discover a single metabolite biomarker or a group of metabolites acting as a biomarker panel or to discover new molecular pathophysiological mechanisms. The typical untargeted metabolomics workflow is shown in Figure 2.

Targeted assays are applied to test a hypothesis and focus on a small number (typically <20) of biologically important metabolites whose chemical identity is known prior to data acquisition, and for which an absolute concentration of each metabolite is reported through the use of isotopically labelled internal standards. It requires a more intensive sample preparation compared to untargeted studies and provides the separation of analytes from the sample matrix and other metabolites.

Semi-targeted assays are also used for hypothesis testing and it is an intermediate approach between untargeted and targeted assays, where low hundreds of metabolites are targeted, whose chemical identity is known prior to data acquisition, and for which semi-quantification is applied to define approximate metabolite concentrations (typically applying one calibration curve and internal standard for multiple metabolites).

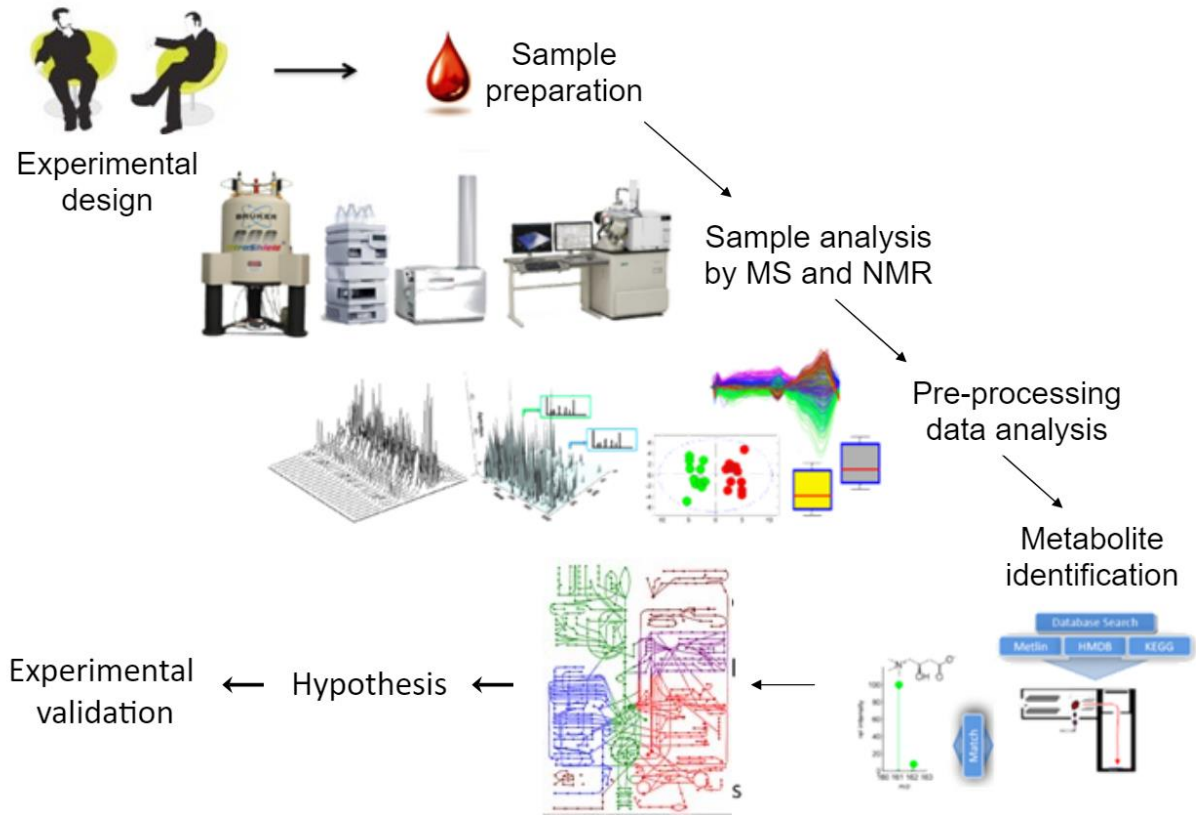


Figure 2. Untargeted metabolomic workflow

4.2 Metabolomics application for lung diseases

Since metabolomics approaches can elucidate the pathophysiological changes related to inflammation and structural disease, they have been used to understand different pulmonary diseases. In acute respiratory distress syndrome patients, metabolomics revealed altered pathways associated with amino acid metabolism, glycolysis and gluconeogenesis, fatty acid biosynthesis, phospholipids and purine metabolism[8]. Fabiano et al conducted a preliminary study to analyze metabolic profiles on the bronchoalveolar lavage fluid (BALF) of preterm infants complicated by RDS[9]. Other authors reported specific metabolic profiles characterizing the development of bronchopulmonary dysplasia[10, 11]. Given the phenotypic heterogeneity observed in asthma, developments in metabolomics were exploited in the attempts to improve the diagnosis of this disease. Several candidate biomarkers have been identified, validating the value of metabolomics in asthma diagnosis[12, 13]. Chronic childhood interstitial lung diseases represent a large spectrum of parenchymatous diseases, prevalent in children. Since many of these diseases directly affect components the pulmonary surfactant system, the investigation of lipid and metabolite profiles could help in uniquely classify them[14]. Finally, metabolomic profiling has allowed discovery of new pathways implicated in cystic fibrosis, including purines, mitochondrial pathways, and different aspects of glucose metabolism[15].

Although, many compounds have been identified as potential biomarkers, none of them has yet been introduced in routine clinical practice. This is due to a lack of standardization of sampling and analysis to ensure reproducibility and to the need of validation in large, independent cohorts. On the other hand, these preliminary studies can be a valuable tool for improving pathophysiological knowledge.[16].

A wide range of biological samples have been used for pulmonary disease metabolomics studies, including blood serum and plasma, induced sputum, exhaled breath condensate, BALF, and lung tissue. Urine and blood are the most commonly used biofluids, as both samples contain thousands of detectable metabolites and can be obtained via non-invasive and minimally invasive methods. A limitation with these biofluids is that the concentration of molecules can be influenced by an inflammatory state in other parts of the body; hence, these are not lung specific. Sputum[17] and BALF/tracheal aspirates[18] reflect the composition of lung epithelial lining fluid (ELF), which represents the first barrier between the lung and the external environment. Moreover, changes in ELF composition have been reported to be involved in the onset of lung diseases. Thus, these matrices result more accurate for the investigation of pulmonary diseases, but untargeted metabolomic studies for are still scarce[8, 17, 19, 20].

Regardless of the disease and matrix, most of the putative indicators of disease states are found to be lipid metabolites. This makes sense in pathophysiological terms because many of the mediators involved in inflammation or its resolution are derived from lipids. Hence, lipidomics may be of particular value.

4.3 Liquid chromatography-mass spectrometry based metabolomics

Despite the advances in high-throughput profiling techniques, there is no single-instrument platform that currently can analyze all metabolites. These compounds are very different in their physical and chemical properties and occur in a wide concentration range.

Numerous analytical platforms have been used for metabolomic applications, such as nuclear magnetic resonance (NMR)[21], Fourier transform-infrared spectroscopy (FT-IR)[22, 23] and mass spectrometry (MS) coupled to separation techniques or using direct flow injection. The great advantages of NMR are that sample preparation is minimal, and that it is a non-discriminating and non-destructive technique. However, only medium to high abundance metabolites will be detected with this approach and the identification of individual metabolites is challenging in complex mixtures.

MS-based metabolomics offers quantitative analyses with high selectivity and sensitivity and the potential to identify metabolites. Combination with a separation technique (Gas-chromatography, GC, and liquid-chromatography, LC) reduces the complexity of the mass spectra due to metabolite separation in a time dimension, provides isobar separation, and delivers additional information on the physico-chemical properties of the metabolites. However, MS-based techniques usually require a sample preparation step, which can cause metabolite losses, and based on the sample introduction system and the ionization technique used, specific metabolite classes may be discriminated[24]. Therefore, combined application of several technique allows for studying the metabolome more comprehensively.

LC can reduce ion suppression caused by coeluting compounds, isobaric interferences in the case of low- resolving mass analyzers, often can separate isomers, and reduce the background noise, thus improving MS data quality. Among LC techniques, reversed phase chromatography is a standard tool for the separation of medium polar and non- polar analytes. Reversed phase chemistries start with a high aqueous content mobile phase and the organic phase fraction is increased, typically operating from 100% aqueous to 100% organic. The organic solvent is typically either MeOH or ACN (or IPA)

and modifiers (e.g. formic acid, ammonium acetate, etc) can improve separation, resolution or the detection. The use of reversed-phase chemistries provides efficient retention and separation of relatively nonpolar metabolites across a large molecular weight range (50 to > 1,500) and includes high-molecular-weight lipid species (e.g., phospholipids and triglycerides) and nonpolar amino acids (e.g., tryptophan). It typically applies a C18 column, but C8 or C30 columns can also be applied depending on the application: C8 columns will retain hydrophilic metabolites to a greater degree C30 columns will provide greater chromatographic specificity and resolution for lipids. However, very polar metabolites are not retained and elute with the void volume. To overcome the problem, Tolstikov and Fiehn[25] reported the use of hydrophilic interaction chromatography (HILIC) for the analysis of highly polar compounds. HILIC uses either pure silica, amino or amide, cationic or anionic stationary phases, and a high % organic to approximately 50% water. It allows for improved sensitivity for electrospray (ESI) mass spectrometry and a very different retention mechanism which is still not fully understood. Polar surface is hydrated to create a biphasic liquid-liquid system. Separation influenced by partitioning between phases, hydrogen donor interactions, weak electrostatic interactions, and it is based on compound polarity and degree of water solvation.

LC-MS based metabolomics studies have been performed using different mass analyzers including ion trap and Orbitrap instruments (Figure 3)[25, 26], triple quadrupole instruments[27], and quadrupole time of flight (Q-TOF) instruments[28, 29]. Triple quadrupole or Q-TOF analyzers provide the ability to perform MS/MS experiments for the structural elucidation of biomarkers. Ion trap instruments have the advantage of MSⁿ capabilities.

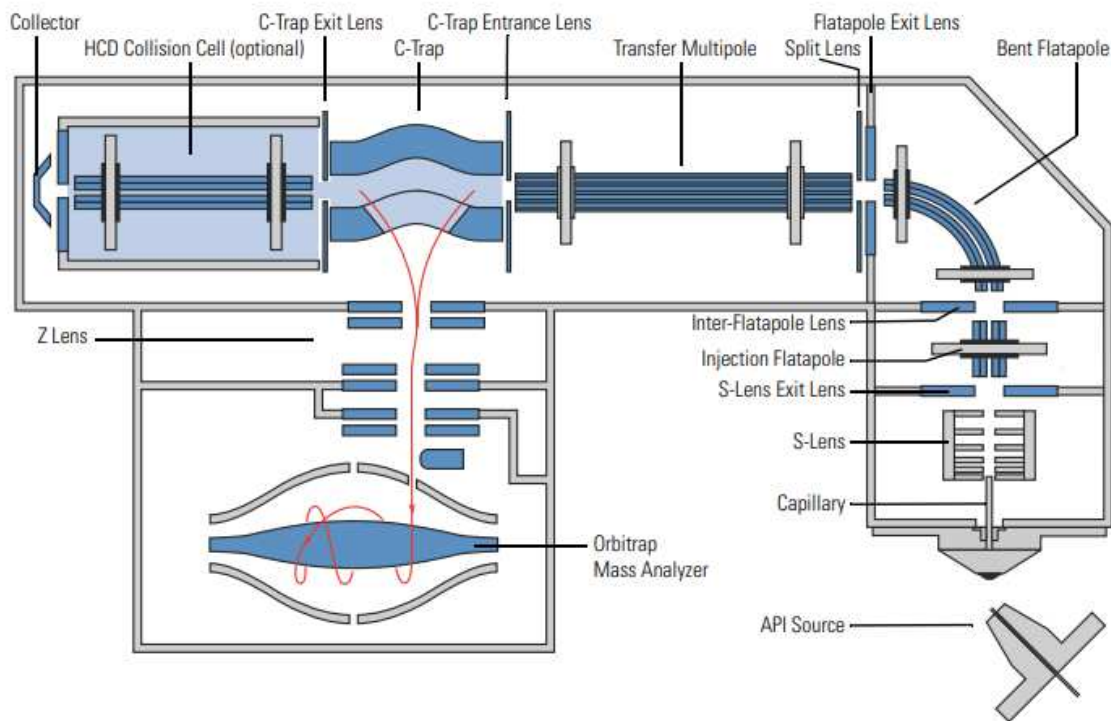


Figure 3. Scheme of a hybrid-quadrupole Orbitrap (Q exactive, Thermo Fisher scientific, Bremen, Germany): the flatapole filters the masses and isolate targeted precursor that subsequently fragmented in the HCD cell and mass analyzed in the Orbitrap

Mass analyzers measure the mass-to-charge (m/z) ratio of metabolites. Most metabolites can only carry a single charge and therefore mass is measured directly. Ions of different m/z are manipulated by electrical or magnetic forces to traverse different paths before detection. One or multiple components operates under high vacuum and the vacuum allows for the ions focusing by removing the gases from the system. Resolving power is a measure of a mass spectrometer's ability to separate ions according to their m/z value. High resolving power allows the distinction between ions of very similar m/z values and allows more confident identification due to increased ability to perform accurate mass measurements. But higher mass resolution corresponds to longer time of analysis. The ionization technique of choice for LC-MS based metabolomics is ESI ionization since it is suitable for ionizing a wide range of molecules. It is a soft ionization technique and imparts very little energy to the analyte leading to no/little in source fragmentation. Can form positive or negative ions via:

- protonation and deprotonation i.e. $[M + H]^+$ or $[M - H]^-$
- adduct formation
- Cationisation in positive ESI e.g. $[M + Na]^+$

- Anionisation in negative ESI e.g. $[M + Cl]^-$

In order to obtain a broad coverage of the metabolome, ionization must be performed in positive and negative mode.

The high selectivity of mass spectrometers in combination with low-detection limits, as well as their compatibility with separation techniques and their ability to deliver quantitative data makes mass spectrometry an ideal tool for metabolomic applications[24].

During my PhD, an LC-ESI-MS/MS untargeted metabolomic approach was used to assess changes in metabolic and lipid profiles in infants with RDS exposed to chorioamnionitis. This part of the PhD project was developed during a 6-month training period at the University of Birmingham – School of Biosciences, under the supervision of Prof. Warwick Dunn. I reported in this chapter the manuscript with the results of the study. The manuscript draft is currently under approval from all the authors and it is going to be submitted in the next few weeks.

Bibliography

1. Kell DB, Brown M, Davey HM, Dunn WB, Spasic I, Oliver SG. Metabolic footprinting and systems biology: The medium is the message. *Nat Rev Microbiol.* 2005; 3:557–565.
2. Kan M, Shumyatcher M, Himes BE. Using omics approaches to understand pulmonary diseases. doi: 10.1186/s12931-017-0631-9
3. Chen T, He P, Tan Y, Xu D. Biomarker identification and pathway analysis of preeclampsia based on serum metabolomics. *Biochem Biophys Res Commun.* 2017; 485:119–125.
4. Diaz SO, Pinto J, Barros AS, Morais E, Duarte D, Negrão F, Pita C, Almeida M do C, Carreira IM, Spraul M, Gil AM. Newborn urinary metabolic signatures of prematurity and other disorders: a case control study. *J Proteome Res.* 2016; 15:311–325.
5. Virgiliou C, Gika HG, Witting M, Bletsou AA, Athanasiadis A, Zafrakas M, Thomaidis NS, Raikos N, Makrydimas G, Theodoridis GA. Amniotic fluid and maternal serum metabolic signatures in the second trimester associated with preterm delivery. *J Proteome Res.* 2017; 16:898–910.
6. Chetwynd AJ, Dunn WB, Rodriguez-Blanco G. Collection and preparation of clinical samples for metabolomics. Springer, Cham, pp 19–44
7. Dunn WB, Broadhurst DI, Atherton HJ, Goodacre R, Griffin JL. Systems level studies of mammalian metabolomes: the roles of mass spectrometry and nuclear magnetic resonance spectroscopy. *Chem Soc Rev.* 2011; 40:387–426.
8. Evans CR, Karnovsky A, Kovach MA, Standiford TJ, Burant CF, Stringer KA. Untargeted LC-MS metabolomics of bronchoalveolar lavage fluid differentiates acute respiratory distress syndrome from health. *J Proteome Res.* 2014; 13:640–9.
9. Fabiano A, Gazzolo D, Zimmermann LJI, Gavilanes AWD, Paolillo P, Fanos V, Caboni P, Barberini L, Noto A, Atzori L. Metabolomic analysis of bronchoalveolar lavage fluid in preterm infants complicated by respiratory distress syndrome: Preliminary results. *J Matern Neonatal Med.* 2011; 24:56–59.
10. Fattuoni C, Pietrasanta C, Pagni L, Ronchi A, Palmas F, Barberini L, Dessì A, Pintus R, Fanos V, Noto A, Mosca F. Urinary metabolomic analysis to identify preterm neonates exposed to histological chorioamnionitis: A pilot study. *PLoS One.* 2017; 12:1–15.

11. Baraldi E, Giordano G, Stocchero M, Moschino L, Zaramella P, Tran MR, Carraro S, Romero R, Gervasi MT. Untargeted metabolomic analysis of amniotic fluid in the prediction of preterm delivery and bronchopulmonary dysplasia. *PLoS One*. 2016; 11:e0164211.
12. Sinha N, Viswan A, Singh C, Rai RK, Azim A, Baronia AK. Metabolomics based predictive biomarker model of ARDS: A systemic measure of clinical hypoxemia. *PLoS One*. 2017; 12:e0187545.
13. Carraro S, Rezzi S, Reniero F, Héberger K, Giordano G, Zanconato S, Guillou C, Baraldi E. Metabolomics Applied to Exhaled Breath Condensate in Childhood Asthma. *Am J Respir Crit Care Med*. 2007; 175:986–990.
14. Griese M, Kirmeier HG, Liebisch G, Rauch D, Stückler F, Schmitz G, Zarbock R. Surfactant lipidomics in healthy children and childhood interstitial lung disease. *PLoS One*. 2015; 10:1–18.
15. Muhlebach MS, Sha W. Lessons learned from metabolomics in cystic fibrosis. *Mol Cell Pediatr*. 2015; 2:9.
16. Devillier P, Salvator H, Naline E, Couderc L-J, Grassin-Delyle S. Metabolomics in the diagnosis and pharmacotherapy of lung diseases. *Curr Pharm Des*. 2017; 23:.
17. Brandsma J, Goss VM, Yang X, Bakke PS, Caruso M, Chanez P, Dahlén S-E, Fowler SJ, Horvath I, Kруг N, Montuschi P, Sanak M, Sandström T, Shaw DE, Chung KF, Singer F, Fleming LJ, Sousa AR, Pandis I, Bansal AT, Sterk PJ, Djukanović R, Postle AD. Lipid phenotyping of lung epithelial lining fluid in healthy human volunteers. *Metabolomics*. 2018; 14:123.
18. Dargaville PA, South M, McDougall PN. Comparison of two methods of diagnostic lung lavage in ventilated infants with lung disease. *Am J Respir Crit Care Med*. 1999; 160:771–777.
19. Piersigilli F, Bhandari V, Lam TT, Vernocchi P, Aghai ZH, Quagliariello A, Putignani L. Identification of new biomarkers of bronchopulmonary dysplasia using metabolomics. *Metabolomics*. 2019; 15:0.
20. Lal CV, Kandasamy J, Dolma K, Ramani M, Kumar R, Wilson L, Aghai Z, Barnes S, Edwin Blalock J, Gaggar A, Bhandari V, Ambalavanan N. Early airway microbial metagenomic and metabolomic signatures are associated with development of severe bronchopulmonary

- dysplasia. *Physiol Am J Physiol Lung Cell Mol Physiol*. 2018; 315:810–815.
21. Nicholson JK, Wilson ID. Understanding “global” systems biology: metabonomics and the continuum of metabolism. *Nat Rev Drug Discov*. 2003; 2:668–676.
 22. Harrigan GG, LaPlante RH, Cosma GN, Cockerell G, Goodacre R, Maddox JF, Luyendyk JP, Ganey PE, Roth RA. Application of high-throughput Fourier-transform infrared spectroscopy in toxicology studies: contribution to a study on the development of an animal model for idiosyncratic toxicity. *Toxicol Lett*. 2004; 146:197–205.
 23. Johnson HE, Broadhurst D, Kell DB, Theodorou MK, Merry RJ, Griffith GW. High-throughput metabolic fingerprinting of legume silage fermentations via Fourier transform infrared spectroscopy and chemometrics. *Appl Environ Microbiol*. 2004; 70:1583–92.
 24. Dettmer K, Aronov PA, Hammock BD. Mass spectrometry-based metabolomics. *Mass Spectrom Rev*. 2007; 26:51.
 25. Tolstikov V V., Fiehn O. Analysis of Highly Polar Compounds of plant origin: combination of hydrophilic interaction chromatography and electrospray ion trap mass spectrometry. *Anal Biochem*. 2002; 301:298–307.
 26. Ancillotti C, Ulaszewska M, Mattivi F, Del Bubba M. Untargeted metabolomics analytical strategy based on liquid chromatography/electrospray ionization linear ion trap quadrupole/orbitrap mass spectrometry for discovering new polyphenol metabolites in human biofluids after acute ingestion of *Vaccinium myrtillus* berry supplement. *J Am Soc Mass Spectrom*. 2019; 30:381–402.
 27. Idborg-Björkman H, Edlund P-O, Kvalheim OM, Schuppe-Koistinen I, Jacobsson SP. Screening of biomarkers in rat urine using LC/Electrospray Ionization-MS and two-way data analysis. *Anal Chem*. 2003; 75:4784–47892.
 28. Gooding J, Cao L, Ahmed F, Mwiza J-M, Fernander M, Whitaker C, Acuff Z, McRitchie S, Sumner S, Ongeri EM. LC-MS-based metabolomics analysis to identify meprin β -associated changes in kidney tissue from mice with STZ-induced type 1 diabetes and diabetic kidney injury. *Am J Physiol Physiol*. 2019; ajprenal.00166.2019.
 29. Nagai K, Uranbileg B, Chen Z, Fujioka A, Yamazaki T, Matsumoto Y, Tsukamoto H, Ikeda H, Yatomi Y, Chiba H, Hui S, Nakazawa T, Saito R, Koshiha S, Aoki J, Saigusa D, Tomioka Y. Identification of novel biomarkers of hepatocellular carcinoma by a high definition mass

spectrometry; UHPLC-QTOF/MS and DESI-MSI. Rapid Commun Mass Spectrom. 2019; rcm.8551.

CHORIOAMNIONITIS EFFECTS ON LUNG SURFACTANT LIPIDOME IN NEWBORNS WITH RESPIRATORY DISTRESS SYNDROME

Sonia Giambelluca¹⁾²⁾, Giovanna Verlatto¹⁾, Manuela Simonato²⁾³⁾, Luca Vedovelli²⁾, Luca Bonadies¹⁾, Lukáš Najdekr⁵⁾, Warwick B. Dunn⁵⁾⁶⁾, Virgilio P. Carnielli⁴⁾, Paola Cogo⁷⁾

1) Padova University Hospital, Department of Women's and Children's Health. Padova, Italy.

2) Fondazione Istituto di Ricerca Pediatrica Città della Speranza, PCare Laboratory. Padova, Italy.

3) Institute of Anesthesiology and Intensive Care, Department of Medicine – DIMED, University of Padova; Padova, Italy.

4) Polytechnic University of Marche and Azienda Ospedaliero-Universitaria Ospedali Riuniti, Division of Neonatology, Department of Clinical Sciences. Ancona, Italy.

5) School of Biosciences, Phenome Centre Birmingham and Institute for Metabolism and Systems Research, University of Birmingham, Birmingham, B15 2TT, UK.

6) Institute for Metabolism and Systems Research, University of Birmingham, Birmingham, B15 2TT, UK

7) University of Udine, Department of Medicine, Udine, Italy.

Corresponding author: Manuela Simonato, Fondazione Istituto di Ricerca Pediatrica Città della Speranza, PCare Laboratory. Corso Stati Uniti, 4F – 35127, Padova, Italy. Tel: +390498211477, Fax: +390499640146 Email: m.simonato@irpcds.org

Author Contributions: Conception and design: V.P.C, P.C., W.B.D. Patient recruitment and data collection: G.V., L.B.. Laboratory experiments: S.G., L.N., L.V. Analysis and interpretation: S.G., W.B.D., P.C., M.S. Drafting of the manuscript: S.G, P.C. Revision of the manuscript and final approval: all authors.

Funding: The study was performed with no specific financial support.

Running title: Chorioamnionitis and lung surfactant lipidome

Subject category: 4.11 Pediatric Critical Care

At a Glance Commentary

Scientific Knowledge on the Subject: Chorioamnionitis is associated with significant maternal, perinatal, and long-term adverse outcomes, including premature birth, neonatal sepsis, and brain injury. However, the relationships between chorioamnionitis and pulmonary outcomes, such as respiratory distress syndrome, for preterm infants remains to be clarified.

What This Study Adds to the Field: Our lipidomics investigation on tracheal aspirates of preterm newborns at birth have suggested that exposure to maternal histological chorioamnionitis may cause changes in epithelial lining fluid composition. These results could provide novel link between placental membrane inflammation and respiratory outcome of the newborn.

CONFIDENTIAL DRAFT

ABSTRACT

Rationale: Chorioamnionitis is an inflammation of fetal membranes often associated with preterm delivery and morbidities. The role in lung disease is controversial.

Objectives: To assess the effect of chorioamnionitis on metabolite and lipid profiles of epithelial lining fluid in preterm newborns with respiratory distress syndrome (RDS).

Methods: The study involved 30 newborns with RDS, born from mothers with or without histological chorioamnionitis (HCA): HCA+, N=10; HCA-, N=20. Patients had a gestational age ≤ 30 weeks and the groups were matched for age and birth weights. Tracheal aspirates were collected within the first 24h after birth and analyzed using liquid chromatography/mass spectrometry based untargeted lipidomics. Blank samples were used to exclude contaminants and QC samples were used to determine within-experiment precision. Differences between groups were assessed by univariate and multivariate analysis.

Measurements and Main Results: After data filtering, we detected over 4000 unique metabolite features. According to Mann-Whitney U tests, 570 metabolite features had statistically significantly higher or lower concentrations ($p < 0.05$) in the tracheal aspirates of HCA+ compared to HCA-, and 246 metabolite features were putatively annotated and classified. The most relevant changes among complex lipids involved higher levels of glycerophospholipids (56% of increased annotated metabolites, fold-change 2.42-17.69) and sphingolipids, with lower concentration of all annotated sphingomyelins in HCA+ (fold-change 0.01-0.50).

Conclusions: Untargeted lipidomic profiling of tracheal aspirates have suggested changes in specific areas of lipid metabolism that are involved in the processes of angiogenesis and cell apoptosis. However, the effect of chorioamnionitis on epithelial lining fluid composition deserves further investigations on a larger group of preterm infants.

Word count: 248

Keyword: Intrauterine inflammation, lung disease, tracheal aspirate, preterm infants, lipidomics

INTRODUCTION

Chorioamnionitis is a complication of pregnancy characterized by neutrophil infiltration in the fetal membranes, with or without a fetal inflammatory response (1). It is characterized by the passage of organisms most commonly from the cervix or the vagina to the chorioamnion (2), and the fetal response will depend on both the type of organism and the duration of fetal exposure (3). It is a major risk factor for preterm delivery (4), with an incidence inversely related to gestational age (GA) (1), and it has been associated with adverse perinatal outcome in preterm infants (5–7). The association with lung disease remains to be clarified. It has been reported that chorioamnionitis correlates with both a decreased risk of respiratory distress syndrome (RDS) and an increased risk of chronic lung disease in preterm infants (8, 9). However, other studies reported no specific effects on the development of chronic lung diseases (10).

RDS is a breathing disorder characterised by lung immaturity and deficiency of lung surfactant, the lipoprotein component of epithelial lining fluid (ELF). In animal models, experimentally induced chorioamnionitis with intra-amniotic application of endotoxin or IL-1 is associated with increased lung maturation in sheep (11, 12) and an increase in surfactant lipids (13) and mRNA for surfactant proteins (14). This is in agreement with the decreased incidence of RDS and the lower early oxygen requirement found in preterm infants exposed to chorioamnionitis. On the other hand, the exposure to intrauterine infection seems to make the fetal lung prone to cytokine-mediated inflammation, along with a subsequent increased risk of chronic lung diseases (15).

Lipidomics and metabolomics are good approaches to identify metabolic changes related to a particular pathophysiological state. A pilot study on metabolomics of urines from preterm newborns born from mothers with or without histological chorioamnionitis (HCA), reported a decrease in concentration for 29 metabolites related to mitochondrial electron transport chain, citric acid cycle, glutamate and carbohydrate metabolism in newborns exposed to chorioamnionitis (16).

When ethically feasible, the use of biospecimen closer to the target organ is usually preferable to proximal biofluids, such as plasma or urine, to investigate specific metabolic perturbations (17). Tracheal aspirates (TAs) are good proxies of ELF composition (18) and could reflect in a more accurate way the effect of intrauterine inflammation on newborn lungs. We recently reported that preterm newborns exposed to HCA had higher concentrations of ELF disaturated phosphatidylcholine (DSPC), surfactant protein B, and myeloperoxidase activity, suggesting a stimulated lung maturation in these babies (19). Moreover, exposure to chorioamnionitis was associated to an elevated presence of pro-inflammatory cells, cytokines and prostaglandins in TAs (7, 8). However, information on TAs metabolomics are scarce (20, 21).

The aim of the present study was to assess the effect of chorioamnionitis on the lipid profiles of TAs in preterm newborns affected by RDS.

METHODS

Study population

The study protocol was approved by the Local Ethics Committee (Prot. n. 1591P) and informed consent was obtained from parents. Prospective recruitment took place from 2014 to 2017 at the Neonatal Intensive Care Unit of the Department of Women's and Children's Health, University Hospital of Padova, and at the Neonatal Intensive Care, Salesi Children's Hospital, Ancona, Italy. Selected case infants were preterm newborns with GA >23 and ≤30 weeks who needed intubation for RDS and met the following criteria at delivery: blood pH >7.20, 5-min Apgar score ≥5, cesarean section delivery to minimize the risk of perinatal hypoxic-ischemic insult. Exclusion criteria were: severe congenital malformations, chromosomal abnormalities, lack of placenta histological examination report.

Based on the diagnosis for HCA, infants were divided in two groups: positive for HCA (HCA+) or negative for HCA (HCA-). In HCA+ group, 9 out of 10 mothers also had clinical diagnosis of chorioamnionitis. The two groups were matched for gestational age, birth weight and sex. Criteria for the diagnosis of RDS, clinical chorioamnionitis and HCA are provided in online data supplement. The basic clinical characteristics are reported in Table 1.

Sample collection

TAs were collected within the first 24h of life, immediately after intubation and before exogenous surfactant administration, as previously reported (22).

Leftover blood from arterial blood gas analysis was collected contemporarily to the TA sample. Further details can be found in online data supplement.

Urea analysis

Plasma and TAs urea was analyzed using a colorimetric assay (QuantiChrom™ Urea Assay kit, BioAssay Systems, Hayward, CA).

Untargeted metabolomics analysis

Sample preparation

Sample preparation is detailed in online data supplement. Briefly, two different aliquots of TA sample were deproteinized adding cold HPLC-grade acetonitrile (ACN) or 2-isopropanol (IPA) for water-soluble metabolite and lipid profiling, respectively. An aliquot from each deproteinized sample was pooled to construct a pooled Quality Control (QC) sample (23). Process blank samples were prepared using the same solvent and procedure used for TA samples but with the absence of any biological sample.

Sample analysis

UHPLC-MS(/MS) analysis were performed on a Vanquish UHPLC system (Thermo Fisher Scientific, Bremen, Germany) coupled to an electrospray (ESI) Q Exactive Plus mass spectrometer (Thermo Fisher scientific, Bremen, Germany) for water-soluble metabolite profiling (HILIC ESI+ and HILIC ESI-) and lipid profiling (LIPIDS ESI+ and LIPIDS ESI-). Details are provided in online data supplement.

Data processing and statistical analysis

Data processing was performed for each analytical batch (LIPIDS ESI+, LIPIDS ESI-, HILIC ESI+, and HILIC ESI-), separately. The filtered and normalized datasets were analyzed in MetaboAnalyst (24) applying the unsupervised multivariate analysis technique Principal Components Analysis (PCA). Volcano plots were constructed to assess statistically significant differences between the two groups ($p\text{-value} < 0.05$ and fold change (FC) $\text{HCA}^+/\text{HCA}^- < 0.9$ or > 1.1). Volcano plot analysis was repeated applying correction for false discovery rate (FDR) using Benjamini-Hochberg procedure (adjusted $p\text{-value}$ threshold 0.05). Statistically significant metabolite features were annotated according to level 2 of the MSI reporting standards (25) using in-house software at the University of Birmingham (BEAMS). Further details are provided in the online data supplement.

RESULTS

TA samples from 30 newborns affected by RDS and born from mothers with HCA (HCA+, N=10) or without HCA (HCA-, N=20) were analyzed via UHPLC/ESI-MS untargeted metabolomic and lipidomic approaches in both ESI+ and ESI-. The use of four complementary UHPLC/ESI-MS assays provided a broad coverage of water-soluble (HILIC ESI+ and HILIC ESI-) and lipid (LIPIDS ESI+ and LIPIDS ESI-) metabolites.

After data filtering using blank and pooled QC samples, we detected over 4000 unique features across all four datasets. The PCA analysis for each dataset (LIPIDS ESI+, LIPIDS ESI-, HILIC ESI+,

HILIC ESI-) showed a tight clustering for pooled QC samples relative to the observed dispersion of biological samples, reflecting a system stability and reproducibility of sample preparation (Fig 1). Small deviations from the origin of the PCA score plot can be due to sample weight discrepancies, since normalization for TA samples dilution factor was performed post-acquisition, during data processing. According to PCA, a sample from HCA+ group (HCA+_8) was observed to be an outlier for both lipid ESI+ and lipid ESI-, and it was removed from both lipid datasets prior to statistical analysis. Three samples (1 from HCA+ group and 2 from HCA- group) were removed from the HILIC ESI+ dataset since the number of metabolite features detected was <20% of the average for all biological samples.

Taken together, the Volcano plot analyses for the 4 datasets identified a total of 570 metabolite features present at a statistically significantly higher or lower concentration in ELF of group HCA+ compared to HCA-. Most of these metabolite features were detected by lipid profiling (334 and 125 for LIPIDS ESI+ and LIPIDS ESI-, respectively), with a lower contribution from water-soluble metabolite profiling (36 and 75 for HILIC ESI+ and HILIC ESI-, respectively). Of the 570 statistically different metabolic features, 246 were putatively annotated and classified (Fig 2). The list of putatively annotated compounds present at lower or higher concentrations in HCA+ with obtained fold change and p-value is reported in Tables E1 and E2 in the online data supplement, respectively. Of the 110 metabolites present at a statistically significantly higher concentration in the ELF of the HCA+ group, 56% was represented by glycerophospholipids (FC 2.42-17.69) and 12% by ceramides (FC 2.12-46.71). Among the 136 metabolites present at a statistically significantly lower concentration in the ELF of the HCA+ group, sphingolipids covered the highest percentage (24%), with 16 sphingomyelins (SMs, FC 0.01-0.50) and 16 ceramides (FC 0.07-0.52), 16% were glycerophospholipids (FC 0.10-0.73), 8% diacylglycerides (DGs, FC 0.14-0.71), 6% short chain (chain length C2-C8) acyl carnitines (FC 0.29-0.53) and about 5% metabolites associated to ubiquinone or other terpenoid-quinone biosynthesis (FC 0.33-0.57).

After applying correction for FDR to the volcano plot analysis, only two unique features were statistically significant. One was putatively annotated as a sphingomyelin (FC 0.01, adjusted p-value 0.046), the second one was unidentified (FC 0.19, adjusted p-value 0.046).

DISCUSSION

Fetal exposure to maternal HCA can affect fetal development resulting in poor outcome for the newborn, such as the onset of neonatal sepsis or increased incidence of early neurologic insults. The association between HCA and lung diseases have been extensively studied, but the results remain

inconsistent. The aim of this study was to explore changes in lipidomic and metabolomic profiles in preterm infants with and without HCA. We observed statistically significant changes in lipid and metabolic profiles between the two groups, although there were only two metabolites that were statistically significantly different when a false discovery rate correction was applied.

Most of the ELF changes were lipids. In lungs, lipids play crucial roles in many processes with unique profiles across lung cell types (26, 27). They represent the primary component of pulmonary surfactant (~90%), with glycerophospholipids being the most represented species (~80–85% by weight) and DSPC accounting for about 50% of total phospholipids. Of the DSPCs, DPPC is the most abundant species (28). We recently reported a higher DSPC concentration in ELF of newborns exposed to HCA compared to age-matched infants born from HCA- mothers (19). In the present study, ELF dipalmitoyl-phosphatidylcholine (DPPC) ([M+H]⁺, m/z 734.5689, rt 415.09) was not statistically different between the two groups, although the median peak intensity of the feature putatively annotated as DPPC was higher in HCA+ (4.7E+11 [1.5E+11-1.1E+12]) than in HCA- (2.8E+10 [1.6E+10-1.9E+11]), according to the hypothesis of a stimulated lung maturation mediated by the prenatal infection. Moreover, 76 different glycerophospholipids were at higher concentration in the HCA+ group. Among these, 16 were phosphatidylserines (PS). The exact physiological role of PS in lung function and surfactant metabolism is not completely understood, although it has been reported that Ca²⁺-PS-dependent protein kinase may be involved in the initiation or regulation of synthesis of surfactant components, in particular phosphatidylcholine in fetal lung cells (29). Phosphatidylglycerol (PG) is the second most abundant lipid species in lung surfactant (up to 11% of lipids), primarily esterified by palmitate (C16:0) and oleate (C18:1 ω 9). PG enhances the spread of PL on the alveolar surface, but it is usually detectable only near term. At this stage, the higher presence of PG species having longer unsaturated chains, together with other acidic PLs, such as phosphatidylinositols (PI), could be related to enhanced innate immune response in HCA+ babies since it has been reported that PG and PI inhibit infection and inflammatory responses in the lung (30–32). Complex glycerophospholipids containing long-chain polyunsaturated fatty acids have been reported in fetal mice lung (33) and have been linked to inflammatory processes, acting as substrates for the generations of lipid mediators having both pro-inflammatory and pro-resolution functions (34).

Sphingolipids represent a small portion (2-3%) of structural lipids of lung surfactant. However, their concentration may increase in the setting of acute or chronic lung injury and during lung development and they have been used as a marker for both pulmonary development and disease (35). In particular, sphingomyelin (SM) levels increase during lung development in rats with the highest levels at birth, due to both an increase in its rate of biosynthesis, and a decreased activity of enzymes involved in SM

degradation (36). The bioactive sphingolipids also include ceramides, sphingosine, sphingosine-1-phosphate (S1P), ceramide-1-phosphate, and others. Ceramides are the center of sphingolipid metabolism and can be synthesized by three main pathways: *de novo* synthesis from serine and palmitoyl co-enzyme A, hydrolysis of SM by sphingomyelinases and reversible production from sphingosine by ceramide synthase in the recycling pathway (salvage pathway). In the salvage pathway, ceramides are also the precursor to sphingosine, which in turn can be phosphorylated into S1P by sphingosine kinase (37). The increase of S1P promotes cell survival, proliferation, migration, and angiogenesis (38), thus playing an important role in alveolar-capillary development during lung maturation. Interestingly, in this study, all the annotated SMs were decreased in the HCA+ group, while long chain ceramides were significantly increased and very long chain ceramides significantly decreased, as it has been previously reported in mice postnatal lung development and in humans with chronic lung diseases (39, 40). Moreover, putatively annotated sphingosine d18:1 ([M+H]⁺, m/z 300.2898, rt 182.91 sec) was detected in 67% of HCA+ patients versus 35% in HCA- group, with higher intensity in HCA+ (2.4E+07 [1.4E+07-4.0E+07]) than in HCA- (7.2E+06 [4.5E+06-1.5E+07]). Thus, from this preliminary work it is conceivable to hypothesize a tendency to an enhanced pro-apoptotic pro-autophagic sphingolipid signaling in HCA+ preterm human lungs already occurring prenatally, as described in an HCA animal model, where the activation of acid-sphingomyelinase has been demonstrated with the generation of ceramides (41).

Additionally, among annotated ceramides, galabiosylceramides/lactosylceramides (LacCer) showed the strongest significant FC (up to 46.7) in TAs of the HCA+ group. This is in agreement with data obtained in amniotic fluid metabolomics of HCA+ women, where LacCer(d18:1/16:0) and LacCer(d18:1/24:1) were suggested as biomarker candidates for predicting subclinical chorioamnionitis (42).

Among the other classes of metabolites, carnitine and short chain acylcarnitines (C2-C8) were lower in ELF of HCA+ newborns. Carnitines are present in cells and tissues as both free carnitine and acylcarnitines, and its most widely known function is the transport of long-chain fatty acids into mitochondria for β -oxidation. However, other possible roles have been reported. Short-chain acylcarnitines have been previously described in both lung and bronchoalveolar lavages in a murine model of influenza pneumonia, indicating a possible role in the host response to the infection (43). In some tissues, short-chain acylcarnitines may be used for energy and as a carbon source for phospholipid synthesis (44). While medium- and long-chain acylcarnitines are derived exclusively from fatty acid metabolism, short-chain acylcarnitines are produced from glucose, amino acids and fatty acid degradation. Under physiological conditions, an organism switches between glucose and

fatty acid metabolism based on the availability of substrates to maintain energy homeostasis (45). Differences in acylcarnitines levels might be related to specific changes in energy metabolism.

Finally, the presence of annotated complex lipids with odd chain fatty acids, usually uncommon in human tissues, could be related to bacterial contamination during the sampling procedure (46).

This study has some limitations. Firstly, the small number of patients included in the study and the unbalanced number of newborns in the two groups could have affected the statistical analysis. In clinical practice, obtaining samples from unbiased matched patients extremely reduces the number of available cases, especially when such a sensitive population, as preterm infants, and specific biospecimen are involved. Nevertheless, the major strength of the present study is that the two groups were accurately matched, in terms of clinical characteristics, drugs and resuscitation strategies during the perinatal period, time of TAs sampling, and more importantly definition of chorioamnionitis that included both clinical and histological criteria. Intubation and oxygen supplementation, are pro-inflammatory factors that may contribute to triggering pro-inflammatory pathways that may be difficult to differentiate from inflammation secondary to chorioamnionitis. However, in the present study there was no difference in the intensive care therapy management between the two groups, being 100% and 70% of babies in both groups treated with oxygen supplementation and endotracheal intubation, respectively, in delivery room.

Please note that this is a thorough selection for this field of research, that enhances the value of our findings. Moreover, this is the first description of lipidomic profiles in preterm infants with and without exposition to chorioamnionitis.

Another limitation is that a post-acquisition normalization method was applied to correct for sample dilution. However, post analysis normalization has been extensively used for urine metabolomics, and TA/plasma urea concentration has been reported to be reliable marker of dilution (47).

Because of these limitations, the present study has to be considered as an explorative study on the application of untargeted lipidomics on TA samples as a promising approach to identify pathway that can be altered in newborns because of maternal infection. Although changes in specific areas of metabolism were found, the hypothesis of an effect of chorioamnionitis on TAs lipidomics/metabolomics deserves a further unbiased investigation on a larger group of patients.

REFERENCES

1. Yoon BH, Romero R, Park JS, Kim M, Oh S-Y, Kim CJ, Jun JK. The relationship among inflammatory lesions of the umbilical cord (funisitis), umbilical cord plasma interleukin 6 concentration, amniotic fluid infection, and neonatal sepsis. *Am J Obstet Gynecol* 2000;183:1124–1129.

2. Romero R, Espinoza J, Chaiworapongsa T, Kalache K. Infection and prematurity and the role of preventive strategies. *Semin Neonatol* 2002;7:259–274.
3. Jobe A. Effects of chorioamnionitis on the fetal lung. *Clin Perinatol* 2012;39:441–457.
4. Goldenberg RL, Hauth JC, Andrews WW. Intrauterine infection and preterm delivery. In: Epstein FH, editor. *N Engl J Med* 2000;342:1500–1507.
5. Ramsey PS, Lieman JM, Brumfield CG, Carlo W. Chorioamnionitis increases neonatal morbidity in pregnancies complicated by preterm premature rupture of membranes. *Am J Obstet Gynecol* 2005;192:1162–1166.
6. Dempsey E, Ch B, Chen M-F, Kokottis T, Vallerand D, Usher R, Dempsey E. Outcome of neonates less than 30 weeks gestation with histologic chorioamnionitis. *Am J Perinatol* 2005;22:155–159.
7. Dooy J DE, Colpaert C, Schuerwegh A, Bridts C, Van Der Planken M, Ieven M, Clerck L DE, Stevens W, Mahieu L. Relationship between histologic chorioamnionitis and early inflammatory variables in blood, tracheal aspirates, and endotracheal colonization in preterm infants. *Pediatr Res* 2003;54:113–119.
8. Watterberg KL, Demers LM, Scott SM, Murphy S. Chorioamnionitis and early lung inflammation in infants in whom bronchopulmonary dysplasia develops. *Pediatrics* 1996;97:210–215.
9. Lahra MM, Beeby PJ, Jeffery HE, Lahra MM. Maternal versus fetal inflammation and respiratory distress syndrome: a 10-year hospital cohort study. *Arch Dis Child Fetal Neonatal* 2009;94:F13-16.
10. Kent A, Dahlstrom J. Chorioamnionitis/funisitis and the development of bronchopulmonary dysplasia. *J Paediatr Child Health* 2004;40:356–359.
11. Kramer B. Antenatal inflammation and lung injury: prenatal origin of neonatal disease. *J Perinatol* 2008;28:S21–S27.
12. Moss TJM, Newnham JP, Willett KE, Kramer BW, Jobe AH, Ikegami M. Early Gestational Intra-Amniotic Endotoxin. *Am J Respir Crit Care Med* 2002;165:805–811.
13. Jobe AH, Newnham JP, Willett KE, Moss TJ, Gore Ervin M, Padbury JF, Sly P, Ikegami M. Endotoxin-induced lung maturation in preterm lambs is not mediated by cortisol. *Am J Respir Crit Care Med* 2000;162:1656–1661.
14. Bachurski CJ, Ross GF, Ikegami M, Kramer BW, Jobe AH. Intra-amniotic endotoxin increases pulmonary surfactant proteins and induces SP-B processing in fetal sheep. *Am J Physiol Cell Mol Physiol* 2001;280:L279-285.
15. Speer CP. Inflammation and bronchopulmonary dysplasia: A continuing story. *Semin Fetal*

- Neonatal Med* 2006;11:354–362.
16. Fattuoni C, Pietrasanta C, Pigni L, Ronchi A, Palmas F, Barberini L, Dessì A, Pintus R, Fanos V, Noto A, Mosca F. Urinary metabolomic analysis to identify preterm neonates exposed to histological chorioamnionitis: A pilot study. *PLoS One* 2017;12:e0189120.
 17. Chetwynd AJ, Dunn WB, Rodriguez-Blanco G. Collection and preparation of clinical samples for metabolomics. *Metabolomics from Fundam to Clin Appl Adv Exp Med Biol*, Sussulini, Springer, Cham; 2017. p. 19–44.
 18. Dargaville PA, South M, McDougall PN. Comparison of two methods of diagnostic lung lavage in ventilated infants with lung disease. *Am J Respir Crit Care Med* 1999;160:771–777.
 19. Verlato G, Simonato M, Giambelluca S, Fantinato M, Correani A, Cavicchiolo ME, Priante E, Carnielli V, Cogo P. Surfactant components and tracheal aspirate inflammatory markers in preterm infants with Respiratory Distress Syndrome. *J Pediatr* 2018;203:442–446.
 20. Lal CV, Kandasamy J, Dolma K, Ramani M, Kumar R, Wilson L, Aghai Z, Barnes S, Edwin Blalock J, Gaggar A, Bhandari V, Ambalavanan N. Early airway microbial metagenomic and metabolomic signatures are associated with development of severe bronchopulmonary dysplasia. *Physiol Am J Physiol Lung Cell Mol Physiol* 2018;315:810–815.
 21. Piersigilli F, Bhandari V, Lam TT, Vernocchi P, Aghai ZH, Quagliariello A, Putignani L. Identification of new biomarkers of bronchopulmonary dysplasia using metabolomics. *Metabolomics* 2019;15:0.
 22. Simonato M, Baritussio A, Carnielli VP, Vedovelli L, Falasco G, Salvagno M, Padalino M, Cogo P. Influence of the type of congenital heart defects on epithelial lining fluid composition in infants undergoing cardiac surgery with cardiopulmonary bypass. *Pediatr Res* 2018;83:791–797.
 23. Broadhurst D, Goodacre R, Reinke SN, Kuligowski J, Wilson ID, Lewis MR, Dunn WB. Guidelines and considerations for the use of system suitability and quality control samples in mass spectrometry assays applied in untargeted clinical metabolomic studies. *Metabolomics* 2018;14:72.
 24. Chong J, Wishart DS, Xia J. Using MetaboAnalyst 4.0 for comprehensive and integrative metabolomics data analysis. *Curr Protoc Bioinforma* 2019;68:e86.
 25. Sumner LW, Amberg A, Barrett D, Beale MH, Beger R, Daykin CA, W-M Fan T, Fiehn O, Goodacre R, Griffin JL, Hankemeier T, Hardy N, Harnly J, Higashi R, Kopka J, Lane AN, Lindon JC, Marriott P, Nicholls AW, Reily MD, Thaden JJ, Viant MR. Proposed minimum reporting standards for chemical analysis Chemical Analysis Working Group (CAWG) Metabolomics Standards Initiative (MSI) NIH Public Access. *Metabolomics* 2007;3:211–221.

26. Kyle JE, Clair G, Bandyopadhyay G, Misra RS, Zink EM, Bloodsworth KJ, Shukla AK, Du Y, Lillis J, Myers JR, Ashton J, Bushnell T, Cochran M, Deutsch G, Baker ES, Carson JP, Mariani TJ, Xu Y, Whitsett JA, Pryhuber G, Ansong C. Cell type-resolved human lung lipidome reveals cellular cooperation in lung function. *Sci Rep* 2018;8:13455.
27. Zemski Berry KA, Murphy RC, Kosmider B, Mason RJ. Lipidomic characterization and localization of phospholipids in the human lung. *J Lipid Res* 2017;58:926–933.
28. Vedovelli L, Baritussio A, Carnielli VP, Simonato M, Giusti P, Cogo PE. Simultaneous measurement of phosphatidylglycerol and disaturated-phosphatidylcholine palmitate kinetics from alveolar surfactant. Study in infants with stable isotope tracer, coupled with isotope ratio mass spectrometry. *J Mass Spectrom* 2011;46:986–992.
29. Samuels ER, Elliott Scott J. Ca²⁺-phosphatidylserine-dependent protein kinase C activity in fetal, neonatal and adult rabbit lung and isolated lamellar bodies. *Life Sci* 1995;57:1557–1568.
30. Numata M, Chu HW, Dakhama A, Voelker DR. Pulmonary surfactant phosphatidylglycerol inhibits respiratory syncytial virus-induced inflammation and infection. *Proc Natl Acad Sci* 2010;107:320–325.
31. Numata M, Kandasamy P, Nagashima Y, Posey J, Hartshorn K, Woodland D, Voelker DR. Phosphatidylglycerol suppresses influenza A virus infection. *Am J Respir Cell Mol Biol* 2012;46:479–87.
32. Kuronuma K, Mitsuzawa H, Takeda K, Nishitani C, Chan ED, Kuroki Y, Nakamura M, Voelker DR. Anionic pulmonary surfactant phospholipids inhibit inflammatory responses from alveolar macrophages and U937 cells by binding the lipopolysaccharide-interacting proteins CD14 and MD-2. *J Biol Chem* 2009;284:25488–25500.
33. Dautel SE, Kyle JE, Clair G, Sontag RL, Weitz KK, Shukla AK, Nguyen SN, Kim YM, Zink EM, Luders T, Frevert CW, Gharib SA, Laskin J, Carson JP, Metz TO, Corley RA, Ansong C. Lipidomics reveals dramatic lipid compositional changes in the maturing postnatal lung. *Sci Rep* 2017;7:1–12.
34. Serhan CN, Chiang N, Van Dyke TE. Resolving inflammation: dual anti-inflammatory and pro-resolution lipid mediators. *Nat Rev Immunol* 2008;8:349–361.
35. Uhlig S, Gulbins E. Sphingolipids in the lungs. *Am J Respir Crit Care Med* 2008;178:1100–1114.
36. Longo CA, Tyler D, Mallampalli RK. Sphingomyelin metabolism is developmentally regulated in rat lung. *Am J Respir Cell Mol Biol* 1997;16:605–612.
37. Trayssac M, Hannun YA, Obeid LM. Role of sphingolipids in senescence: Implication in aging and age-related diseases. *J Clin Invest* 2018;128:2702–2712.

38. Gault CR, Obeid LM, Hannun YA. An overview of sphingolipid metabolism: from synthesis to breakdown. *Adv Exp Med Biol* 2010;688:1–23.
39. Tibboel J, Reiss I, de Jongste JC, Post M. Sphingolipids in lung growth and repair. *Chest* 2014;145:120–128.
40. Grösch S, Schiffmann S, Geisslinger G. Chain length-specific properties of ceramides. *Prog Lipid Res* 2012;51:50–62.
41. Kunzmann S, Collins JJP, Yang Y, Uhlig S, Kallapur SG, Speer CP, Jobe AH, Kramer BW. Antenatal inflammation reduces expression of caveolin-1 and influences multiple signaling pathways in preterm fetal lungs. *Am J Respir Cell Mol Biol* 2011;45:969–976.
42. Dudzik D, Revello R, Barbas C, Bartha JL. LC–MS-Based metabolomics identification of novel biomarkers of chorioamnionitis and its associated perinatal neurological damage. *J Proteome Res* 2015;14:1432–1444.
43. Cui L, Zheng D, Lee YH, Chan TK, Kumar Y, Ho WE, Chen JZ, Tannenbaum SR, Ong CN. Metabolomics investigation reveals metabolite mediators associated with acute lung injury and repair in a murine model of influenza pneumonia. *Sci Rep* 2016;6:1–13.
44. Jones LL, McDonald DA, Borum PR. Acylcarnitines: Role in brain. *Prog Lipid Res* 2010;49:61–75.
45. Makrecka-Kuka M, Sevostjanovs E, Vilks K, Volska K, Antone U, Kuka J, Makarova E, Pugovics O, Dambrova M, Liepinsh E. Plasma acylcarnitine concentrations reflect the acylcarnitine profile in cardiac tissues. *Sci Rep* 2017;7:17528.
46. Brandsma J, Goss VM, Yang X, Bakke PS, Caruso M, Chanez P, Dahlén S-E, Fowler SJ, Horvath I, Krug N, Montuschi P, Sanak M, Sandström T, Shaw DE, Chung KF, Singer F, Fleming LJ, Sousa AR, Pandis I, Bansal AT, Sterk PJ, Djukanović R, Postle AD. Lipid phenotyping of lung epithelial lining fluid in healthy human volunteers. *Metabolomics* 2018;14:123.
47. Dargaville PA, South M, Vervaart P, Dougall PNMC. Validity of markers of dilution in small volume lung lavage. *Am J Respir Crit Care Med* 1999;160:778–784.

FIGURE CAPTION

Figure 1

PCA score plots for LIPIDS ESI+(A), LIPIDS ESI- (B), HILIC ESI+(C), HILIC ESI- (D).

* Sample HCA+_8 observed to be an outlier and removed from both lipid datasets prior to statistical analysis

Figure 2

Effects of HCA on TAs metabolome of RDS newborns (A) Metabolites at higher concentration in newborns exposed to HCA (B) Metabolites at lower concentration in newborns exposed to HCA

CONFIDENTIAL DRAFT

Table 1. Clinical characteristics of the study population

	HCA+ (N=10)*	HCA- (N=20)**
GA mean±SD (weeks)	26.5±2.4	27.9±2.0
GA range (weeks)	23.6-29.4	24.0-30.7
Birth weight mean±SD (g)	893±274	970±304
Birth weight range (g)	550-1280	470-1660
Male N(%)	4(40%)	12(60%)
Apgar 5' median(range)	8 (5-9)	8 (5-9)
Umbilical blood pH mean±SD	7.33± 0.04	7.32 ± 0.07
Oxygen in delivery room	10(100%)	20(100%)
Endotracheal intubation in delivery room	7(70%)	13(65%)
Surfactant therapy in delivery room	5(50%)	5(25%)
Prenatal steroids (Bentelan 12 mg) N(%)	10(100%)	16(80%)
Other drugs N(%)	1(10%)	4(20%)
Time of collection (h post birth)	2.0 (0.1-14.2)	2.0 (0.1-9.1)
Mean (min-Max)		
Maternal age	29.6±7.3	33.4±6.7
Clinical chorioamnionitis	9(90%)	2(10%)
Maternal antibiotics	5(50%)	1(5%)
Pre-eclampsia	1(10%)	3(15%)

* HCA+= newborns from mother with histological chorioamnionitis

** HCA-= newborns from mother without histological chorioamnionitis

Figure 1

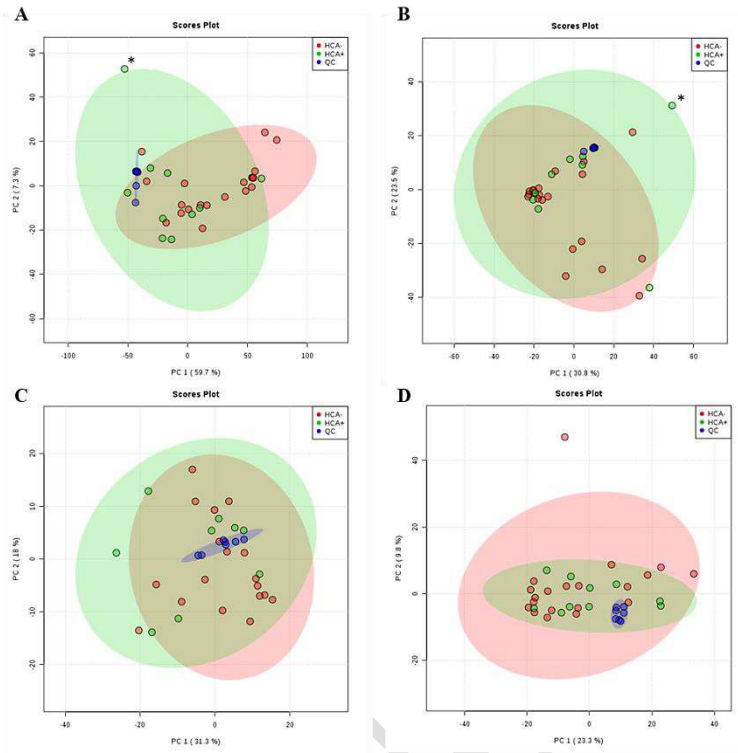
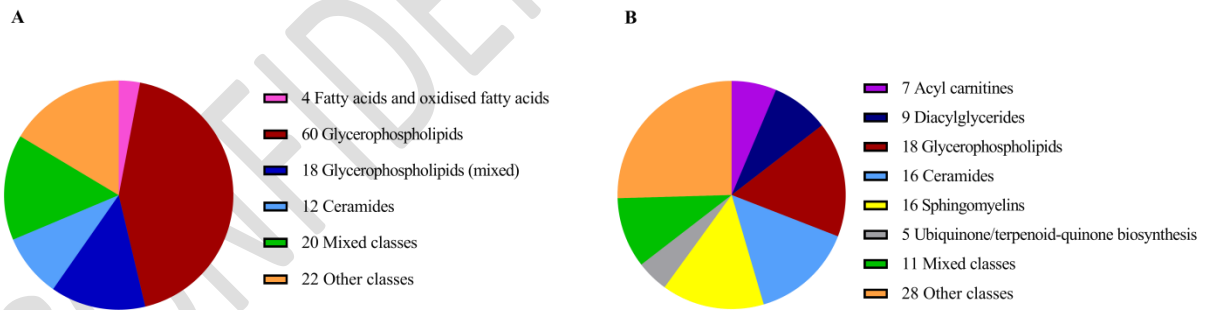


Figure 2



ONLINE DATA SUPPLEMENT

SUPPLEMENTARY METHODS

Study population

RDS was defined as indicated by the Vermont-Oxford Neonatal Network (1). Clinical chorioamnionitis was diagnosed by mother fever ($T > 37.8^{\circ}\text{C}$) associated with two of the following clinical symptoms: uterine tenderness, purulent and/or foul-smelling amniotic fluid, and fetal (>160 BPM) and maternal (>100 BPM) tachycardia.

HCA was diagnosed when acute inflammation was observed in any placental tissue samples (amnion, chorion-decidua, umbilical cord, and chorionic plate). The presence of acute inflammation was classified as grade 1 or 2 and 3 according to previously published criteria (2). For the purpose of this study only stage 2 and 3 involving the chorionic plate and/or the umbilical cord were considered for the study. Funisitis was diagnosed when neutrophil infiltration was observed in the umbilical vessel walls or Wharton's jelly. Placentas and umbilical cords were evaluated by the same pathologist.

Sample collection

Tracheal aspirates (TAs) were collected within the first 24h of life, immediately after intubation and before exogenous surfactant administration. Briefly, after instillation of 0.5 ml saline (0.9% NaCl) in the endotracheal tube, the preterm newborn was gently hand-bagged for 30 seconds and then tracheal secretions were collected (E1). The samples were brought to a final volume of 1.5 ml with 0.9% saline and centrifuged at $400 \times g$ for 10 minutes. Cell-free supernatant was aliquoted and stored at -80°C within 3 hours of collection.

Leftover blood from arterial blood gas analysis was collected contemporarily to the TA sample. Arterial blood gas syringes with dry lithium heparin (Smiths Medical ASD, Keene, NH, USA) were used. Blood was transferred in 1.5 ml Eppendorf tubes (Eppendorf AG, Hamburg, Germany), centrifuged at $1400 \times g$ for 10 minutes and the plasma was stored at -80°C until analysis.

Untargeted metabolomics analysis

Sample preparation

Sample preparation order was randomized and re-randomized before sample analysis to ensure no systematic biases. TA samples were thawed on ice and vortexed. Two different $40 \mu\text{L}$ aliquots were deproteinised adding $80 \mu\text{L}$ of cold HPLC grade acetonitrile (ACN) or 2-isopropanol (IPA) for water-soluble metabolite and lipid profiling, respectively, followed by vortex mixing and centrifugation ($15000 \times g \times 15$ minutes at 4°C). Supernatant was collected and $40 \mu\text{L}$ aliquots were transferred in to LC-vials for the analysis. Another $40 \mu\text{L}$ aliquot from each sample was pooled to construct a pooled

Quality Control (QC) sample (E2). The pooled QC sample was vortexed for 5 minutes and then 40 μ l aliquots were transferred in to LC-vials. Process blank samples were prepared using the same solvent and procedure used for TA samples but with the absence of any biological sample. Samples were analysed within 48 hours after preparation.

Sample analysis

UHPLC-MS(/MS) analysis were performed on a Vanquish UHPLC system (Thermo Fisher Scientific, Bremen, Germany) coupled to an electrospray (ESI) Q Exactive Plus mass spectrometer (Thermo Fisher scientific, Bremen, Germany). All reagents used were of HPLC Grade purity.

For water-soluble metabolite profiling (HILIC ESI+ and HILIC ESI-), chromatographic separations were performed on a 2.1 mm x 100 mm, 2.6 μ m Accucore 150 Amide hydrophilic interaction liquid chromatography (HILIC) LC column (Thermo Fisher Scientific, Bremen, Germany) at 35 °C. The mobile phase A consisted of 10mM ammonium formate in ACN:H₂O (95:5, v:v) + 0.1% formic acid; the mobile phase B consisted of 10mM ammonium formate in ACN:H₂O (50:50, v:v). The flow rate was 0.5 ml/min with the following gradient: the ratio of mobile phase B was started at 1%, increased to 15% B at 3 min, to 50% B at 6 min and to 95% B at 9 min, maintained at 95% B for 1.5 min, then decreased to 1% B and kept constant for 4 min. A 2 μ L injection volume was used. All samples were analysed in both positive (ESI+) and negative (ESI-) ionisation mode at following mass spectrometer conditions: spray voltage +3.5 kV, sheath gas 53.0, aux gas 14.0, spare gas 3.0, S-lens level 30, resolution 70,000 FWHM (at 200 m/z), capillary temperature 269.0 °C, probe heater temperature 438.0 °C for ESI+; spray voltage -2.5 kV, sheath gas 52.5, aux gas 13.75, spare gas 2.75, S-lens level 30, mass resolution 70,000 (FWHM at m/z 200), capillary temperature 268.8 °C, probe heater temperature 437.5 °C for ESI-. Data were collected in the m/z range 70-1050.

For lipid profiling (LIPIDS ESI+ and LIPIDS ESI-), chromatographic separations were performed on a 2.1 mm x 100 mm, 1.9 μ m Hypersil GOLD C₁₈ column (Thermo Fisher Scientific, Bremen, Germany) at 55 °C. The mobile phase A consisted of 10mM ammonium formate in ACN:H₂O (60:40, v:v) + 0.1% formic acid; the mobile phase B consisted of 10mM ammonium formate in IPA:ACN:H₂O (85.5:9.5:5, v:v:v). The flow rate was 0.4 ml/min with the following gradient: the ratio of mobile phase B was started at 20%, increased to 100% B at 8.5, maintained at 100% B for 3 min, then decreased to 20% B and kept constant for 3 min. A 2 μ L injection of each sample was used. All samples were analysed in both positive (ESI+) and negative (ESI-) ion mode at following mass spectrometer conditions: spray voltage +3.2 kV, sheath gas 48.0, aux gas 15.0, spare gas 0, S-lens 60, resolution 70000, capillary T 350.0 °C, probe heater T 400 °C for ESI+; spray voltage -2.7 kV, sheath gas 48.0, aux gas 15.0, spare gas 0.0, S-lens 60, mass resolution 70,000 (FWHM at m/z 200), capillary T 268.8 °C, probe heater T 400.0 °C for ESI-.

Data were collected in the m/z range 100-1500.

All samples were maintained at 4°C during analysis.

Ten QC samples were analysed at the start of each analytical batch to condition the analytical system, a QC sample was then analysed every 6th injection and two QC samples were analysed at the end of the sequence. Two process blank samples were analysed after the fifth pooled QC sample and at the end of the sequence to detect contaminants from sample preparation or sample carryover (E2).

Data processing and statistical analysis

Data obtained in the instrument-specific data format (.RAW) were converted to open source data format mzML files in ProteoWizard – MSConvert (5). Data processing was performed for each analytical batch (lipids ESI+, lipids ESI-, polar ESI+, polar ESI-), separately. The deconvolution was performed using the XCMS R-package (E4–7) to obtain a data matrix of metabolite feature (m/z -retention time pairs) vs chromatographic peak areas in samples. The obtained datasets were filtered by removing metabolite features with a relative standard deviation greater than 30% for QC samples and/or were detected in <60% of pooled QC samples. Metabolite features were removed if the blank response was >5% of the average QC response. The ratio between urea concentration in plasma and in TA was used to normalize peak intensity in samples for the epithelial lining fluid volume (E8), as follows:

$$\text{Normalized peak intensity} = \text{peak intensity} * \frac{\text{plasma urea}}{\text{TA urea}}$$

The filtered and normalized datasets were analysed in MetaboAnalyst (E9) applying the unsupervised multivariate analysis technique Principal Components Analysis (PCA). For multivariate analysis, features with >50% missing values were removed and the remaining missing values were replaced with a value estimated using k-nearest neighbor (KNN). The data were normalized by sum and subjected to log transformation and Pareto scaling.

Volcano plots were constructed to assess statistically significant differences between the two groups (p -value<0.05 and fold change (FC) HCA+/HCA- <0.9 or >1.1). Volcano plot analysis was repeated applying correction for false discovery rate (FDR) using Benjamini-Hochberg procedure (adjusted p -value threshold 0.05). Statistically significant metabolite features were annotated according to level 2 of the MSI reporting standards (E10) using in-house software at the University of Birmingham (BEAMS). Full-scan MS1 data was applied to generate molecular formulas which were searched for in the Human Metabolome Database and Lipid Maps databases with settings as follows: a mass error window of <5 ppm was used and for feature grouping a maximum RT difference of 5 sec was

applied. Metabolites were manually clustered into classes defining similar chemical structure or metabolic pathway.

CONFIDENTIAL DRAFT

REFERENCES

- E1. Sweet DG, Carnielli V, Greisen G, Hallman M, Ozek E, Plavka R, Didrik Saugstad O, Simeoni U, Speer CP, Vento M, Visser GHA, Halliday HL. European consensus guidelines on the management of Respiratory Distress Syndrome-2016 Update. *Neonatology* 2017;111:107–125.
- E2. Redline RW. Inflammatory responses in the placenta and umbilical cord. *Semin Fetal Neonatal Med* 2006;11:296–301.
- E3. Simonato M, Baritussio A, Carnielli VP, Vedovelli L, Falasco G, Salvagno M, Padalino M, Cogo P. Influence of the type of congenital heart defects on epithelial lining fluid composition in infants undergoing cardiac surgery with cardiopulmonary bypass. *Pediatr Res* 2018;83:791–797.
- E4. Broadhurst D, Goodacre R, Reinke SN, Kuligowski J, Wilson ID, Lewis MR, Dunn WB. Guidelines and considerations for the use of system suitability and quality control samples in mass spectrometry assays applied in untargeted clinical metabolomic studies. *Metabolomics* 2018;14:72.
- E5. Chambers MC, MacLean B, Burke R, Amodei D, Ruderman DL, Neumann S, Gatto L, Fischer B, Pratt B, Egertson J, Hoff K, Kessner D, Tasman N, Shulman N, Frewen B, Baker TA, Brusniak MY, Paulse C, Creasy D, Flashner L, Kani K, Moulding C, Seymour SL, Nuwaysir LM, Lefebvre B, Kuhlmann F, Roark J, Rainer P, Detlev S, *et al.* A cross-platform toolkit for mass spectrometry and proteomics. *Nat Biotechnol* 2012;30:918–920.
- E6. Dunn WB, Broadhurst D, Brown M, Baker PN, Redman CWG, Kenny LC, Kell DB. Metabolic profiling of serum using Ultra Performance Liquid Chromatography and the LTQ-Orbitrap mass spectrometry system. *J Chromatogr B* 2008;871:288–298.
- E7. Smith CA, Want EJ, O’Maille G, Abagyan R, Siuzdak G. XCMS: Processing mass spectrometry data for metabolite profiling using nonlinear peak alignment, matching, and identification. *Anal Chem* 2006;78:779–787.
- E8. Tautenhahn R, Bottcher C, Neumann S. Highly sensitive feature detection for high resolution LC/MS. *BMC Bioinformatics* 2008;9:504.
- E9. Benton HP, Want EJ, Ebbels TMD. Correction of mass calibration gaps in liquid chromatography-mass spectrometry metabolomics data. *Bioinformatics* 2010;26:2488–9.
- E10. Dargaville PA, South M, Vervaart P, Dougall PNMC. Validity of markers of dilution in small volume lung lavage. *Am J Respir Crit Care Med* 1999;160:778–784.
- E11. Chong J, Wishart DS, Xia J. Using MetaboAnalyst 4.0 for comprehensive and integrative metabolomics data analysis. *Curr Protoc Bioinforma* 2019;68:e86.

- E12. Sumner LW, Amberg A, Barrett D, Beale MH, Beger R, Daykin CA, W-M Fan T, Fiehn O, Goodacre R, Griffin JL, Hankemeier T, Hardy N, Harnly J, Higashi R, Kopka J, Lane AN, Lindon JC, Marriott P, Nicholls AW, Reily MD, Thaden JJ, Viant MR. Proposed minimum reporting standards for chemical analysis Chemical Analysis Working Group (CAWG) Metabolomics Standards Initiative (MSI) NIH Public Access. *Metabolomics* 2007;3:211–221.

CONFIDENTIAL DRAFT

Table E1

Metabolite name	Assay	mz	rt (sec)	raw.pval	FC (HCA+/HCA-)
Fatty acids and oxidised fatty acids					
Hydroxy-oxohexadecanoic acid;Hexadecanedioic acid	HILIC ESI-	345.2287	40.85	3.92E-02	2.16
3-Hexadecanoyloleanoic acid	Lipids ESI+	733.5567	394.21	9.69E-03	2.33
Dimethyl-heptadienoic acid;Oxo-nonenal	HILIC ESI+	193.0621	529.91	4.62E-02	2.46
Hydroxy-decenoic acid;2-Methylbutyl 3-hydroxy-2-methylidenebutanoate;Oxodecanoic acid	HILIC ESI-	245.1396	39.97	4.90E-02	2.99
Glycerophospholipids					
Lysoglycerophospholipids					
LysoPC(16:1);LysoPE(19:1)	Lipids ESI+	494.3244	95.07	4.91E-02	1.78
LysoPS(21:0);LysoPE(20:1);LysoPC(17:1)	Lipids ESI-	566.3466	144.48	2.64E-02	4.11
Phosphatidic acid (PA)					
PA(40:0)	Lipids ESI-	781.5701	413.02	3.86E-02	2.25
PA(42:1)	Lipids ESI-	807.5857	414.66	2.01E-02	2.44
PA(40:1)	Lipids ESI-	779.5542	391.98	1.31E-02	3.31
PA(41:7)	Lipids ESI-	819.5205	389.36	4.36E-02	3.61
PA(41:1)	Lipids ESI+	811.5626	430.58	1.31E-02	3.69
Phosphatidylcholine (PC) and/or phosphatidylethanolamine (PE)					
PC(16:0/O-16:0);PC(O-14:0/18:0);PC(O-18:0/14:0);PC(O-20:0/12:0);PE(O-16:0/19:0);PE(O-18:0/17:0);PE(O-20:0/15:0)	Lipids ESI+	720.5896	430.35	1.13E-02	1.99
PC(30:0);PE(33:0)	Lipids ESI+	706.5376	391.71	8.28E-03	2.22
PC(36:3);PE(39:3)	Lipids ESI-	782.5726	413.01	4.91E-02	2.22
PC(32:1);PE(35:1);PE-NMe(16:0/18:1);PE-NMe(16:0/18:1);PE-NMe(18:1/16:0)	Lipids ESI+	732.5532	394.21	9.69E-03	2.34
PC(30:2);PE(33:2)	Lipids ESI+	702.5072	356.77	4.91E-02	2.46
PC(O-14:0/16:0);PC(O-16:0/14:0);PC(O-18:0/12:0);PC(o-14:0/16:0);PE(O-16:0/17:0);PE(O-18:0/15:0);PE(O-20:0/13:0)	Lipids ESI+	692.5587	408.23	1.75E-02	2.48
PC(32:0);PE(35:0);PE(P-16:0/20:0);PE(P-16:0/20:0);PE(P-18:0/18:0);PE(P-20:0/16:0);PE(dm18:0/18:0)	Lipids ESI-	768.5325	413.01	4.91E-02	2.49
PC(O-16:0/15:0);PC(O-18:0/13:0);PE(O-16:0/18:0);PE(O-18:0/16:0);PE(O-20:0/14:0)	Lipids ESI+	706.5735	419.75	3.86E-02	2.54
PC(38:3);PE(41:3)	Lipids ESI-	848.5547	413.01	2.31E-02	2.54
PC(20:1/P-18:1);PC(20:2/P-18:0);PC(22:2/P-16:0);PC(O-18:0/20:3);PC(O-20:0/18:3);PC(P-16:0/22:2);PC(P-18:0/20:2);PC(P-18:1/20:1);PC(P-20:0/18:2);PC(o-20:0/18:3)	Lipids ESI-	832.5986	417.37	1.75E-02	2.58
PC(40:4);PE(43:4)	Lipids ESI-	874.5704	415.17	1.52E-02	2.58
PC(32:3);PE(35:3);PC(30:0);PE(33:0);PE-NMe(32:0)	Lipids ESI+	728.5196	391.71	4.25E-03	2.69
PC(18:1/P-18:0);PC(O-18:0/17:2);PC(P-16:0/19:1);PC(P-18:0/17:1);PC(P-20:0/15:1);PE(20:0/P-18:1);PE(20:0/P-18:1);PE(20:1/P-18:0);PE(22:1/P-16:0);PE(O-16:0/22:2);PE(O-18:0/20:2);PE(O-20:0/18:2);PE(P-16:0/22:1);PE(P-16:0/22:1);PE(P-18:0/20:1);PE(P-18:0/20:1);PE(P-18:0/20:1);PE(P-18:1/20:0);PE(P-20:0/18:1);PC(34:1);PE(37:1)	Lipids ESI-	794.5464	415.16	1.52E-02	2.72
PC(18:0/O-16:0);PC(O-16:0/18:0);PC(O-17:0/17:0);PC(O-18:0/16:0);PC(O-20:0/14:0);PC(o-16:0/18:0);PE(O-16:0/21:0);PE(O-18:0/19:0);PE(O-20:0/17:0)	Lipids ESI+	748.6214	450.47	3.41E-02	2.79
PC(37:6);PE(40:6);PE(P-18:0/22:6(14OH));PE(DiMe(11,3)/DiMe(11,5));PE(DiMe(11,5)/DiMe(11,3));PE(DiMe(11,5)/DiMe(9,5));PE(DiMe(13,5)/DiMe(9,3));PE(DiMe(9,3)/DiMe(13,5));PE(DiMe(9,5)/DiMe(11,5));PE(MonoMe(11,3)/MonoMe(13,5));PE(MonoMe(11,5)/MonoMe(11,5));PE(MonoMe(13,5)/MonoMe(11,3));PE(MonoMe(13,5)/MonoMe(9,5));PE(MonoMe(9,5)/MonoMe(13,5));PS(41:5)	HILIC ESI-	850.5618	205.60	3.50E-02	3.10
PC(18:2/P-18:1);PC(18:3/P-18:0);PC(20:3/P-16:0);PC(O-16:0/20:4);PC(O-18:0/18:4);PC(O-18:2/18:2);PC(P-16:0/20:3);PC(P-18:0/18:3);PC(P-18:1/18:2);PC(o-16:0/20:4);PC(o-18:2/18:2);PC(18:2/P-18:1);PC(18:3/P-18:0);PC(20:3/P-16:0);PC(O-16:0/20:4);PC(O-18:0/18:4);PC(O-18:2/18:2);PC(P-16:0/20:3);PC(P-18:0/18:3);PC(P-18:1/18:2);PC(o-16:0/20:4);PC(o-18:2/18:2);PC(16:0/P-18:0);PC(18:0/P-16:0);PC(O-16:0/18:1);PC(O-16:1/18:0);PC(O-18:0/16:1);PC(O-18:1/16:0);PC(O-20:0/14:1);PC(P-16:0/18:0);PC(P-18:0/16:0);PC(P-20:0/14:0);PC(o-16:1/18:0);PC(o-18:1/16:0);PE(O-18:0/19:1);PE(O-20:0/17:1);PE(P-16:0/21:0);PE(P-18:0/19:0);PE(P-20:0/17:0)	Lipids ESI+	768.5873	431.30	2.31E-02	3.28
PC(18:0/P-18:1);PC(20:1/P-16:0);PC(O-16:0/20:2);PC(O-18:0/18:2);PC(O-18:1/18:1);PC(P-16:0/20:1);PC(P-18:0/18:1);PC(P-18:1/18:0);PC(P-20:0/16:1);PC(o-18:0/18:2);PC(o-18:1/18:1);PE(P-20:0/19:1)	Lipids ESI-	806.5828	414.64	2.97E-03	3.37
PC(16:0/P-18:0);PC(18:0/P-16:0);PC(O-16:0/18:1);PC(O-16:1/18:0);PC(O-18:0/16:1);PC(O-18:1/16:0);PC(O-18:1/16:0);PC(O-20:0/14:1);PC(P-16:0/18:0);PC(P-16:0/18:0);PC(P-18:0/16:0);PC(P-18:0/16:0);PC(P-20:0/14:0);PC(o-16:1/18:0);PC(o-18:1/16:0);PC(o-18:1/16:0);PE(O-18:0/19:1);PE(O-20:0/17:1);PE(P-16:0/21:0);PE(P-18:0/19:0);PE(P-20:0/17:0)	HILIC ESI-	780.5680	213.63	2.76E-02	3.47
PC(O-16:0/O-18:1);PC(O-18:1/O-16:0)	Lipids ESI-	766.5885	429.31	3.86E-02	3.64
PC(O-14:0/15:0);PC(O-16:0/13:0);PE(O-16:0/16:0);PE(O-18:0/14:0);PE(O-20:0/12:0)	Lipids ESI-	736.5506	406.35	3.86E-02	3.87
PC(38:4);PE(41:4)	Lipids ESI-	846.5393	392.14	3.00E-02	4.40
PC(18:0/P-18:0);PC(20:0/P-16:0);PC(O-16:0/20:1);PC(O-16:0/20:1);PC(O-16:1/20:0);PC(O-18:0/18:1);PC(O-20:0/16:1);PC(P-16:0/20:0);PC(P-16:0/20:0);PC(P-18:0/18:0);PC(P-18:0/18:0);PC(P-20:0/16:0);PC(o-16:1/20:0);PC(o-18:1/18:0);PE(O-20:0/19:1);PE(P-18:0/21:0);PE(P-20:0/19:0)	Lipids ESI+	774.6357	451.29	1.13E-02	6.48
PC(O-14:0/22:0);PC(O-16:0/20:0);PC(O-18:0/18:0);PC(O-20:0/16:0);PC(o-16:0/20:0);PC(o-18:0/18:0);PE(O-18:0/21:0);PE(O-20:0/19:0)	Lipids ESI+	776.6529	468.43	4.91E-02	9.77
PC(24:0/P-18:1);PC(24:1/P-18:0);PC(O-18:2/24:0);PC(O-20:0/22:2);PC(P-18:0/24:1);PC(P-18:1/24:0);PC(P-20:0/22:1);PC(o-18:2/24:0)	Lipids ESI+	856.7157	485.23	1.67E-03	17.69
Phosphatidylglycerol (PG)					
PG(44:7)	Lipids ESI-	875.5833	435.12	4.36E-02	1.88
PG(40:2)	Lipids ESI-	865.5725	414.89	4.36E-02	2.12
PG(42:7)	Lipids ESI-	847.5515	413.01	2.64E-02	2.46
PG(44:8)	Lipids ESI-	873.5674	415.17	1.13E-02	2.60
PG(O-20:0/17:2);PG(P-18:0/19:1);PG(P-20:0/17:1)	Lipids ESI-	795.5494	413.82	2.31E-02	2.64
PG(42:8)	Lipids ESI-	845.5360	392.23	7.05E-03	4.27
Glycerophospholipid (PI)					
PI(36:1)	Lipids ESI-	863.5660	414.88	4.36E-02	2.13
PI(38:5)	Lipids ESI+	885.5454	398.78	3.41E-02	2.21
PI(37:4)	Lipids ESI-	931.5548	415.18	2.31E-02	2.64

PI(35:4)	Lipids ESI-	903.5222	393.77	2.64E-02	2.71
PI(O-18:0/19:1);PI(O-20:0/17:1);PI(P-16:0/21:0);PI(P-18:0/19:0);PI(P-20:0/17:0)	Lipids ESI-	899.5829	417.83	7.05E-03	2.91
PI(38:3);PI(40:6)	Lipids ESI-	909.5507	385.43	3.86E-02	4.29
PI(36:2)	HILIC ESI-	861.5511	242.36	1.67E-02	4.50
Phosphatidylserine (PS)					
PS(37:2)	Lipids ESI-	860.5650	423.98	3.00E-02	2.16
PS(40:7)	Lipids ESI-	892.5385	413.02	4.36E-02	2.40
PS(43:6)	Lipids ESI-	914.5359	412.74	1.52E-02	2.43
PS(O-16:0/18:0);PS(O-18:0/16:0);PS(O-20:0/14:0)	Lipids ESI-	770.5302	413.01	4.91E-02	2.50
PS(38:3)	Lipids ESI-	872.5640	415.16	1.75E-02	2.53
PS(42:8)	Lipids ESI-	918.5542	415.17	9.69E-03	2.61
PS(O-18:0/19:1);PS(O-20:0/17:1);PS(P-16:0/21:0);PS(P-18:0/19:0);PS(P-20:0/17:0);	HILIC ESI-	848.6033	210.74	4.90E-02	2.63
PS(35:2)	Lipids ESI+	796.5066	391.52	8.28E-03	2.64
PS(40:4)	Lipids ESI-	898.5797	417.75	9.69E-03	2.88
PS(O-20:0/17:2);PS(P-18:0/19:1);PS(P-20:0/17:1)	Lipids ESI+	810.5586	430.43	1.52E-02	3.23
PS(P-20:0/19:1)	HILIC ESI-	874.6184	208.76	4.90E-02	3.47
PS(40:8)	Lipids ESI-	890.5224	392.24	3.41E-02	3.67
PS(O-16:0/20:2);PS(O-18:0/18:2);PS(P-16:0/20:1);PS(P-18:0/18:1);PS(P-20:0/16:1)	Lipids ESI-	832.5688	429.23	3.41E-02	3.67
PS(O-16:0/19:1);PS(O-18:0/17:1);PS(O-20:0/15:1);PS(P-16:0/19:0);PS(P-18:0/17:0);PS(P-20:0/15:0)	HILIC ESI-	820.5723	212.54	1.67E-02	3.91
PS(41:6)	Lipids ESI-	886.5049	389.10	4.25E-03	4.23
PS(36:3)	Lipids ESI-	844.5325	392.24	7.05E-03	4.34
Glycerophospholipids (mixed)					
PS(37:0);PC(33:1);PE(36:1)	Lipids ESI-	804.5765	414.65	2.31E-02	2.42
PG(O-16:0/19:1);PG(O-18:0/17:1);PG(O-20:0/15:1);PG(P-16:0/19:0);PG(P-18:0/17:0);PG(P-20:0/15:0);PA(O-16:0/22:4);PA(O-18:0/20:4);PA(O-20:0/18:4);PA(P-18:0/20:3);PA(P-20:0/18:3);PA(P-20:0/18:3)	Lipids ESI-	769.5352	413.02	4.91E-02	2.43
PI(P-18:0/22:6);PGP(36:1);PI(37:1)	Lipids ESI-	915.5389	412.64	1.52E-02	2.46
PC(34:4);PE(37:4);PC(32:1);PE(35:1);PE-NMe(16:0/18:1)	Lipids ESI+	754.5352	394.63	3.56E-03	2.88
PC(35:3);PE(38:3);PS(39:2)	HILIC ESI-	828.5758	208.72	3.50E-02	3.09
PC(29:1);PE(32:1);PS(33:0)	Lipids ESI-	748.5141	365.21	4.91E-02	3.27
PC(31:0);PE(34:0);PE-NMe2(32:0)	HILIC ESI-	778.5614	213.48	1.11E-02	3.35
PI(P-16:0/22:6);PGP(34:1);PI(35:1)	Lipids ESI-	887.5081	389.10	4.36E-02	3.61
PS(O-16:0/21:0);PS(O-18:0/19:0);PS(O-20:0/17:0);PC(15:0/P-18:0);PC(O-16:0/17:1);PC(O-18:0/15:1);PC(P-16:0/17:0);PC(P-18:0/15:0);PC(P-18:0/15:0);PC(P-20:0/13:0);PE(18:0/P-18:0);PE(20:0/P-16:0);PE(O-16:0/20:1(11Z));PE(O-18:0/18:1(9Z));PE(O-20:0/16:1(9Z));PE(P-16:0/20:0);PE(P-16:0/20:0);PE(P-18:0/18:0);PE(P-18:0/16:0);PE(P-20:0/16:0);PE(dm18:0/18:0)	Lipids ESI-	790.5972	430.29	1.13E-02	3.63
PC(33:1);PE(36:1);PE-NMe2(16:0/18:1);PS(37:0)	HILIC ESI-	804.5772	210.99	1.67E-02	4.04
PC(33:2);PE(36:2);PS(37:1);PT(36:1)	HILIC ESI-	802.5618	210.96	2.44E-02	4.16
PC(44:11);PS(42:5)	Lipids ESI-	900.5558	429.24	4.91E-02	4.22
PC(35:1);PE(38:1);PS(39:0)	HILIC ESI-	832.6060	209.56	4.39E-02	4.42
PC(33:3);PE(36:3);PS(37:2)	HILIC ESI-	800.5460	210.32	1.11E-02	4.90
PC(35:2);PE(38:2);PS(39:1)	HILIC ESI-	830.5927	209.16	9.62E-03	5.10
PA(44:8);PG(O-16:0/22:4);PG(O-18:0/20:4);PG(O-20:0/18:4);PG(P-18:0/20:3);PG(P-20:0/18:3);PG(P-20:0/18:3)	Lipids ESI+	823.5253	394.87	3.00E-02	5.64
PC(31:1);PE(34:1);PS(35:0)	HILIC ESI-	776.5461	212.52	9.62E-03	6.87
PC(29:0);PE(32:0);GlcCer(d15:1/20:0);GlcCer(d14:1/20:0(2OH))	HILIC ESI-	750.5305	215.00	6.17E-03	7.50
Sphingolipids					
Ceramide					
Cer(d16:1/17:0)	Lipids ESI-	582.5104	414.62	3.86E-02	2.12
Cer(m18:1/18:0)	Lipids ESI-	584.5169	414.63	3.41E-02	2.13
Cer(d18:1/16:0);Cer(d14:1/20:0);Cer(d16:1/18:0)	Lipids ESI-	536.5046	414.63	3.41E-02	2.18
MIPC(t18:0/16:0(2OH))	Lipids ESI-	1010.5543	435.06	3.86E-02	2.20
PE-Cer(d15:2/24:0(2OH))	Lipids ESI-	765.5497	401.90	3.41E-02	2.21
PE-Cer(d14:1/22:0(2OH));PE-Cer(d16:1/20:0(2OH))	HILIC ESI-	741.4976	211.56	3.50E-02	2.33
PI-Cer(d18:0/16:0(2OH));PI-Cer(t18:0/16:0);PS(34:2)	Lipids ESI-	818.5169	389.36	4.36E-02	3.72
PE-Cer(d14:1/24:1(2OH));PE-Cer(d14:2/24:0(2OH));PE-Cer(d16:1/22:1(2OH));PE-Cer(d16:2/22:0(2OH))	HILIC ESI-	751.5338	215.11	9.62E-03	7.95
Galabiosylceramide (d18:1/24:0);LacCer(d18:0/24:1);Lactosylceramide (d18:1/24:0)	Lipids ESI+	996.7334	469.70	1.67E-03	11.08
Galabiosylceramide (d18:1/24:1);LacCer(d18:1/24:1);Lactosylceramide (d18:1/24:1)	Lipids ESI+	972.7355	453.14	2.82E-04	31.99
Galabiosylceramide (d18:1/22:0);Lactosylceramide (d18:1/22:0)	Lipids ESI+	968.7013	453.09	2.31E-02	33.82
Galabiosylceramide (d18:1/16:0);Lactosylceramide (d18:1/16:0)	Lipids ESI+	862.6247	391.94	8.99E-04	46.71
Other classes					
bacteriohopane-,32,33,34-triol-35-cyclitol;bacteriohopanetetrol cyclitol	Lipids ESI+	708.5440	391.71	8.28E-03	2.21
Plastoquinone 9	Lipids ESI+	749.6248	450.47	3.86E-02	2.50
Notoginsenoside R1	Lipids ESI-	953.5067	415.17	1.13E-02	2.62
CDP-DG(16:0/16:0)	Lipids ESI-	952.5075	415.18	4.25E-03	3.12
MGDG(36:2)	HILIC ESI-	803.5651	210.93	2.16E-02	4.40
MGDG(34:1);MGDG(36:4)	HILIC ESI-	777.5495	212.54	7.18E-03	6.95
Tetranor-PGF1alpha	HILIC ESI-	359.2081	40.17	1.90E-02	7.07
Diacylglyceride					
DG(38:6);DG(40:9)	Lipids ESI+	663.4969	363.07	3.86E-02	1.93
Ubiquinone and other terpenoid-quinone biosynthesis					
2-Decaprenyl-6-methoxy-1,4-benzoquinone;2-decaprenyl-6-methoxy-1,4-benzoquinone;3-Decaprenyl-4-hydroxybenzoic acid	Lipids ESI+	819.6671	472.69	4.36E-02	1.84
Decaprenyl diphosphate	Lipids ESI-	893.5409	413.01	3.41E-02	2.52
Acyl carnitine					
3-Dehydroxycarnitine	Lipids ESI+	184.0733	415.36	4.91E-02	1.55
Drug metabolism					
Aspartyl-Glycine;Carglumic acid	HILIC ESI+	191.0659	499.11	4.62E-02	2.25

Pirbuterol	HILIC ESI+	241.1542	459.95	1.05E-02	2.58
Fatty ester					
Arachidyl linoleate;Linoleyl arachidate	Lipids ESI-	581.5266	420.65	3.86E-02	2.07
Mercapto/thiol metabolite					
Cysteinylglycine disulfide	HILIC ESI+	298.0521	551.88	2.68E-02	3.64
Peptides					
Angiotensin III	Lipids ESI-	951.4866	396.68	4.36E-02	3.17
Isoleucyl-Lysine;Leucyl-Lysine	HILIC ESI+	260.1965	510.32	6.25E-03	4.45
Glycyl-Lysine	HILIC ESI+	204.1340	534.16	1.24E-02	6.10
Polyamine					
N1,N12-Diacetylspermine	HILIC ESI+	287.2437	487.85	2.68E-02	3.99
N1-Acetylspermidine;N8-Acetylspermidine	HILIC ESI+	188.1754	484.06	2.90E-03	12.78
Vitamin A metabolism					
Siphonaxanthin dodecenoate	HILIC ESI-	779.5650	213.52	1.11E-02	3.47
2'-Apo-beta-carotenal	Lipids ESI+	509.3800	169.64	1.31E-02	4.68
Mixed classes					
DGTA(18:1/22:4);PC(35:0);PE(38:0);PE-NMe2(18:0/18:0);GalCer(d18:1/23:0);GlcCer(d18:1/23:0)	Lipids ESI-	834.6239	454.16	3.86E-02	1.81
PI-Cer(d18:0/20:0(2OH));PI-Cer(d20:0/18:0(2OH));PI-Cer(t18:0/20:0);PI-Cer(t20:0/18:0);PS(38:2)	Lipids ESI-	874.5798	435.22	4.36E-02	1.89
LacCer(d14:1/16:0);LacCer(d18:1/12:0);PS(40:2)	Lipids ESI-	864.5694	414.88	3.86E-02	2.11
2,5-Dihydroxycinnamic acid methyl ester;3-(2-Hydroxy-3-methoxyphenyl)-2-propenoic acid;Isoferulic acid;trans-Ferulic acid	HILIC ESI+	233.0215	509.20	4.05E-02	2.21
GlcCer(d15:1/22:0);GlcCer(d14:1(4E)/22:0(2OH));GlcCer(d16:1(4E)/20:0(2OH));PC(31:0);PE(34:0);PE-NMe2(16:0/16:0);PE-NMe2(16:0/16:0)	Lipids ESI-	778.5608	413.02	4.36E-02	2.24
PA(O-20:0/20:5);PA(P-18:0/22:4);PA(P-20:0/20:4);Cholesteryl-6-O-myristoyl-alpha-D-glucoside	HILIC ESI-	795.5577	214.67	3.50E-02	2.33
PI-Cer(d18:0/18:0(2OH));PI-Cer(d20:0/16:0(2OH));PI-Cer(t18:0/18:0);PI-Cer(t20:0/16:0);PS(36:2)	Lipids ESI-	846.5481	413.01	2.64E-02	2.44
1alpha,25-dihydroxy-24-oxo-23-azavitamin D2;N-oleoyl tyrosine;LysoPC(14:0);PC(O-12:0/2:0);LysoPE(17:0);Buprenorphine;N-arachidonoyl tyrosine	Lipids ESI+	468.3087	86.20	4.36E-02	2.56
DGTS(34:2);PC(35:2);PE(38:2);PE-NMe2(36:2)	Lipids ESI-	770.5706	417.55	4.91E-02	2.81
1-Pyrroline-4-hydroxy-2-carboxylate;5-Oxoprolinate;Pyroglutamic acid;Pyrrolidonecarboxylic acid	HILIC ESI+	152.0322	529.96	1.54E-03	2.90
11-deoxy-11-methylene-PGD2;13,14-dihydroxy-11-mulinen-20-oic acid;5a-Tetrahydrocorticosterone;5alpha-Tetrahydrocorticosterone;9-deoxy-9-methylene-PGE2;MG(18:4);Pregnenetriolone;Tetrahydrocorticosterone;Tetrahydrocorticosterone;Tetrahydrodeoxycortisol;Tetrahydrodeoxycortisol;None;(13E)-11a-Hydroxy-9,15-dioxoprost-13-enoic acid;(5Z)-(15S)-11alpha-Hydroxy-9,15-dioxoprostanoate;(ent-6alpha,7alpha,16alphaH)-6,7,17-Trihydroxy-19-kauranoic acid;10,11-dihydro-Resolvin E1;11b-PGE2;11beta-PGE2;12-D2c-IsoP;12-D2t-IsoP;12-epi-12-D2c-IsoP;12-epi-12-D2t-IsoP;12-epi-12-iso-LGD2;12-epi-12-iso-LGE2;12-iso-LGD2;12-iso-LGE2;13,14-Dihydro-15-keto-PGD2;13,14-Dihydro-15-keto-PGE2;13,14-Dihydro-15-oxo-lipoxin A4;13,14-Dihydro-15-oxo-lipoxin A4;13,14-dihydro-15-keto-LXA4;13,14-dihydro-15-keto-PGD2;13,14-dihydro-15-keto-PGE2;15-D2c-IsoP;15-D2t-IsoP;15-E2c-IsoP;15-Epi-lipoxin A4;15-Keto-prostaglandin F2a;15-epi-15-D2c-IsoP;15-epi-15-D2t-IsoP;15-epi-15-E2c-IsoP;15-epi-15-E2t-IsoP;15-epi-15-iso-LGD2;15-epi-15-iso-LGE2;15-epi-lipoxin A4;15-iso-LGD2;15-iso-LGE2;15-keto-PGE1;15-keto-PGF2alpha;15R-PGD2;15R-PGE2;20-Hydroxy-leukotriene B4;20-hydroxy-LTB4;20-hydroxy-LTB4;5-D2c-IsoP;5-D2t-IsoP;5-epi-5-D2c-IsoP;5-epi-5-D2t-IsoP;5-epi-5-iso-LGD2;5-epi-5-iso-LGE2;5-iso-LGD2;5-iso-LGE2;5-trans-PGE2;8,15-diepi-15-D2c-IsoP;8-D2c-IsoP;8-D2t-IsoP;8-epi-15-D2c-IsoP;8-epi-15-E2c-IsoP;8-epi-8-D2c-IsoP;8-epi-8-D2t-IsoP;8-epi-8-iso-LGD2;8-epi-8-iso-LGE2;8-iso-15-keto-PGF2a;8-iso-15-keto-PGF2alpha;8-iso-LGD2;8-iso-LGE2;8-iso-PGE2;8-iso-PGF3a;8-iso-PGF3alpha;8-isoprostaglandin E2;Cinnassiol D1;Cinnassiol D4;D17-PGE1;Grayanotoxin II;Isograyanotoxin II;LGD2;LGE2;Levuglandin D2;Levuglandin E2;Lipoxin A4;Lipoxin A4;Lipoxin B4;LipoxinB4;PGD2;PGE2;PGF3alpha;PGH2;PGI2;PGK1;Prostaglandin D2;Prostaglandin E2;Prostaglandin F3a;Prostaglandin H2;Prostaglandin I2;Sterebin B;Sterebin C;TXA2;Thromboxane A2;delta-12-PGD2;ent-12-D2c-IsoP;ent-12-D2t-IsoP;ent-12-epi-12-D2c-IsoP;ent-12-epi-12-D2t-IsoP;ent-12-epi-12-iso-LGD2;ent-12-epi-12-iso-LGE2;ent-12-iso-LGD2;ent-12-iso-LGE2;ent-15-D2c-IsoP;ent-15-D2t-IsoP;ent-15-E2c-IsoP;ent-15-E2t-IsoP;ent-15-epi-15-D2c-IsoP;ent-15-epi-15-D2t-IsoP;ent-15-epi-15-E2c-IsoP;ent-15-epi-15-E2t-IsoP;ent-15-epi-15-iso-LGD2;ent-15-epi-15-iso-LGE2;ent-15-iso-LGD2;ent-15-iso-LGE2;ent-5-D2c-IsoP;ent-5-D2t-IsoP;ent-5-epi-5-D2c-IsoP;ent-5-epi-5-D2t-IsoP;ent-5-epi-5-iso-LGD2;ent-5-epi-5-iso-LGE2;ent-5-iso-LGD2;ent-5-iso-LGE2;ent-8,15-diepi-15-D2c-IsoP;ent-8,15-diepi-15-	HILIC ESI-	387.1935	31.90	4.90E-02	3.15
GlcCer(d18:0/18:0);PC(O-16:0/15:0);PC(O-18:0/13:0);PE(O-16:0/18:0);PE(O-18:0/16:0);PE(O-20:0/14:0)	Lipids ESI-	764.5818	429.13	1.31E-02	3.27
PA(37:1);PG(36:1);DG(44:10);PE-Cer(d16:2/24:1)	Lipids ESI-	775.5492	419.28	4.91E-02	3.30
3-Amino-2-piperidone;N-Mononitrosopiperazine	HILIC ESI+	115.0865	508.45	4.62E-02	3.41
PE-Cer(d14:1/26:0);PE-Cer(d16:1/24:0);SM(d18:1/19:0);SM(d19:1/18:0)	Lipids ESI-	765.5856	429.36	1.13E-02	3.48
DGCC(16:0/20:5);PS(O-16:0/17:0);PS(O-18:0/15:0);PS(O-20:0/13:0)	HILIC ESI-	794.5560	215.00	2.16E-02	4.34
PI-Cer(d18:0/20:0);PI-Cer(d20:0/18:0);PI-Cer(d18:0/20:0);PI-Cer(d20:0/18:0);PS(O-18:0/20:3);PS(O-20:0/18:3);PS(O-20:0/18:3);PS(P-16:0/22:2);PS(P-18:0/20:2);PS(P-20:0/18:2)	Lipids ESI-	858.5833	430.34	1.31E-02	4.35
PA(35:1);PG(34:1);DG(42:10);PE-Cer(d14:2/24:1);PE-Cer(d16:2/22:1)	Lipids ESI-	747.5185	397.98	3.41E-02	4.39
PGP(36:2);PI(37:2)	Lipids ESI-	913.5233	392.24	1.52E-02	4.48
PA(37:2);PG(36:2);DG(44:11)	HILIC ESI-	773.5352	42.08	2.05E-04	36.80

Table E2

Metabolite name	Assay	mz	rt (sec)	raw.pval	FC (HCA+/HCA-)
Acyl carnitines					
Hexanoylcarnitine	Lipids ESI+	260.1858	34.42	7.05E-03	0.29
Acetylcarnitine	Lipids ESI+	204.1231	32.57	3.56E-03	0.30
3-hydroxyoctanoyl carnitine	Lipids ESI+	304.2122	34.44	1.31E-02	0.31
Butyrylcarnitine;Isobutyrylcarnitine	Lipids ESI+	232.1544	33.11	2.31E-02	0.36
Isovalerylcarnitine;Valerylcarnitine	Lipids ESI+	246.1701	33.38	3.41E-02	0.39
Propionylcarnitine	Lipids ESI+	218.1387	33.06	3.00E-02	0.43
Carnitine	Lipids ESI+	162.1124	32.35	1.52E-02	0.53
Glycerophospholipids					
Phosphatidic acid (PA)					
PA(O-18:0/21:0);PA(O-20:0/19:0)	Lipids ESI+	733.6124	418.26	4.25E-03	0.34
PA(41:6)	Lipids ESI+	763.5304	399.77	7.05E-03	0.37
PA(O-16:0/18:1);PA(O-18:0/16:1);PA(O-20:0/14:1);PA(P-16:0/18:0);PA(P-18:0/16:0);PA(P-20:0/14:0);PA(O-16:0/20:4);PA(O-18:0/18:4);PA(P-16:0/20:3);PA(P-18:0/18:3);PA(P-18:0/18:3)	Lipids ESI+	683.5013	447.04	7.05E-03	0.39
PA(16:0e/18:0);PA(O-16:0/18:0);PA(O-18:0/16:0);PA(O-20:0/14:0);PA(O-16:0/20:3);PA(O-18:0/18:3);PA(P-16:0/20:2);PA(P-18:0/18:2)	Lipids ESI+	685.5168	455.53	1.13E-02	0.42
Phosphatidylcholine (PC) and/or phosphatidylethanolamine (PE)					
PC(40:2);PE(43:2);PC(42:5)	Lipids ESI+	864.6488	430.80	8.99E-04	0.10
PC(18:1/P-18:1);PC(18:2/P-16:0);PC(20:2/P-16:0);PC(O-16:0/20:3);PC(O-18:0/18:3);PC(O-18:1/18:2);PC(P-16:0/20:2);PC(P-18:0/18:2);PC(P-18:1/18:1);PC(O-18:1/18:2);PC(20:4/P-18:1);PC(20:5/P-18:0);PC(22:5/P-16:0);PC(O-16:0/22:6);PC(P-16:0/22:5);PC(P-18:0/20:5);PC(P-18:1/20:4);PC(dm18:1/20:4);PC(o-16:0/22:6)	Lipids ESI+	792.5898	405.36	1.37E-03	0.29
PC(O-22:1/22:3);PC(O-22:2/22:2);PC(O-24:0/20:4);PC(o-22:1/22:3);PC(o-22:2/22:2);PC(o-24:0/20:4)	Lipids ESI+	880.7180	504.94	3.56E-03	0.38
PE(22:6/P-18:1)	Lipids ESI+	774.5419	429.45	4.91E-02	0.44
PC(15:0/P-18:1);PC(18:1(9Z)/P-16:0);PC(P-16:0/17:1);PC(P-18:0/15:1);PC(P-18:1/15:0);PE(18:1/P-18:0);PE(20:1/P-16:0);PE(O-16:0/20:2);PE(O-18:0/18:2);PE(P-16:0/20:1);PE(P-18:0/18:1);PE(P-18:1/18:0);PE(P-20:0/16:1);PE(dm18:0/18:1);PE(20:3/P-18:1);PE(20:4/P-18:0);PE(22:4/P-16:0);PE(O-16:0/22:5);PE(O-18:0/20:5);PE(O-18:1/20:4);PE(P-16:0/22:4);PE(P-18:0/20:4);PE(P-18:0/20:4);PE(P-18:1/20:3);PE(P-20:0/18:4)	Lipids ESI+	752.5588	429.45	1.31E-02	0.46
PE(18:2/P-18:1);PE(18:3/P-18:0);PE(20:3/P-16:0);PE(O-16:0/20:4);PE(O-18:0/18:4);PE(P-18:0/18:3);PE(P-18:1/18:2);PE(20:5/P-18:1);PE(22:6/P-16:0);PE(O-16:1/22:6);PE(P-16:0/22:6);PE(P-18:1/20:5)	Lipids ESI+	748.5273	399.55	3.00E-02	0.48
PC(36:1);PE(39:1);PC(38:4);PE(41:4)	Lipids ESI+	810.6000	415.10	1.52E-02	0.54
PC(P-16:0/15:1);PE(16:0/P-18:1);PE(18:1/P-16:0);PE(O-16:0/18:2);PE(P-16:0/18:1);PE(P-18:0/16:1);PE(P-18:1/16:0);PE(P-20:0/14:1);PE(P-16:0/18:1)	Lipids ESI+	702.5434	431.30	4.36E-02	0.64
PC(15:0/P-18:1);PC(18:1/P-16:0);PC(O-16:0/17:2(9Z,12Z));PC(P-16:0/17:1(9Z));PC(P-18:0/15:1(9Z));PC(P-18:1(11Z)/15:0);PC(P-18:1(9Z)/15:0);PE(18:0/P-18:1(11Z));PE(18:0/P-18:1(9Z));PE(18:1(11Z)/P-18:0);PE(18:1(9Z)/P-18:0);PE(20:1(11Z)/P-16:0);PE(O-16:0/20:2(11Z,14Z));PE(O-18:0/18:2(9Z,12Z));PE(P-16:0/20:1(11Z));PE(P-16:0/20:1(11Z));PE(P-18:0/18:1(9Z));PE(P-18:0/18:1(9Z));PE(P-18:1(11Z)/18:0);PE(P-18:1(9Z)/18:0);PE(P-20:0/16:1(9Z));PE(dm18:0/18:1(11Z))	Lipids ESI+	730.5747	449.97	2.64E-02	0.66
PC(33:1);PE(36:1)	Lipids ESI+	746.5697	439.39	4.91E-02	0.73
Phosphatidylglycerol (PG)					
PG(36:1)	Lipids ESI+	777.5619	421.48	4.36E-02	0.52
Phosphatidylserine (PS)					
PS(34:1)	Lipids ESI+	762.5275	399.59	4.91E-02	0.55
Glycerophospholipids (mixed)					
PC(42:5);PS(O-20:0/21:0);PC(44:7)	Lipids ESI+	886.6316	405.35	1.52E-02	0.33
PG(36:5);PI(O-16:0/13:0);PA(39:8);PG(38:8)	Lipids ESI-	789.4678	31.76	2.64E-02	0.57
Sphingolipids					
Xestoaminol C	Lipids ESI+	230.2480	65.16	1.75E-02	0.15
Ceramides					
Cer(t18:0/18:0(2OH));Cer(t20:0/16:0(2OH))	Lipids ESI+	622.5370	465.28	1.13E-02	0.07
Cer(t18:0/20:0(2OH));Cer(t20:0/18:0(2OH))	Lipids ESI+	650.5681	480.81	4.91E-02	0.08
Cer(m18:1/22:0)	Lipids ESI+	628.6028	457.90	2.31E-02	0.22
1-O-behenoyl-Cer(d18:1/16:0)	Lipids ESI+	860.8433	566.13	4.91E-02	0.23
Cer(d14:1/22:0(2OH));Cer(d16:1/20:0(2OH))	Lipids ESI+	604.5276	430.82	3.00E-02	0.23
Cer(m18:1/24:1)	Lipids ESI+	632.6343	488.81	1.67E-03	0.39
GalCer(d18:1/24:1);GlcCer(d18:1/24:1)	Lipids ESI+	810.6826	472.29	3.86E-02	0.41
Cer(d15:1/22:0);Cer(d18:1/19:0)	Lipids ESI+	602.5486	447.71	4.91E-02	0.43
Cer(m18:0/22:0)	Lipids ESI+	630.6186	473.90	9.69E-03	0.44
Cer(d18:0/24:1);Cer(d18:1/24:0)	Lipids ESI+	650.6450	488.75	2.97E-03	0.44
Cer(d16:2/24:0);Cer(d18:1/22:1);Cer(d18:2/22:0)	Lipids ESI+	642.5799	457.36	5.98E-03	0.45
Cer(d14:1/26:0);Cer(d16:1/24:0);Cer(d18:0/22:1);Cer(d18:1/22:0)	Lipids ESI+	622.6134	473.93	5.05E-03	0.46
Cer(d18:1/26:1)	Lipids ESI+	698.6425	488.18	4.91E-02	0.47
Cer(d18:1/24:1)	Lipids ESI+	670.6111	473.72	7.05E-03	0.47
Cer(d14:1/24:0);Cer(d16:1/22:0);Cer(d18:1/20:0);Cer(d14:1/24:0);Cer(d16:1/22:0);Cer(d18:1/20:0)	Lipids ESI+	594.5820	456.86	3.41E-02	0.48
Cer(d18:0/24:1);Cer(d18:0/24:1);Cer(d18:1/24:0)	Lipids ESI+	688.6002	488.83	3.86E-02	0.52
Sphingomyelins					
SM(d18:1/25:0);SM(d19:0/24:1);SM(d19:1/24:0);SM(d20:1/23:0)	Lipids ESI+	851.6987	482.74	5.29E-05	0.01
SM(d19:1/24:1)	Lipids ESI+	828.7041	466.35	2.82E-04	0.18
SM(d18:0/26:1);SM(d18:1/26:0);SM(d20:0/24:1)	Lipids ESI+	843.7326	490.61	7.23E-04	0.21
SM(d18:1/26:0)	Lipids ESI+	844.7362	490.47	2.31E-02	0.34
SM(d16:0/22:0);SM(d18:0/20:0);SM(d18:0/20:0)	Lipids ESI+	761.6531	447.27	3.56E-03	0.35
SM(d16:1/24:0);SM(d18:0/22:1(13Z));SM(d18:1/22:0);SM(d18:1/22:0)	Lipids ESI+	809.6509	458.19	2.97E-03	0.37
SM(d18:0/24:1(OH))	Lipids ESI+	829.6790	429.16	2.97E-03	0.37
SM(d17:1/24:0)	Lipids ESI+	802.6887	467.07	2.97E-03	0.38
SM(d17:1/26:1);SM(d18:2/25:0);SM(d19:1/24:1)	Lipids ESI+	827.7007	466.43	2.31E-02	0.40
SM(d16:1/24:0);SM(d18:0/22:1);SM(d18:1/22:0);SM(d18:1/22:0)	Lipids ESI+	787.6689	458.19	3.56E-03	0.42
SM(d16:1/25:0);SM(d17:1/24:0);SM(d18:1/23:0);SM(d18:1/23:0)	Lipids ESI+	801.6848	467.11	3.56E-03	0.44
SM(d16:0/20:0);SM(d18:0/18:0);SM(d18:0/18:0);SM(d19:0/17:0)	Lipids ESI+	733.6219	426.98	1.31E-02	0.44
SM(d16:1/22:0);SM(d18:1/20:0);SM(d18:1/20:0)	Lipids ESI+	759.6376	439.30	5.98E-03	0.46
SM(d18:0/22:0);SM(d18:0/22:0);SM(d18:2/24:1)	Lipids ESI+	811.6687	440.46	1.75E-02	0.47
SM(d16:1/22:1);SM(d18:1/20:1);SM(d18:2/20:0)	Lipids ESI+	757.6219	419.16	2.31E-02	0.50

Diacylglycerides						
DG(48:0)	Lipids ESI+	831.7242	482.41	4.58E-04		0.28
DG(39:0)	Lipids ESI+	689.6037	488.92	1.52E-02		0.34
DG(40:7);DG(38:4)	Lipids ESI+	667.5275	447.25	1.67E-03		0.37
DG(46:0)	Lipids ESI+	803.6922	466.96	2.64E-02		0.38
DG(39:1);DG(40:4);DG(42:8)	Lipids ESI+	687.5893	473.64	3.86E-02		0.38
DG(36:4);DG(38:7)	Lipids ESI+	639.4962	507.09	2.01E-02		0.38
DG(38:7);DG(36:4)	Lipids ESI+	639.4961	427.69	3.41E-02		0.41
DG(42:7);DG(40:4)	Lipids ESI+	695.5593	460.29	2.01E-02		0.48
DG(40:6);DG(42:9)	Lipids ESI+	691.5273	439.83	3.86E-02		0.53
Ubiquinone and other terpenoid-quinone biosynthesis						
Arachispreol 10;Decaprenol	Lipids ESI+	699.6446	488.21	1.75E-02		0.33
2-Decaprenyl-3-methyl-6-methoxy-1,4-benzoquinone;2-decaprenyl-5-hydroxy-6-methoxy-3-methyl-1,4-benzoquinone;3-Decaprenyl-4-hydroxy-5-methoxybenzoate;3-decaprenyl-4-hydroxy-5-methoxybenzoic acid	Lipids ESI+	887.6349	405.39	2.31E-02		0.34
Ubiquinol-10	Lipids ESI+	887.6893	493.21	3.86E-02		0.35
Coenzyme Q10	Lipids ESI+	901.6476	504.95	1.31E-02		0.41
2-demethylmenaquinone-8	Lipids ESI+	703.5470	431.49	3.86E-02		0.57
Other classes						
PGF2alpha-11-acetate	Lipids ESI+	419.2407	78.29	4.36E-02		0.21
Cytosine	Lipids ESI+	112.0506	33.74	3.60E-04		0.24
Citronellyl beta-sophoroside	Lipids ESI+	481.2620	33.10	4.91E-02		0.25
Thiomorpholine 3-carboxylate	Lipids ESI+	148.0427	33.38	1.13E-02		0.27
Bilirubin	Lipids ESI+	585.2709	38.83	1.52E-02		0.32
Indoleacrylic acid	Lipids ESI+	188.0706	33.69	2.31E-02		0.38
2-Aminooctanoic acid	Lipids ESI+	160.1332	32.32	5.05E-03		0.40
Cholesteryl-6-O-myristoyl-alpha-D-glucoside	Lipids ESI+	781.5927	443.29	7.05E-03		0.43
Histidine	Lipids ESI+	156.0768	34.23	2.01E-02		0.44
Peroxydisulfuric acid	HILIC ESI-	192.9115	240.74	3.84E-03		0.51
Neurine	Lipids ESI+	104.1070	31.78	4.91E-02		0.55
Triacylglycerides						
TG(15:0/16:0/o-18:0);TG(15:0/o-18:0/16:0);TG(16:0/15:0/o-18:0)	Lipids ESI+	845.7392	490.63	7.23E-04		0.19
Cysteine and methionine metabolism						
S-Adenosylhomocysteine	HILIC ESI+	385.1281	428.81	4.62E-02		0.37
Carbohydrate metabolism						
3-Galactosyllactose;3-beta-Cellobiosyllglucose;3-beta-Gentiobiosyllglucose;4-beta-Laminaribiosyllglucose;6-Kestose;6-O-Glucosylmaltose;D-Gal alpha 1->6D-Gal alpha 1->6D-Glucose;Dextrin;Fagopyritol A2;Fagopyritol B2;Galactotriose;Gentianose;Gentiotriose;Levan;Maltotriose;Melezitose;Neokestose;Nephritogenoside;Panose;Raffinose;Sophorotriose;Umbelliferose;alpha-D-Glucopyranosyl-(1->4)-alpha-D-galactopyranosyl-(1->6)-D-glucose;alpha-D-Glucopyranosyl-(1->6)-alpha-D-glucopyranosyl-(1->2)-D-glucose;beta-D-Fructofuranosyl alpha-D-glucopyranosyl-(1->4)-D-glucopyranoside;beta-D-Galactopyranosyl-(1->2)-[beta-D-galactopyranosyl-(1->4)]-D-galactose;beta-D-Galactopyranosyl-(1->3)-beta-D-galactopyranosyl-(1->6)-D-galactose;beta-D-Galactopyranosyl-(1->4)-beta-D-galactopyranosyl-(1->4)-D-galactose	HILIC ESI-	503.1626	452.47	5.00E-04		0.26
Drug metabolism						
Dihydroartemisinin	Lipids ESI+	307.1520	38.34	3.86E-02		0.14
Bupivacaine;Levobupivacaine	Lipids ESI+	289.2276	36.39	3.00E-02		0.26
Ethopropazine	HILIC ESI-	347.1352	40.46	4.39E-02		0.61
Fatty acids and oxidised fatty acids						
Cohibin C;Cohibin D	Lipids ESI+	599.5037	507.05	9.69E-03		0.30
Mercapto/thiol metabolite						
(S)-3-Mercaptohexyl butyrate;3-Mercaptohexyl butyrate;Hexyl 3-mercaptobutanoate;Hexyl 3-mercaptobutanoate	Lipids ESI+	205.1264	32.59	8.28E-03		0.29
(S1)-Methoxy-3-heptanethiol	Lipids ESI+	163.1158	32.46	1.52E-02		0.53
Nicotinate and nicotinamide metabolism						
N1-Methyl-2-pyridone-5-carboxamide;N1-Methyl-4-pyridone-3-carboxamide	Lipids ESI+	153.0659	33.63	7.05E-03		0.25
Niacinamide	HILIC ESI-	121.0408	364.37	2.44E-02		0.83
Peptides						
Gamma-glutamyl-Glutamate;Glutamyl-Glutamate;Prolyl-Histidine	Lipids ESI+	275.1102	33.68	2.01E-02		0.13
Alanyl-Isoleucine;Alanyl-Leucine	Lipids ESI+	203.1391	33.09	4.25E-03		0.38
Polyamine						
Caffeoylferuloylspermidine	HILIC ESI+	522.2020	490.31	4.62E-02		0.29
Creatinine	Lipids ESI+	114.0662	33.10	1.52E-02		0.47
Vitamin D metabolism						
1alpha,22-dihydroxy-23,24,25,26,27-pentanorvitamin D3	Lipids ESI+	369.2405	212.61	1.75E-02		0.15
(6RS)-22-oxo-23,24,25,26,27-pentanorvitamin D3 6,19-sulfur dioxide adduct	Lipids ESI+	393.2095	33.33	2.31E-02		0.30
Mixed classes						
2-Hydroxy-2-(2-oxopropyl)butanedioic acid;3,7-dideoxy-D-threo-hepto-2,6-diulosonic acid;3-Dehydroquinone	HILIC ESI-	225.0172	32.21	1.46E-02		0.19
4-Imidazolone-5-propionic acid;5-Hydroxymethyl-4-methyluracil;Imidazolelactic acid	Lipids ESI+	157.0608	34.89	5.05E-03		0.35
5-Aminopentanoic acid;Betaine;Valine;N-Methyl-a-aminoisobutyric acid;Norvaline	Lipids ESI+	118.0862	33.10	7.05E-03		0.38
PE-Cer(d15:2/22:0(2OH));SM(d18:0/16:1(OH))	Lipids ESI+	717.5547	357.82	3.41E-02		0.40
4-Amino-2-methylenebutanoic acid;Proline	Lipids ESI+	116.0706	33.33	2.01E-02		0.45
PE-Cer(d14:1(4E)/26:0);PE-Cer(d16:1(4E)/24:0);SM(d18:1/19:0);SM(d19:1/18:0)	Lipids ESI+	745.6226	429.05	2.01E-02		0.46
Dihydrothymine;L-Cyclo(alanylglucyl);Squamolone	Lipids ESI+	129.0659	33.62	1.75E-02		0.51
2-Pyrrolidineacetic acid;Pipelicolic acid	Lipids ESI+	130.0863	33.63	2.64E-02		0.52
LBPA(34:1);PG(34:1)	Lipids ESI+	749.5311	399.55	4.91E-02		0.54
Alanylglycine;Glutamine	Lipids ESI+	147.0764	33.57	3.86E-02		0.54
Glutamyl-Valine;Valyl-Glutamate;Adenosine;Deoxyguanosine	Lipids ESI+	268.1041	33.37	4.91E-02		0.60

CONCLUSIONS

Neonatal pulmonary diseases and respiratory failure are common in neonates and often associated with maternal pathology, prematurity, or congenital anomalies. During my PhD we explored the feasibility of applying two different high resolution mass spectrometry approaches for the study of a pulmonary disease, the RDS, by investigating both the efficiency of surfactant replacement therapy and the effects of maternal inflammation.

Firstly, we developed a novel method by which the exogenous and endogenous surfactant can be distinguished in the alveolar pool *in vivo* without the need for administering any artificially labelled compound. Our novel stable isotopes approach at ^{13}C natural abundance is non-invasive and risk-free. It could then be suitable for *in vivo* studies involving preterm infants. Moreover, under the premises of a significant difference in stable isotope content between the exogenous compound and the biological counterpart, this method could also be extended to other drug therapies.

The analysis of principal surfactant components suggested an effect of fetal exposure to chorioamnionitis on the concentration of ELF DSPC, SP-B, and MPO activity. In accordance with these results, LC-MS/MS untargeted lipidomics investigation on TAs revealed interesting changes in specific areas of metabolism making this approach a promising technique to identify pathways that can be altered in newborns as a consequence of maternal infection. The small number of patients included in the study and the unbalanced number of newborns in the two groups represent a limitation to the study that has to be considered as a pilot study. However, the developed methodology applied to an unbiased investigation on a larger group of patients will be helpful in the assessment of effect of chorioamnionitis on the onset of respiratory diseases.

A better knowledge on the pathophysiology of lung disease and on the effectiveness of the therapy administered to the babies will hopefully lead to the development of more effective and less invasive personalized treatments.

ACKNOWLEDGEMENTS

Vorrei innanzitutto ringraziare la Prof.ssa Paola Cogo e il Prof. Carnielli per avermi dato la possibilità di lavorare a questo progetto e per la grande disponibilità e professionalità con cui mi hanno seguita nella sua realizzazione.

Un grandissimo ringraziamento va ai miei compagni di avventura, Manuela, Luca e Alessio, per tutto quello che mi hanno insegnato, per la pazienza e tutto l'aiuto ricevuto in questi tre anni. Senza di loro, nessuno dei risultati raggiunti sarebbe stato possibile.

Vorrei inoltre ringraziare il Prof. Warwick Dunn e tutto il suo gruppo per la formazione sul campo della metabolomica, per avermi incoraggiata e fatta sentire in poco tempo parte integrante del gruppo di ricerca.

Grazie a “quelli delle 13.30”, per le risate e le merende che hanno allietato anche le giornate più grigie.

Grazie a tutti i nuovi amici che sono stati la parte più bella di questi anni. E grazie soprattutto a Virginia, Pia, Flavia, Martina, Adal, Giulia e Alessandra per avermi fatta sentire meno sola lontana da casa e avermi tirata fuori dal laboratorio quando avevo bisogno di staccare, rendendo così leggere anche le settimane più pesanti.

Grazie agli amici di sempre, quelli che non hai bisogno di sentire tutti i giorni per sapere che ci sono, a cui non serve dire come stai perchè lo sentono anche a km di distanza. Grazie a Lady, Laura, Daniele, Giusi, Velia, Mary, Eri, Sergio e Azzurra per le telefonate in cui avete dovuto darmi la carica e per quelle in cui abbiamo condiviso la gioia per i risultati raggiunti.

Infine il più importante ringraziamento va alla mia famiglia, per avermi sempre sostenuta nelle mie scelte, anche in quelle che mi portavano via da casa. E in particolare ringrazio i miei genitori, perchè da loro ho imparato a non arrendermi e a lavorare sodo, perchè nella vita con il giusto impegno si può raggiungere qualsiasi obiettivo.